

# Roadmap to Iodine and Mercury Abatement Materials Selection in Nuclear Waste Processing Off-Gas Streams

December 2022

MS Fountain  
RM Asmussen  
BJ Riley  
S Chong  
S Choi  
J Matyáš

## DISCLAIMER

This report was prepared as an account of work sponsored by an agency of the United States Government. Neither the United States Government nor any agency thereof, nor Battelle Memorial Institute, nor any of their employees, makes **any warranty, express or implied, or assumes any legal liability or responsibility for the accuracy, completeness, or usefulness of any information, apparatus, product, or process disclosed, or represents that its use would not infringe privately owned rights.** Reference herein to any specific commercial product, process, or service by trade name, trademark, manufacturer, or otherwise does not necessarily constitute or imply its endorsement, recommendation, or favoring by the United States Government or any agency thereof, or Battelle Memorial Institute. The views and opinions of authors expressed herein do not necessarily state or reflect those of the United States Government or any agency thereof.

PACIFIC NORTHWEST NATIONAL LABORATORY  
*operated by*  
BATTELLE  
*for the*  
UNITED STATES DEPARTMENT OF ENERGY  
*under Contract DE-AC05-76RL01830*

Printed in the United States of America

Available to DOE and DOE contractors from the  
Office of Scientific and Technical Information,  
P.O. Box 62, Oak Ridge, TN 37831-0062;  
ph: (865) 576-8401  
fax: (865) 576-5728  
email: [reports@adonis.osti.gov](mailto:reports@adonis.osti.gov)

Available to the public from the National Technical Information Service  
5301 Shawnee Rd., Alexandria, VA 22312  
ph: (800) 553-NTIS (6847)  
email: [orders@ntis.gov](mailto:orders@ntis.gov) <<https://www.ntis.gov/about>>  
Online ordering: <http://www.ntis.gov>

# **Roadmap to Iodine and Mercury Abatement Materials Selection in Nuclear Waste Processing Off-Gas Streams**

December 2022

MS Fountain  
RM Asmussen  
BJ Riley  
S Chong  
S Choi  
J Matyáš

Prepared for  
the U.S. Department of Energy  
under Contract DE-AC05-76RL01830

Pacific Northwest National Laboratory  
Richland, Washington 99354

## Executive Summary

This work provides a guide for candidate mercury (Hg) and iodine-129 ( $^{129}\text{I}$ ) abatement material identification, screening, evaluation, technical gap identification, and bench-scale testing prioritization while also conceptualizing a materials deployment roadmap for implementation of new materials in the Hanford Waste Treatment and Immobilization Plant (WTP) Low-Activity Waste (LAW) Facility at Hanford in Richland, Washington, and elsewhere in the U.S. Department of Energy (DOE) complex for similar applications. The study was prompted by the need to replace the Kombisorb BAT-37 due to uncertainties in Hg and  $^{129}\text{I}$  capture performance and future availability for use in the WTP LAW Facility secondary off-gas system, specifically the Carbon Adsorber units. However, replacement of this material could also mitigate two other issues with Kombisorb BAT-37 (and its successor BAT-37 II): (1) fire safety risk due to exothermic heat generated by adsorption reactions between the carbon material and Hg and (2) the risk of low retention of  $^{129}\text{I}$  in glass and subsequent downstream impacts on secondary liquid waste treatment at the Effluent Treatment Facility. The objectives and benefits of this work for application at Hanford include:

- Mitigation of mercury-adsorbent material (Kombisorb BAT-37) source/availability risk
- Avoidance of future operational downtime and inefficiencies due to  $^{129}\text{I}$  limits for secondary liquid waste receipt at the Effluent Treatment Facility
- Early and informed maturation of  $^{129}\text{I}$  removal and immobilization technologies for current and future phases of the waste treatment mission (e.g., WTP HLW Facility, supplemental LAW)
- Improved protection of the thermal catalytic oxidizer and selective catalytic reducer catalyst beds from potential poisoning and more frequent replacement leading to increased facility downtime
- Efficient and effective abatement of Hg and  $^{129}\text{I}$  for compliance with multiple facility air emission and waste disposal assumptions
- Immobilization of  $^{129}\text{I}$  into a durable waste form

Pacific Northwest National Laboratory conducted a search of commercial and literature sources, developed an evaluation methodology, and then screened and evaluated potential candidate materials (both commercially available materials for near-term application and developmental materials for potential long-term integration) with the intent to rank and recommend materials for subsequent bench-scale testing for Hg and/or I abatement under dynamic flow using simple gas conditions initially, followed by complex gas conditions for the most promising materials.

Reference-based application details were established relating to the design of the WTP LAW and High-Level Waste (HLW) facilities, abatement needs specifically for Hg and  $^{129}\text{I}$ , the Carbon Adsorber infrastructure and configuration, existing Carbon Adsorber media specifications, prior work on baseline Carbon Adsorber media, and waste form planning assumptions. These details directly influenced the evaluation criteria developed for the material candidates and the information extracted from commercial/literature sources.

A diverse array of materials were screened for gas-phase capture of Hg and I, and each material group was summarized. The evaluation methodology first binned materials as commercially available (near-term replacements) or developmental (long-term replacements) and then evaluated them using the following criteria (listed in order of importance by this assessment):

- Material cost
- Safety risks

- Hg/I loading capacity
- Test conditions relative to the WTP LAW Facility
- Thermal and chemical stability in service
- Mechanical stability and physical form
- Waste form demonstration

Each criterion was given a qualitative measure to rank and prioritize these materials for potential use in the WTP LAW Facility off-gas application. Top priority materials were inherently biased to commercial candidates for near-term implementation, and the highest ranked materials were carbon-based, driven primarily by low-cost, but also maturity in safety, loading, and stability. Porous inorganic crystalline matrices and inorganic sulfide sorbents were deemed the next most-promising commercially available binned materials.

Developmental materials were also ranked and prioritized; these materials need more time for development and have a lower maturity, but that is counteracted by their significant potential to improve safety and operational stability and reduce long-term mission costs. The order of priority for the top three developmental materials is aerogels, xerogels, and engineered membranes, with multiple additional developmental material groups provided at lower ranking.

Laboratory-scale testing priorities were established based on the material rankings and known near-term needs. The near-term needs are believed to be best met through investigation of commercially available activated carbons for Hg and I abatement.

Attractive materials for long-term implementation were identified, in priority order, as

1. inorganics aerogels,
2. engineered membranes (like carbon foam), and
3. development of new sorbents through modification (impregnate/functionalize) of emerging substrates.

Planned laboratory testing to advance material candidacy will follow this evaluation work and be conducted in three phases:

- Static testing for Hg and I capture where limited capture data exists to quickly screen out material candidates
- Simplified off-gas composition (i.e., only Hg and/or I in moist air without competitors) testing in dynamic flow conditions to screen materials prior to complex off-gas composition testing
- Complex off-gas composition (i.e., additional chemistry including NO<sub>x</sub>, SO<sub>2</sub>, etc.) testing in dynamic conditions to select a limited material set for future scaled testing under full prototypic and representative WTP LAW Facility melter off-gas conditions

Finally, the testing priorities listed above are only a portion of the evaluation steps needed to reach a material development maturity for deployment in the WTP LAW Facility or elsewhere in the DOE complex. A conceptualized deployment roadmap was derived and is presented that groups major activities by “candidacy evaluation” and “deployment assessment” to serve as a guide to DOE and DOE contractors

for anticipating total budget, schedule, and risk impacts for replacing a sorbent material to abate constituent emissions for regulatory compliance in a radioactive melter off-gas stream.

## Acknowledgments

The authors would like to thank Nicholas Machara (DOE-EM) for his recognition of the technical merit of this work and securing the funding to complete this materials evaluation and deployment roadmap report and subsequent bench-scale testing. Krista Carlson is also recognized for her discussions with the team and collaborations on other related material development work. The authors also wish to thank Phil Schonewill for his technical review, Dave MacPherson for quality assurance, and Matt Wilburn for the technical editing. We also thank technical staff at Donau Carbon, Molecular Products, ResinTech, Calgon, Purolite, Norit Carbon, Honeywell and Ecologix for product discussions. Thanks also to Melanie Chiaradia for her essential help with the project controls and Cassie Martin for her management of project records.

## Acronyms and Abbreviations

AC	activated carbon
AC-S	sulfur-impregnated activated carbon
Ag <sup>0</sup>	elemental silver
AgX	silver faujasite (zeolite)
AgZ	silver mordenite (zeolite)
Bi <sup>0</sup>	elemental bismuth
BNI	Bechtel National, Inc.
CMP	conjugated microporous polymer
COF	covalent organic framework
Cu <sup>0</sup>	elemental copper
DF	decontamination factor
DMSO	dimethyl sulfoxide
DOE	U.S. Department of Energy
DRE	destruction and removal efficiency
EDS	energy-dispersive X-ray spectroscopy
EM	Office of Environmental Management
EMF	Effluent Management Facility
ETF	Effluent Treatment Facility
FY	fiscal year
HEPA	high-efficiency particulate air
Hg <sup>0</sup>	elemental mercury
HLW	high-level waste
HTA	heat-treated aerogel
HTX	heat-treated xerogel
I <sub>2(g)</sub>	iodine gas/vapors
IDF	Integrated Disposal Facility
LAW	low-activity waste
LDR	land disposal restriction
LERF	Liquid Effluent Retention Facility
MACT	Maximum Achievable Control Technology
MDS	mechanical data sheet
MOF	metal organic framework
ORNL	Oak Ridge National Laboratory
PAF	porous aromatic framework
PAN	polyacrylonitrile (polymer)
PNNL	Pacific Northwest National Laboratory



POP	porous organic polymer
POP-SH	thiol-functionalized porous organic polymer QA quality assurance
R&D	research and development
RCRA	Resource Conservation and Recovery Act
SBS	submerged bed scrubber
SCR	selective catalytic reducer
SEM	scanning electron microscopy
SFSA	Ag <sup>0</sup> -functionalized silica aerogel
Sn <sup>0</sup>	elemental tin
SOW	statement of work
SSA	specific surface area (m <sup>2</sup> /g)
TCO	thermal catalytic oxidizer
TEDA	triethylenediamine
TRL	technology readiness level
VSL	Vitreous State Laboratory
WESP	wet electrostatic precipitator
WRPS	Washington River Protection Solutions, LLC
WTP	Hanford Waste Treatment and Immobilization Plant
WWFTP	WRPS Waste Form Testing Program
XRD	X-ray diffraction

# Contents

Executive Summary .....	ii
Acknowledgments.....	v
Acronyms and Abbreviations .....	vi
Contents .....	viii
1.0 Introduction.....	1.1
1.1 Background.....	1.2
1.2 Scope and Objective .....	1.4
1.3 Report Content.....	1.4
2.0 Quality Assurance.....	2.1
3.0 Hanford Melter Off-Gas Abatement of Mercury and Iodine .....	3.1
3.1 WTP Design Basis Requirements/Needs for Mercury and Iodine Abatement .....	3.1
3.2 Carbon Adsorber Configuration and Design Basis Conditions .....	3.3
3.3 Existing Activated Carbon Media Specifications .....	3.7
3.4 Prior Work on Baseline Media .....	3.7
3.5 Existing Waste Form and Disposition Planning for Spent Media .....	3.9
4.0 State of Gas-Phase Mercury Sorbent Technology .....	4.1
4.1 Porous Inorganic Crystalline Matrices (e.g., Zeolites) .....	4.2
4.2 Inorganic Aerogels.....	4.3
4.3 Inorganic Sulfide Materials.....	4.4
4.4 Porous Organic Materials .....	4.7
4.4.1 Metal Organic Frameworks .....	4.7
4.4.2 Covalent Organic Frameworks .....	4.9
4.4.3 Porous Organic Polymers .....	4.10
4.5 Carbon-Based Sorbents.....	4.10
4.6 Metal Substrates and Other Materials.....	4.11
5.0 State of Gas-Phase Iodine Sorbent Technology.....	5.1
5.1 Porous Inorganic Crystalline Matrices (e.g., Zeolites) .....	5.2
5.2 Inorganic Aerogels.....	5.4
5.3 Inorganic Sulfide Materials.....	5.7
5.4 Inorganic Xerogels.....	5.8
5.5 Porous Organic Sorbents .....	5.9
5.5.1 Metal Organic Frameworks .....	5.9
5.5.2 Covalent Organic Frameworks .....	5.10
5.5.3 Porous Aromatic Frameworks .....	5.11
5.5.4 Porous Organic Polymers .....	5.12
5.6 Carbon-Based Sorbents.....	5.13
5.7 Metal Substrates (e.g., Metal Particles, Metal Wires) .....	5.14

6.0	Sorbent Screening and Evaluation .....	6.1
6.1	Criteria for Material Evaluation.....	6.1
6.2	Sorbent Screening, Evaluation, and Ranking Analysis.....	6.3
6.2.1	Commercially Available.....	6.4
6.2.2	Developmental.....	6.5
7.0	Testing and Material Development Priorities .....	7.1
7.1	Testing Priorities.....	7.1
7.1.1	Near Term: Activated Carbons in Combination.....	7.1
7.1.2	Long Term: Inorganic Aerogels for Hg and I Capture .....	7.2
7.1.3	Long Term: Engineered Membranes (Carbon Foam) .....	7.2
7.1.4	Long Term: Development of Other Stable Sorbent Materials.....	7.3
8.0	Material Deployment Roadmap .....	8.1
9.0	Conclusions.....	9.1
10.0	References.....	10.1
	Appendix A – Detailed Material Screening, Evaluation, and Ranking Tables.....	A.1

## Figures

Figure 3.1.	Simplified diagram of the WTP LAW melter off-gas system. ....	3.2
Figure 3.2.	General physical arrangement of the WTP LAW Carbon Adsorbers with two units in series (from Sweeney 2020). ....	3.5
Figure 3.3.	WTP LAW Carbon Adsorber beds – Top view (from Tuck 2016). ....	3.6
Figure 3.4.	WTP LAW Carbon Adsorber beds – End view (from Tuck 2016). ....	3.6
Figure 4.1.	Hg <sup>0</sup> removal efficiency of Ag-loaded zeolite 4A and raw zeolite 4A (Sun et al. 2018). ....	4.2
Figure 4.2.	Effect of gas composition on Hg <sup>0</sup> removal efficiency for Mn-modified layered MCM-22 zeolites under different atmospheric conditions (Ma et al. 2021). ....	4.3
Figure 4.3.	(a) Mercury removal efficiency of different sulfides and (b) the effect of temperature on CuS materials (Liu et al. 2019). ....	4.5
Figure 4.4.	Normalized Hg outlet concentration mercury removal efficiency for ZnS sorbents with different surface areas (Li et al. 2016). ....	4.5
Figure 4.5.	Comparison of mercury adsorption capacity on Nano-ZnS and commercial activated carbons (Li et al. 2016). ....	4.6
Figure 4.6.	Effect of (a) vulcanization temperature, (b) vulcanization time, and (c) adsorption temperature on the adsorption capacity of Hg <sup>0</sup> on H <sub>2</sub> S/Fe <sub>2</sub> O <sub>3</sub> (Wu et al. 2021). ....	4.6
Figure 4.7.	Mercury removal mechanism on H <sub>2</sub> S/Fe <sub>2</sub> O <sub>3</sub> material (Wu et al. 2021). ....	4.7
Figure 4.8.	Hg <sup>0</sup> removal efficiency of MIL-101-Cr. SFG denotes simulated flue gas (Dong et al. 2019). ....	4.8

Figure 4.9.	Hg <sup>0</sup> concentration changes for (a) different MOFs at 300 °C and (b) UiO-66-Br at different temperatures; Hg <sup>0</sup> loading capacities of (c) four types of UiO-66 MOFs and (d) UiO-66-Br at different temperatures (Zhao et al. 2021).....	4.9
Figure 4.10.	Effect of flue gas composition on the Hg <sup>0</sup> removal efficiency for S/FeS <sub>2</sub> material (H Li et al. 2018).....	4.12
Figure 5.1.	SiO <sub>2</sub> -Al <sub>2</sub> O <sub>3</sub> -(alkali or alkaline earth) ternary diagram for zeolite minerals that shows the acid stability (Jubin 1988) (modified from ORNL drawing 78-15097).....	5.2
Figure 5.2.	General summary of zeolite structures, including BEA, FAU (faujasite), MFI, MOR (mordenite), and TON, including the crystal structures on top and the building blocks below (modified from Baerlocher et al. 2007). ....	5.3
Figure 5.3.	Pathway for producing SFSA iodine sorbents and subsequent waste forms (after iodine loading) showing the various synthesis stages, including the host material, the Ag-functionalization process, the iodine capture process, and the final waste form. ....	5.5
Figure 5.4.	(left) Chemical uptake (measured with energy dispersive X-ray spectroscopy) vs. gravimetric uptake (measured by mass change during uptake experiment) of various aluminosilicate aerogels and xerogels loaded with different metal getters (Riley et al. 2020). (right) Summary of iodine loadings in terms of iodine loadings (g/g) as well as mass% iodine in the final materials, including thiolated Ag <sup>0</sup> AlSiO <sub>4</sub> aerogels (SH-Ag <sup>0</sup> ), Ag <sup>0</sup> AlSiO <sub>4</sub> aerogels (Ag <sup>0</sup> ), thiolated Ag <sup>+</sup> AlSiO <sub>4</sub> aerogels (SH-Ag <sup>+</sup> ), Ag <sup>+</sup> AlSiO <sub>4</sub> aerogels (Ag <sup>+</sup> ), thiolated NaAlSiO <sub>4</sub> aerogels (before Ag exchange), and silver mordenite (AgZ) for comparison (Riley et al. 2017). ....	5.6
Figure 5.5.	(a) Picture of Pt <sub>2</sub> Ge <sub>5</sub> S <sub>10</sub> chalcogels (Riley et al. 2011). (b) Summary of iodine capture with chalcogels in a 4.2-ppm iodine stream over different times, including Pt <sub>2</sub> Ge <sub>5</sub> S <sub>10</sub> , Co <sub>0.5</sub> Ni <sub>0.5</sub> MoS <sub>4</sub> , and Sn <sub>2</sub> S <sub>3</sub> aerogels (Riley et al. 2013). (c) Scanning electron and transmission electron micrographs of different chalcogels (Riley et al. 2013). ....	5.7
Figure 5.6.	(a) Summary of PAN-Bi <sub>2</sub> S <sub>3</sub> composite synthesis process (Yu et al. 2020). SnS <sub>2</sub> study for iodine capture including pure SnS <sub>2</sub> powder (b) before and (d) after iodine loading as well as SnS <sub>2</sub> -PAN composites (c) before and (e) after iodine loading (Yu et al. 2021). ....	5.8
Figure 5.7.	(left) Hardness comparison between heat-treated NaAlSiO <sub>4</sub> aerogels (Na-HTA), as-made NaAlSiO <sub>4</sub> xerogels (Na-X), and heat-treated NaAlSiO <sub>4</sub> xerogels (Na-HTX) prior to Ag-loading (i.e., AgAlSiO <sub>4</sub> shown in the top right as Ag-HTX) and iodine loading (AgAlSiO <sub>4</sub> +I shown in the bottom right as AgI-HTX-150) (Chong et al. 2021). ....	5.9
Figure 5.8.	(a) Picture of activated HKUST-1@PES composite sorbent beads, (b) pictures of these beads at different sizes, (c) picture of the surface of a bead, and (d) a scanning electron microscopy (SEM) micrograph of the cross-sectional view of the outside of a bead. (Taken from Valizadeh et al. 2018). ....	5.10
Figure 5.9.	(a) Summary of iodine uptake of the TPB-DMTP (red) and TTA-TTB (black) COFs during iodine exposure time at ~77 °C (350 K). (b) Iodine retention after exposure to 25 °C in air. (c) Iodine capacities of different porous organic sorbents, including various COFs and MOFs. (Taken from Wang et al. 2018.).....	5.11
Figure 5.10.	Summary of I <sub>2(g)</sub> mass loadings for COFs (a) TJNU-203 and (b) TJNU-204 over time at 77 °C in air (Zhang et al. 2021). ....	5.11
Figure 5.11.	Summary of iodine loading kinetics for PAFs P-DPDA, P-TPB, and P-PC in saturated conditions at 75 °C (Wang et al. 2021). ....	5.12

Figure 5.12. SEM images of (a,c) POP-1 and (b,d) POP-2 and (e) iodine loading over time (Qian et al. 2017). .....	5.12
Figure 5.13. (a) Summary of the production process for making Bi-functionalized carbon foams along with (b) schematics showing the structure of the carbon foam followed by bismuth functionalization of the carbon foam without and with iodine loading (from Baskaran et al. 2022). .....	5.14
Figure 5.14. (a) A summary of the iodine capture performance of pure metal wires in saturated iodine environments and (b) a magnified version of the lower left corner in (a) (Riley et al. 2021). .....	5.15
Figure 5.15. Process for making metal-PAN composites, including (a) dissolving PAN in dimethyl sulfoxide (DMSO), (b) suspending metal particles in the PAN+DMSO mixture, (c) dropping the PAN+DMSO+metal mixture into water to create spheres, and (d) drying the spheres into the final product (Chong et al. 2022). .....	5.16
Figure 5.16. (a) Process by which metal-functionalized Ni foams are produced. (b) SEM and energy-dispersive X-ray spectroscopy (EDS) results of Bi-Ni foam before iodine loading and Bi-Ni foam loaded with iodine. (c) SEM and EDS results of Ag-Ni foam before iodine loading and Ag-Ni foam loaded with iodine. This data is from Tian et al. (2021).....	5.17
Figure 8.1. Deployment roadmap for maturation candidate materials for sustained Hg and I capture in WTP operations. ....	8.2

## Tables

Table 3.1.	WTP LAW Facility melter off-gas design basis conditions. ....	3.4
Table 3.2.	Mercury concentration and decontamination factor (DF) design basis in WTP LAW Facility melter off-gas.....	3.5
Table 3.3.	Kombisorb BAT-37 material properties. ....	3.7
Table 4.1.	Overview of mercury capture material types and commercial availabilities.....	4.1
Table 4.2.	Summary of properties and Hg <sup>2+</sup> removal of ZTS chalcogel (Oh et al. 2011). ....	4.4
Table 4.3.	Summary of low-temperature Hg vapor capture materials (Johnson et al. 2008). ....	4.11
Table 5.1.	Overview of iodine capture material types and commercial availabilities. ....	5.1
Table 6.1.	Summary of the material evaluations for commercially available materials.....	6.7
Table 6.2.	Summary of the material evaluations for developmental materials.....	6.8

## 1.0 Introduction

Across the world, there are many different facilities requiring efficient treatment systems to abate chemical and radionuclide emissions from their associated off-gas stacks to meet regulatory requirements imposed for the protection of the environment and people. These facilities include radioactive waste incinerators, used nuclear fuel reprocessing, nuclear waste processing, and energy-producing nuclear reactors. A common technology employed in these facilities and others is packed-bed adsorber units designed to remove specific constituents such as mercury (Hg), iodine-129 ( $^{129}\text{I}$ ), and/or volatile organic compounds. At the Hanford Site, near Richland Washington, carbon bed adsorber units are specifically used to remove Hg from process emissions to meet incinerator standards. The efficiency of this abatement relies on the material selected and its associated characteristics, such as Hg capacity, thermal and chemical stability under service conditions, and robust physical form. However, other factors, such as material cost, safety risks, and disposition waste form, also play an important role in selecting the best material for each application. This roadmap report intends to guide material selection and required testing to facilitate time-sensitive decisions and subsequent vendor actions for the Hanford Waste Treatment and Immobilization Plant (WTP) application, but has applicability and potential use for both other U.S. Department of Energy (DOE) Office of Environmental Management (EM) facilities and, more generally, nuclear processing off-gas emission treatment systems.

Operational and flowsheet mission risks continue to persist for the primary and secondary off-gas systems at the WTP Low-Activity Waste (LAW) Facility. These risks are due to low retention values of iodine-129 ( $^{129}\text{I}$ ) and mercury (Hg) in the melter pool, uncertainty in partitioning of both species in the off-gas system, and poor  $^{129}\text{I}$  retention in the sulfur-impregnated activated carbon (AC-S) bed (currently designed to use AC-S Kombisorb BAT-37, Donau Carbon, USA) (Fountain et al. 2019). It is assumed that at least 99 mass% of the gas-phase Hg is retained by the Carbon Adsorber units, and these must be functional for the WTP LAW Facility to be compliant with the associated WTP Dangerous Waste Permit (WA7890008967), the WTP LAW Facility air emissions operating license application (Haggard 2019), and supporting emissions estimates documented by Brar (2019).

The sorbent material, when loaded in Carbon Adsorber units in the WTP LAW Facility secondary off-gas system, provides the sole Hg abatement function to achieve regulatory compliance during waste processing operations. It was recently declared that the Kombisorb BAT-37 material is no longer commercially available from the sole-source manufacturer (Donau Carbon, USA), the current inventory is being fully utilized with no spare material, and Carbon Adsorber beds are designed to have a minimum service life of 2 years (Wong 2017). The replacement for the Kombisorb BAT-37 is Kombisorb BAT-37 II (Donau Carbon, USA), which has a lower sulfur impregnation level (2 wt% compared with 9 wt% for BAT-37), allowing safer production. Lower sulfur impregnation levels have been correlated to lower sorption capacity for Hg. The performance of BAT-37 II is assumed to be identical to that of BAT-37, but no data supports this assumption in WTP conditions to date. The BAT-37 (or BAT-37 II) material is also not optimized for performance in the WTP LAW Facility off-gas conditions and more suitable material alternatives may exist.

Hence, replacement of Kombisorb BAT-37/BAT-37 II with a robust, efficient, and commercially available or high technology readiness level (TRL) material to resolve future Hg abatement risks could improve off-gas system performance at WTP. However, there are related operational risks pertaining to the abatement of  $^{129}\text{I}$  in the LAW melter off-gas that warrant simultaneous consideration.

Similar to Hg, regulatory limits on air and liquid discharges require abatement of  $^{129}\text{I}$ . The WTP LAW Facility design to remove  $^{129}\text{I}$  was, until recently, primarily credited to the Carbon Adsorber units. However, a recent Vitreous State Laboratory (VSL) report (Matlack et al. 2020) concluded that as much as 75 mass% of feed iodine bypassed the Carbon Adsorber bed in demonstration testing using the DM10 melter with the

baseline Kombisorb BAT-37 as the bed material. Instead, the iodine was shown to partition to the caustic scrubber solution. The most significant impact of this poor retention and observed partitioning is that much of the I that is volatilized in the WTP LAW melter would bypass both the Effluent Management Facility (EMF) and the recycle to the WTP LAW melter, ending up in secondary liquid effluent to be processed at the Liquid Effluent Retention Facility (LERF) and the Effluent Treatment Facility (ETF). Other consequences include greater release of  $^{129}\text{I}$  to the WTP LAW stack, required modification of the ETF hazard categorization, new radiological monitoring and controls in the liquid process and ventilation systems at ETF, and possible impacts to the Hanford Integrated Disposal Facility (IDF) performance assessment. These challenges can be averted if viable abatement material(s) to efficiently adsorb I and Hg can be identified and deployed in the Carbon Adsorber units at WTP.

Pacific Northwest National Laboratory (PNNL) has proposed to replace Kombisorb BAT-37 with a dual-function material for capture of Hg and I, or a combination of Hg- and I-specific materials, to improve overall performance of the Carbon Adsorber units and prevent bypassing of these contaminants to the WTP LAW Facility off-gas stack, the LERF, and/or ETF. This report screens and then evaluates potential candidate materials (both commercially available for near-term application and developmental materials for potential long-term integration) with the intent to rank and recommend materials for subsequent lab-scale testing and eventual larger-scale testing for demonstration and implementation into WTP LAW Facility operations. This effort was prompted by the need to replace the Kombisorb BAT-37 due to uncertainties in performance (or failure) and future availability. However, replacement of this material could also mitigate two other issues with Kombisorb BAT-37: (1) fire safety risk due to exothermic heat generated by adsorption reactions between the carbon material and Hg and (2) the risk of low retention of I in glass and the downstream impacts on ETF.

## 1.1 Background

The WTP LAW Facility secondary off-gas system, as designed, incorporates two activated Carbon Absorber units (LVP-ADBR-00001A/B), typically operated in series, to abate Hg, acid gas, and halides [e.g., chlorine ( $\text{Cl}^-$ ), fluorine ( $\text{F}^-$ ),  $\text{I}^-$ ] from the melter off-gas stream. Each unit includes a primary bed and a guard bed. A downstream guard bed filled with Sofnolime RG (manufactured by Molecular Products) was designed into the secondary off-gas system to abate acid gases and halides (including all forms of I, but specifically targeting  $^{129}\text{I}$ ). However, due to significant material degradation in high- $\text{NO}_x$  conditions ( $\sim 10,000$  ppm), the guard bed material was removed from the WTP LAW Facility design, and a shift was made to credit the overall off-gas system for I, HCl, and HF removal efficiencies (Stiver 2019). The guard bed unit is still physically retained in the secondary off-gas system and will now be filled with Kombisorb BAT-37 instead (Sweeney 2020). The primary and guard beds, in series, abate mercury through adsorption on the Kombisorb BAT-37 material. The removal of acid gases, Hg, and halides (e.g.,  $\text{Cl}^-$ ,  $\text{F}^-$ ,  $\text{I}^-$ ) is essential to protecting the downstream thermal catalytic oxidizer (TCO) and selective catalytic reducer (SCR) catalyst beds from poisoning/damage and for meeting off-gas treatment targets (for Hg and  $^{129}\text{I}$  specifically) documented by Brar (2019) for regulatory permitting.

The current Carbon Adsorber units employ a sulfur-impregnated carbon (Kombisorb BAT-37) that is credited for Hg,  $^{129}\text{I}$ , and acid gas removal and a minimum change-out frequency of every 2 years (Sweeney 2020). The disposition of the contaminant-loaded bed material is planned via grout stabilization (microencapsulation) and final land disposal restriction (LDR) disposition in the IDF (Prindville 2016). Recent experimental results presented by Bechtel National, Inc. (BNI) report that the  $^{129}\text{I}$  removal efficiency (tested with a potassium iodide surrogate) in the WTP LAW Facility off-gas Carbon Adsorber beds decreased from 99.8% after 6.1 h down to 74.4% after 32.6 h.<sup>1</sup> These demonstration results were unexpected

<sup>1</sup> PowerPoint presentation by Robert Hanson and Brad Stiver, titled “LAW Offgas System Iodine 129 Removal,” presented in December of 2018 on behalf of Bechtel National, Inc.



and cast doubt on the ability of the Carbon Adsorber units to abate  $^{129}\text{I}$  prior to release from the WTP LAW Facility off-gas stack and the receipt and treatment of secondary liquid effluents at ETF. Note that testing at VSL has shown a possible synergistic effect of continued Hg uptake by activated carbon (AC), leading to improved iodine retention (Abramowitz 2019a).

Further complicating the issue is more recent work by Matlack et al. (2020) claiming a significant risk of I partitioning to the liquid phase in the caustic scrubber solution if sufficient I capture does not occur in the submerged bed scrubber (SBS), wet electrostatic precipitator (WESP), and/or Carbon Adsorber units. These tests at the VSL reported 59% to 75% of the I was found to partition to the gas phase. Inductively coupled plasma mass spectrometry measurements of the sodium hydroxide (NaOH) impinger solutions using the three different feed I species showed this behavior. Also note that while carbon-based sorbents are widely used for iodine capture at nuclear power plants using KI-impregnated or triethylenediamine (TEDA)-impregnated ACs (Kulyukhin 2012), they are not considered for I removal during reprocessing of spent nuclear fuel because of poor I retention at high temperatures, a relatively low ignition point, and the potential to form unstable or explosive compounds in the carbon bed in the presence of nitrogen oxides ( $\text{NO}_x$ ).

Currently, proposed approaches to I mitigation are being developed. One approach includes recycling the caustic scrubber stream to the EMF evaporator feed tank to recycle the I back into the melter (for glass retention). The effectiveness of this approach relies on the dominant partitioning of I into the concentrate fraction (i.e., bottoms liquor) during evaporation, which has been experimentally supported (Matlack et al. 2019). However, this approach approximately doubles the volume of secondary liquid to be evaporated by EMF and increases Na mass, carbonate, Tc-99, and corrosive halides (e.g.,  $\text{F}^-$  and  $\text{Cl}^-$ ) recycled into the melter feed. This approach was assessed by Tardiff et al. (2022) and was shown to offer a reduced  $^{129}\text{I}$  concentration to ETF, but still did not fully address the potential for  $^{129}\text{I}$  concentrations in the liquid effluent to exceed the ETF waste acceptance criterion of 357 pCi/L (Tardiff 2022). An evaluation of glass and operational impacts from the caustic scrubber recycle approach was provided in Fountain (2022) and was found to have no significant glass impacts except for much greater I retention in the glass due to recycle. However, results suggest this approach will reduce overall throughput (due to reduced treated LAW feed volume and EMF treatment capacity issues because of the increased evaporation volume) and likely will have negative impacts of secondary solid waste disposition due to higher Tc-99 and  $^{129}\text{I}$  feed concentrations to the melter, then pushing more mass to the secondary wastes.

A second approach being matured is abatement of  $^{129}\text{I}$  in the secondary liquid effluent stream to LERF and ETF through ion exchange in the liquid phase. This approach is technically viable, ion exchange media candidates have been screened, and recommendations have been provided for this application (Asmussen et al. 2021a). However, significant throughput capacity is required for the large volumes of liquid effluents anticipated, approximately 84 kgal every 2-5 days. This potential approach adds considerable capital and operational costs for the DOE-EM not previously in the baseline.

Another viable mitigation approach to the risks associated with Hg and I focuses specifically on abating these constituents as originally intended by the WTP LAW Facility secondary off-gas system design. The most simplistic approach is replacing the Carbon Adsorber unit materials inserted in the guard bed and primary bed to effectively and efficiently abate releases of off-gas species from the stack and avoid other negative downstream consequences. The PNNL-proposed work seeks to provide a full evaluation of candidate materials that could be used in the off-gas for both Hg and I capture in place of the Kombisorb BAT-37/BAT-37 II. The materials presented may be individual or dual-capture, or a combination, to remove both Hg and I.

The overall solution approach, to mitigate the I and Hg risks, is based on simple replacement of the WTP LAW secondary off-gas Carbon Adsorber material to avoid any equipment design changes or new unit

operations. Significant cost and schedule consequences are likely if risk mitigation actions are not implemented in the next couple years. Given the significant risk that I and Hg present to the flowsheet, the proposed work seeks to mitigate the persistent risks by replacing the Carbon Adsorber unit material with a highly efficient alternative individual or dual-capture material for capture and abatement of  $^{129}\text{I}$  and Hg, ensuring long-term success of processing LAW through the WTP LAW Facility.

## 1.2 Scope and Objective

This report is intended to serve as the first step in a deployment roadmap that will guide material selection and required testing to facilitate time-sensitive decisions and subsequent vendor actions. This report identifies, screens, and then evaluates potential candidate materials for individual or dual-capture capability to abate  $^{129}\text{I}$  and Hg. The material candidates will be ranked and prioritized for subsequent bench-scale testing by PNNL in pursuit of maturation testing of the materials toward deployment in the WTP LAW Facility Carbon Adsorber units (to be reported separately). The material candidates identified in this report will be further down-selected based on the results of the bench-scale testing, and the best material(s) will be proposed for demonstration in larger-scale testing before full-scale implementation in WTP LAW Facility operations.

Evaluated materials are first binned as commercially available (near-term replacements) or developmental (long-term replacements) and then evaluated based on the following criteria (listed in order of importance for this assessment):

- Material cost
- Safety risks
- Hg/I loading capacity
- Test conditions relative to the WTP LAW Facility
- Thermal and chemical stability in service
- Mechanical stability and physical form
- Waste form demonstration

The evaluation criteria establish a basis for future material down-selection, or if needed, identify technical gaps to be filled at the bench/laboratory or engineering scale. A deployment roadmap is provided to illustrate the action path to mature, demonstrate, and implement a new sorbent material in the WTP LAW Facility with the intent to inform DOE and other DOE contractors on anticipated total budget and schedule impacts, as well as risk, for replacing this sorbent material.

## 1.3 Report Content

The logical approach to developing a roadmap for the identification of viable candidate materials starts with a thorough discussion of the WTP LAW Facility design basis and needs for Hg and I abatement, Carbon Adsorber configuration and basis conditions, properties of the Kombisorb BAT-37 materials, and prior testing conducted, which is primarily captured in Section 3.0. Potential candidate materials for gas-phase capture of Hg are discussed in Section 4.0 and those for I are in Section 5.0, while their potential to capture both is discussed in Section 6.0. Section 6.0 includes definition of screening and evaluation criteria used (Section 6.1), followed by the screening, evaluation rating, and ranking analysis (Section 6.2). The primary objective of the report is met with final the down-selection and laboratory-scale testing priorities in Section 7.0. Lastly, a material maturation and deployment roadmap is conceptualized and discussed in Section 8.0

to identify key future actions to demonstrate performance and implement the new Hg and/or I sorbent material in the WTP LAW Facility or similar facilities, as applicable.

## 2.0 Quality Assurance

This work was conducted under PNNL project 80673, “Abatement of Hg and I-129 in WTP LAW Off-gas Streams,” with funding from the DOE-EM Office of Technology Development (EM-3.2).

All research and development (R&D) work at PNNL is performed in accordance with PNNL’s Laboratory-level Quality Management Program, which provides overall guidance to staff based on a graded application of NQA-1-2000, *Quality Assurance Requirements for Nuclear Facility Applications*, to R&D activities. The quality assurance (QA) controls of the WRPS Waste Form Testing Program (WWFTP) QA program, which implements requirements of NQA-1-2008, *Quality Assurance Requirements for Nuclear Facility Applications*, and NQA-1a-2009, *Addenda to ASME NQA-1-2008 Quality Assurance Requirements for Nuclear Facility Applications*, graded on the approach presented in NQA-1-2008, Part IV, Subpart 4.2, “Guidance on Graded Application of Quality Assurance (QA) for Nuclear-Related Research and Development,” were also applied to this work. The WWFTP QA program includes procedures that provide detailed instructions for performing and documenting research activities and categorizes R&D work into three technology levels based on the amount of QA rigor required: Basic Research, Applied Research, and Development Work (in order of increasing rigor).

The work described in this report was assigned the technology level “Basic Research” and was conducted in accordance with procedure QA-NSLW-1101, *Scientific Investigation for Basic Research*. All staff members contributing to the work received proper technical and QA training prior to performing quality-affecting work, and the report was independently reviewed by technical, QA, and project management staff before being issued.

### 3.0 Hanford Melter Off-Gas Abatement of Mercury and Iodine

The development of this roadmap for identifying, testing, and implementing a replacement material(s) to abate Hg and I was primarily prompted by a realized risk that existing inventories of Kombisorb BAT-37 AC materials are being fully utilized, and no spare (or replacement) material has been identified. A replacement, Kombisorb BAT-37 II, appears to be a likely candidate for use and is presumed to have identical performance, but a thorough material down-selection process has not been reported.

In the current WTP design, the abatement of Hg, potentially released to the environment, is mitigated solely by the adsorption on the Kombisorb BAT-37 AC material in the WTP LAW Facility secondary off-gas system, specifically by the Carbon Adsorber units. Additional unrealized risks persist related to I abatement (e.g., variability and uncertainty in partitioning, speciation, poisoning of TCO/SCR catalysts) and the observed failure of the Kombisorb BAT-37 to provide continued, meaningful adsorption of I. The overall objective of this work is to identify a material or materials capable of abating Hg and I using existing facility equipment while achieving regulatory performance needs.

The discussion that follows is intended to establish reference details related to design and abatement needs of the WTP LAW and High-Level Waste (HLW) facilities, specifically for Hg and I, Carbon Adsorber infrastructure and configuration, existing Carbon Adsorber media specifications, prior work on baseline Carbon Adsorber media, and waste form planning assumptions. These discussions provide foundational/baseline conditions to enable comparisons and largely justify subsequent assumptions, limitations, and derived evaluation criteria used in selecting potential candidate materials. Finally, note that, although the focus of the discussion lies primarily with implementation in the WTP LAW Facility, the candidate Hg and I materials (Section 4.0 and Section 5.0, respectively) and evaluation criteria (Section 6.0) are relevant to potential replacement of the Hg and I sorbent media used in the WTP HLW Facility, at other DOE waste treatment sites (e.g., Savannah River Site), and within the nuclear energy industry (i.e., primarily iodine).

#### 3.1 WTP Design Basis Requirements/Needs for Mercury and Iodine Abatement

Deng et al. (2016) provide a detailed compilation of flowsheet bases, assumptions, and requirements that serves as a definitive reference basis to understand the purpose of unit operations in the WTP LAW, HLW, and Pretreatment (PT) facilities. To significantly simplify the discussion, focused attention will be given to describing the WTP LAW Facility off-gas system as it relates specifically to abating Hg and <sup>129</sup>I<sup>2</sup>. This discussion is instructive as a baseline/foundation to the conditions and infrastructure available when implementing a replacement material(s) to abate Hg and I in the gas-phase downstream of the melter.

As stated verbatim in Deng et al. (2016):

*“[E]ach LAW melter system has its own primary offgas equipment, including a film cooler, submerged bed scrubber (SBS), and wet electrostatic precipitator (WESP). Particulates and condensables, including entrained or volatilized radionuclides in the melter offgas stream, are captured in the SBS and WESP. Condensables from the SBS and the WESP are collected in the*

<sup>2</sup> The radionuclide <sup>129</sup>I is the constituent that must be managed for regulatory compliance; however, other isotopes of iodine (primarily <sup>127</sup>I) also exist in tank waste. The ratio of <sup>127</sup>I to <sup>129</sup>I is typically 3:1 (Fountain 2020). The I-capture material doesn't have selectivity toward <sup>129</sup>I, so the I-loading capacity needs must account for total I present when designing an I-abatement unit operation.

liquid effluent system and recycled to the treated LAW evaporator in the PT Facility in the baseline WTP configuration. Primary offgas effluents are transferred to the Effluent Management Facility (EMF) in the Direct Feed LAW configuration. The primary offgas systems join after the WESP, and are routed to the secondary offgas system. At this point, the LAW vessel vent header joins the offgas. The secondary offgas system provides final filtration, removes halides and mercury, destroys organics, and reduces NO<sub>x</sub>. This is done by using high-efficiency particulate air (HEPA) filters, activated carbon columns, a thermal catalytic oxidizer, a selective catalytic reducer, and a caustic scrubber.”

Figure 3.1 presents a basic flow diagram of this described configuration to illustrate the unit operations and material flows. The Carbon Adsorbers (also called mercury adsorbers) are located just downstream of the HEPA filters, were originally designed to remove halides and Hg, and are composed of a primary bed and a guard bed in each unit operating in series. The two Carbon Adsorber units are typically operated in a lead/lag series arrangement but can be run in parallel to enable maintenance and bed material replacement without shutdown of the off-gas system. The downstream TCO functions to destroy organics and the subsequent SCR destroys NO<sub>x</sub>. Finally, the caustic scrubber provides final removal of residual gas-phase containments prior to releases to the WTP LAW Facility ventilation stack.

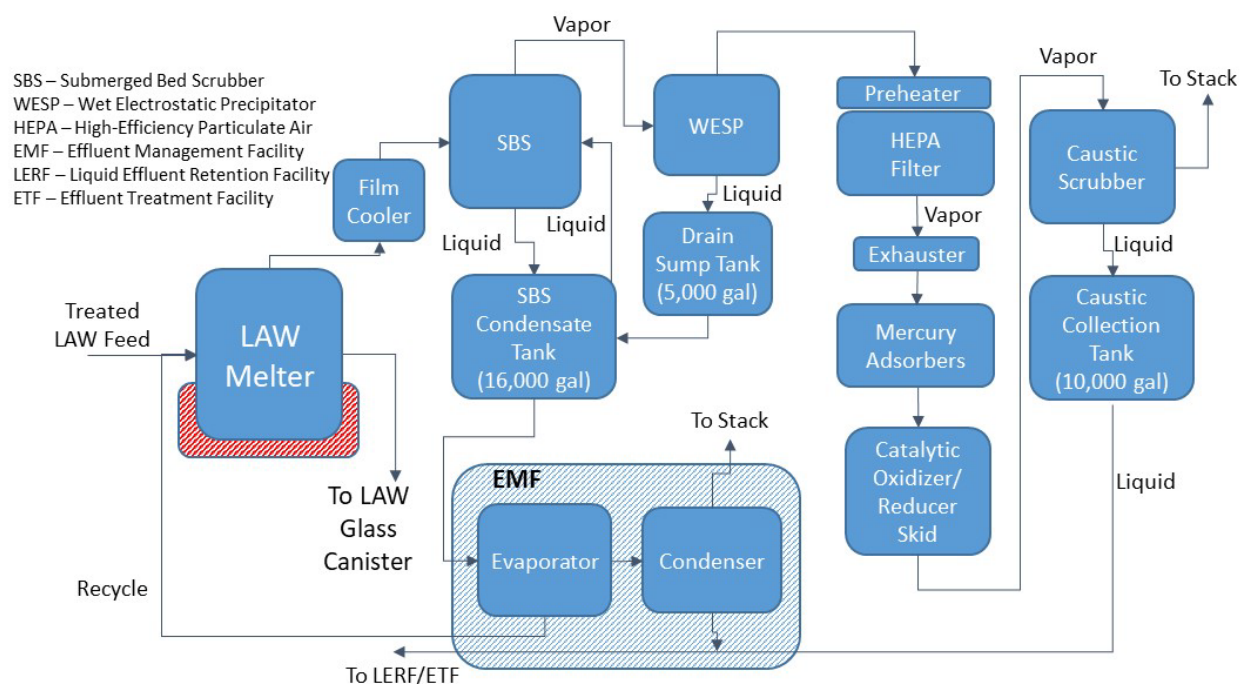


Figure 3.1. Simplified diagram of the WTP LAW melter off-gas system.

The WTP melter off-gas system was designed specifically to maintain compliance with Maximum Achievable Control Technology (MACT) incinerator standards for control by applying destruction and removal efficiency (DRE) limits for Hg and organics. The control of Hg emissions to incinerator standards using sulfur-impregnated AC materials in a radioactive waste treatment system has been selected previously as the best option in one study (WERF MACT Study Team 1998) and as only one of several viable technologies in another (Barnes et al. 1999).

Scaled tests to demonstrate that DREs could be achieved, under prototypic LAW and HLW conditions, were conducted at VSL to satisfy third-party permit testing for organics (Matlack and Pegg 2003) and later

for mercury (Abramowitz et al. 2019a,b). Removal efficiencies cited in Rickettson (2011) are summarized as follows:

For LAW Facility

- Mercury decontamination factor  $\geq 450$
- HCl removal efficiency  $> 97\%$
- Iodine (specifically  $^{129}\text{I}$ ) removal efficiency  $> 99\%$

For HLW Facility

- Mercury decontamination factor  $\geq 1,000$
- HCl removal efficiency  $\geq 90\%$
- Iodine (specifically  $^{129}\text{I}$ ) removal efficiency  $\geq 90\%$
- $\text{SO}_2$  removal efficiency  $\geq 90\%$

## 3.2 Carbon Adsorber Configuration and Design Basis Conditions

The design and configuration of the Carbon Adsorbers is based on a set of specified requirements and expected conditions. The specification of requirements for the design, analysis, fabrication, quality, inspection, testing, and qualification of the Carbon Adsorbers is thoroughly documented in Rickettson (2011). Expected normal and bounding operating conditions are conveyed through mechanical data sheets (MDSs). Key and pertinent details from Rickettson (2011) are summarized below (with the corresponding sections from Rickettson 2011 given in parentheses) to establish expected design-basis requirements for the Carbon Adsorbers relative to the treatment of the off-gas stream:

- Can be operated in series or parallel with isolation of one unit for maintenance during operation (Section 3.2.1.1).
- HLW Carbon Adsorbers shall remove mercury, HCl, HF,  $\text{SO}_2$ , and iodine (Section 3.2.2.1).
- LAW Carbon Adsorbers shall remove mercury, HCl, HF, and iodine (Section 3.2.3.1).
- 24 h a day, 365 days a year operation to establish minimum adsorbent life (Section 3.4.1.2).
- Pneumatically loaded media (Section 3.7.2).
- Spent media unloaded into 55-gallon drums via gravity (Section 3.7.3.1).
- Each Carbon Adsorber unit has a discharge filter rated for 99% efficiency at 5 microns and has a minimum capacity of two times the design flowrate (Section 3.8.1).
- The removal efficiency of the LAW Carbon Adsorber media is for HCl, HF, and  $^{129}\text{I}$ . The HLW Carbon Adsorbers shall also include  $\text{SO}_2$ . Media design life shall also include other acid gases (i.e.,  $\text{SO}_2$ ,  $\text{HNO}_2$ , and  $\text{HNO}_3$ ) (paraphrased from Section 4.1.4).

Multiple changes to the Rickettson (2011) specification have been documented since 2011, with a substantial change in the performance expectations for the Carbon Adsorber media presented by Stiver (2018). The specified capability of the Carbon Adsorbers to comply with MACT incinerator standards was reduced to only Hg abatement in LAW and Hg and  $\text{SO}_2$  abatement in HLW; this change relies on and credits the overall off-gas system for I, HCl, and HF removal efficiencies. This was a notable change for the iodine abatement strategy, which was originally achieved, by design, through the Carbon Adsorber

guard bed Sofnolime RG material (discussed in more detail in Section 3.4). However, the removal efficiencies summarized in Section 3.1 of this report are still valid and drive abatement needs.

The design of the Carbon Adsorber units and associated Hg system was and is based on operating conditions specified in the MDSs. The latest update to the Carbon Adsorber MDS is documented by Sweeney (2020), and Table 3.1 below summarizes the design-basis operating conditions. These conditions serve as reference here and will be used for evaluating candidate materials for selection and subsequent laboratory-scale test conditions used to demonstrate the viability of the candidate materials for application at Hanford. This gas composition is notable for its high NO<sub>x</sub> concentration along with high humidity and thus material degradation that can occur or consumption of sorption sites (Matlack et al. 2005). For gas phase interactions, the halides Cl and I can form mercurous halides, e.g., HgCl<sub>2</sub> and HgI<sub>2</sub>. Furthermore, SO<sub>2</sub> has been shown to inhibit Hg oxidizing reactions and could potentially damage downstream catalyst beds in the WTP off-gas system.

Table 3.1. WTP LAW Facility melter off-gas design basis conditions.

Parameter	Nominal	Maximum
Volumetric flow (m <sup>3</sup> /min) [acfm]	106.4 [3759]	127.1 [4490]
Temperature (°C) [°F]	71 [160]	77 [171]
Pressure (atm) [in. WG]	0.81 [-78]	0.77 [-94.0]
Density (kg/m <sup>3</sup> ) [lb/ft <sup>3</sup> ]	0.780 [0.0487]	0.718 [0.0448]
Relative humidity (%)	23.9 to 23.5	100
Allowable pressure drop (atm) [in. WG]	N/A	0.034 [14]
N <sub>2</sub> (% vol)	69.3	66.4
O <sub>2</sub> (% vol)	18.6	17.8
H <sub>2</sub> O (% vol)	9.7	13.2
CO <sub>2</sub> (% vol)	1.01	1.09
Ar (% vol)	0.83	0.79
NH <sub>3</sub> (kg/h)	2.69E-02	5.98E-02
NO (kg/h)	1.29E+01	1.83E+01
N <sub>2</sub> O (kg/h)	3.44E+00	5.83E+00
NO <sub>2</sub> (kg/h)	1.72E+01	2.27E+01
CO (kg/h)	9.25E-01	1.67E+00
H <sub>2</sub> (kg/h)	3.24E-02	4.52E-02
HCl	4.40E-02	2.37E-02
HF	2.39E-03	9.97E-02
I-129	1.29E-04	1.29E-04
SO <sub>2</sub>	2.78E-02	6.34E-02
HNO <sub>2</sub>	2.45E-01	5.22E-01
HNO <sub>2</sub>	6.17E-02	5.27E-01
VOC	4.88E-01	1.87E+00
Particulate	1.08E-05	3.07E-05
acfm = actual cubic feet per minute; in. WG = inches of water gauge; VOC = volatile organic content		



The design life of the primary beds, operating in series, is further defined to be a minimum of 2 years at nominal conditions presented in Table 3.1 (Sweeney 2020). The Hg concentration and target Hg decontamination factor (DF) are specified by Sweeney (2020) and are captured in Table 3.2.

Table 3.2. Mercury concentration and decontamination factor (DF) design basis in WTP LAW Facility melter off-gas.

Parameter	Nominal		Maximum	
	µg/dscm	kg/hr	µg/dscm	kg/hr
Hg mass flow	702	2.69E-03	1,647	6.73E-03
Required DF for Hg to comply with <45 µg/dscm	≥40			

µg/dscm = micrograms per dry standard cubic meter

Operating conditions, process design requirements, and configuration inputs for the LAW Carbon Adsorber units are further detailed by Wong (2017), who performed calculations to predict system pressure drop, expected media change-out frequency, and other parameters. Most relevant here is the calculated bed service life result of 3.9 years based on a 3153.7 kg mass of AC in each bed, when assuming a 2.9 mass% Hg loading (half of actual loading capacity) and the nominal Hg mass rate of  $2.69 \times 10^{-3}$  kg/h. With the primary bed and guard bed each containing a 3153.7 kg mass of carbon, a significant Carbon Adsorber bed service life of up to 7.8 years is predicted.

An inherent constraint of a replacement Hg and I sorbent material at Hanford is the need to use the existing infrastructure and the physical configuration of the WTP LAW and HLW Carbon Adsorbers. The configuration and basic operation of the WTP LAW Facility Carbon Adsorbers are provided for this background. The two Carbon Adsorbers are physically connected, as depicted in Figure 3.2, with the housing of each unit measuring approximately 20 ft long, 10 ft high, and 8 ft wide. The Carbon Adsorbers are typically operated in series, but can operate in parallel to allow for maintenance.

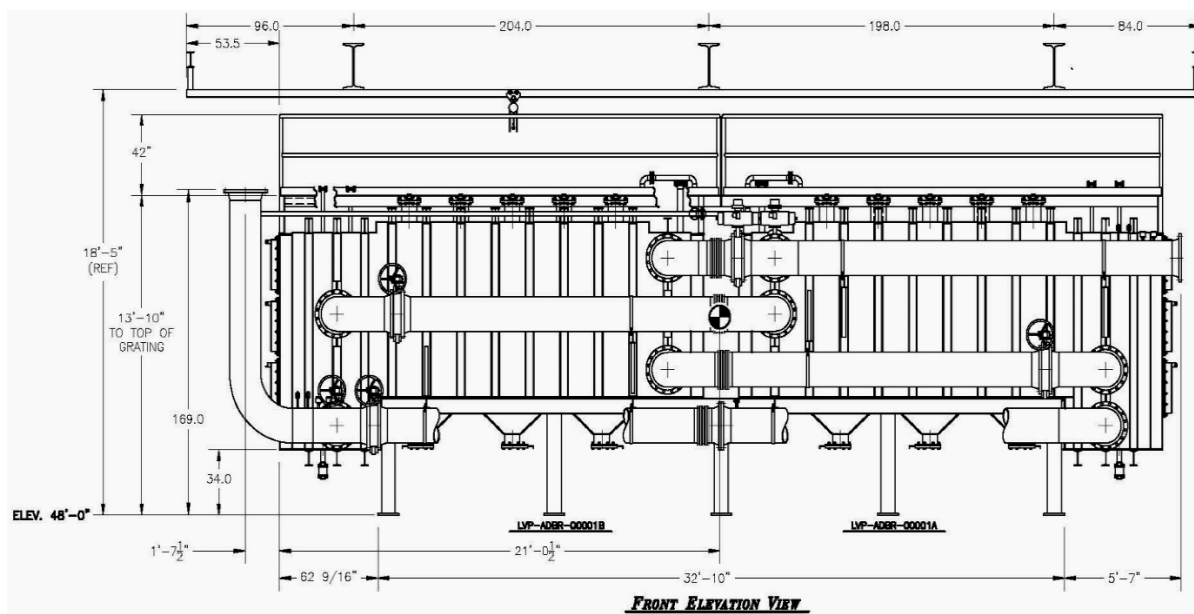


Figure 3.2. General physical arrangement of the WTP LAW Carbon Adsorbers with two units in series (from Sweeney 2020).

Figure 3.3 illustrates the top view of a single Carbon Adsorber and depicts the configuration of the three 30-inch-deep guard beds and three 30-inch-deep primary beds (labeled “carbon bed” in the figure). Melter off-gas enters through an inlet header on the left-side side of the unit (based on Figure 3.3), flows through the guard bed first and then the primary bed, then exits through particulate filters on the right side of the unit within the discharge header. Each guard bed and primary bed has a capacity of 265 ft<sup>3</sup> corresponding to rectangular bed dimensions of 30 inches deep, 154 inches wide, and 84 inches high (Sweeney 2020). Each Carbon Adsorber unit has six tapered 8-inch ports (three per guard bed and three per primary bed) on the bottom of each rectangular bed, as shown in Figure 3.3 and Figure 3.4, for gravity discharging spent media to 55-gallon drums.

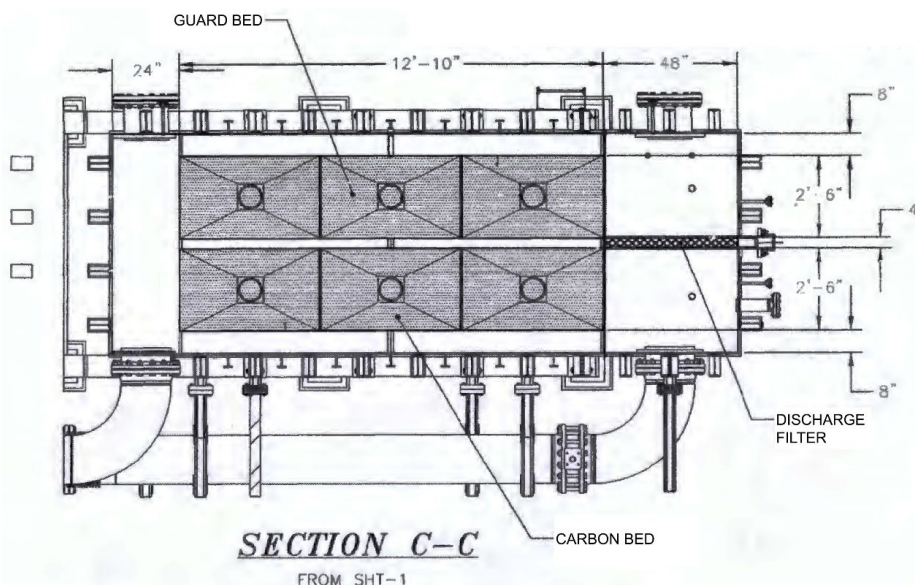


Figure 3.3. WTP LAW Carbon Adsorber beds – Top view (from Tuck 2016).

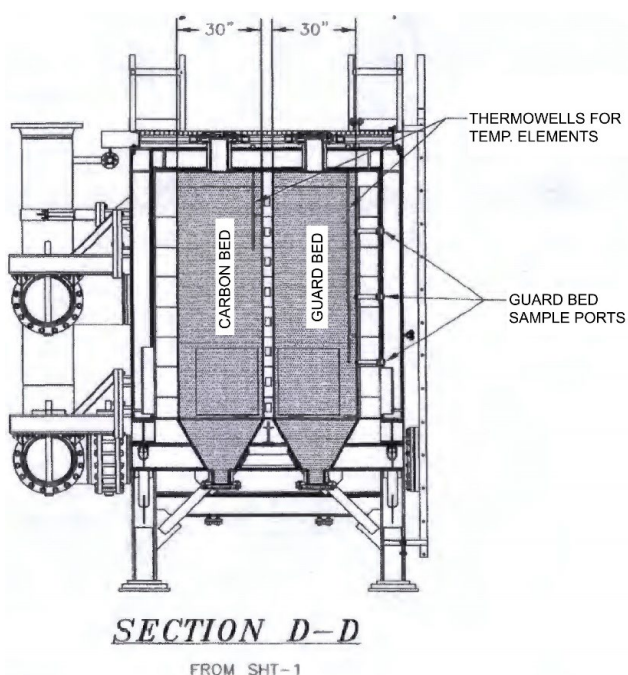


Figure 3.4. WTP LAW Carbon Adsorber beds – End view (from Tuck 2016).

### 3.3 Existing Activated Carbon Media Specifications

The Carbon Adsorber material currently specified for use in the WTP LAW Facility is Kombisorb BAT- 37 (trade name), manufactured by Donau Carbon (USA). The granular AC is a mixture of an inert zeolite filler and coal-based carbon with an approximate 9 mass% sulfur impregnation (Brown 2012). Key material properties and performance are summarized in Table 3.3 for reference to alternative materials being considered in this report.

Table 3.3. Kombisorb BAT-37 material properties.

Parameter	Value BAT-37	Value BAT-37 II
Physical form	Inert zeolite - Granular shaped (3-5 mm) AC - Cylinders (~4 mm diameter)	Inert zeolite - Granular shaped (5-8 mm) AC - Cylinders (~4 mm diameter)
Surface area	~ 800 m <sup>2</sup> /g	~ 800 m <sup>2</sup> /g
Bulk density	37.5 lb/ft <sup>3</sup> (600.7 kg/m <sup>3</sup> )	37.5 lb/ft <sup>3</sup> (600.7 kg/m <sup>3</sup> )
Carbon to inert ratio	7:3 (by volume)	7:3 (by volume)
Impregnation level	~9 wt%	~2 wt%
Particle size distribution	5% maximum retained on #4 sieve 90% minimum on #8 sieve 5% maximum through #8 sieve	Not reported
Ball-pan hardness	92 minimum	Not reported
Moisture content	<5% for inert fraction and <20% for activated carbon	<5% for inert fraction and <20% for activated carbon
Ash content	<10.1 mass%	Not reported
Average Hg loading <sup>(a)</sup>	5.8 mass%	Not reported

(a) Provided by Wong (2017).

### 3.4 Prior Work on Baseline Media

In 2005, VSL was commissioned to operate the DM1200 melter system with a prototypic carbon absorber bed as well as other off-gas unit operations (e.g., SBS, WESP, HEPA, TCO, SCR, and caustic scrubber) to demonstrate sampling and analysis and to characterize melter and stack emissions (i.e., organic, particulate, aerosol, and gaseous) under steady state and worst-case operations using HLW and LAW simulants, derived from and represented by Hanford tanks C-106/AY-102 and AP-101, respectively (Matlack et al. 2005). This early testing of AC-S media indicated acceptable performance, but tests were stopped early due to concerns about excessive heat being generated in the AC-S bed. The heat generation was observed when the AC-S was first exposed to water vapor and then further heated from exposure to high nitrogen oxide (NO<sub>x</sub>) concentrations and organic compounds. These tests resumed after a review of the literature, operating conditions, and potential safety issues. There were indications that elements, mostly sulfur, were stripped off the AC-S bed. Desorbing sulfur (measured as SO<sub>2</sub>) is a concern due to potential catalyst poisoning in the TCO and/or catalyst bed clogging from formation of ammonium sulfate particulate.

In the 2005 VSL testing (Matlack et al. 2005), a full-size bed was installed for testing and the system configuration was consistent with current design where the carbon bed is directly upstream of the TCO. According to Matlack et al. (2005):

*“The carbon unit contains 606 lb of granulated, sulfur impregnated activated carbon mixed with an inert mineral material in the ratio of 7:3 by volume; the material is manufactured by Donau Carbon, EU, under the trade name Kombisorb BAT37.”*

The exact reasoning for the selection of Kombisorb BAT-37 is not apparent in available documents. The inert material is added to the AC-S bed to help with temperature control and prevent localized hot spots from reaching ignition temperatures from heat of adsorption reactions. The testing matrix targeted an AC-S bed outlet temperature of 70–75 °C (nominal condition) and 85–90 °C (challenge condition), but difficulty in achieving this outlet temperature due to heat generation during adsorption led to a specification change based on the inlet temperature. Carbon monoxide emissions were continuously monitored; however, no Hg was present in the exhaust stream during this testing and so no data on Hg removal efficiency or temperature response could be assessed.

In response to this information gap, VSL received a statement of work (SOW) in 2013 from BNI to propose and prepare testing specifically to assess the performance of the Kombisorb BAT-37 AC media and Sofnolime RG guard bed material in prototypical LAW melter off-gas conditions, in a lead and lag configuration, respectively (Brandys et al. 2014). Testing was delayed for unknown reasons and then significant changes in the SOW were provided to VSL in 2017, which prompted a substantial revision of the AC media test plan, updated and documented by Brandys et al. (2018). Testing was conducted under the updated (Brandys et al. 2018) test plan and, during shakedown testing, the Sofnolime RG guard bed material was found to be unstable under the necessary performance conditions (Abramowitz et al. 2018). However, although the guard bed was deemed redundant to the acid gas removal function largely achieved in the SBS and WESP, the guard bed was credited (at that time) as the iodine removal technology and could not be removed from the design.

In response to this new challenge for the guard bed material, a new test plan was developed by Abramowitz et al. (2018) to conduct small-scale testing on several guard bed media as candidates to abate Hg and I in the WTP LAW Facility secondary off-gas system. The small-scale testing was performed by VSL using the following three sorbent materials as directed:

- Sulfur-impregnated AC and inert zeolite mixture (Kombisorb BAT-37, 4×8 mesh), manufactured by Donau Carbon
- TEDA-impregnated AC (Chemsorb 705 G1, 4×8 mesh) combined with an inert filler, provided by IONEX Research Corporation
- Silver mordenite (IONEX Type Ag-900-E16, 8×16 mesh), provided by IONEX Research Corporation

Small-scale testing to assess alternative media capacity and DFs for Hg and I was documented in Abramowitz et al. (2019a,b). Major conclusions from Abramowitz et al. 2019a relevant to this discussion were extracted and include the following:

- All the materials tested (i.e., Kombisorb BAT-37, Chemsorb 705 G1, and IONEX Type Ag-900-E16) exceeded the required capacities for mercury and iodine.
- All measured capacities exceeded 1 and 3 wt% for I and Hg, respectively.
- The results supported the use of BAT-37 and, based on Hg capacity alone, BAT-37 will have sufficient service life (i.e., minimum of 2 years) for use at WTP.
- Measured Hg capacities were higher in tests with I in the test gas due to the conversion of elemental Hg to ionic and particulate forms, which are more readily removed and held by the sorbent media. The proportion of total mercury detected as elemental was 70% and 84% for Chemsorb 705 G1,

77% and 96% for Kombisorb BAT-37, and 69% and 92% for IONEX Type Ag-900-E16, with and without iodine being introduced into the system, respectively.

Based on this last observation, it was recommended that iodine be omitted from “Appendix M” testing to provide the most conservative results from the testing for Hg performance. Follow-on “Appendix M” testing by Abramowitz et al. 2019b focused on Hg abatement with Kombisorb BAT-37 in a small-scale prototypic melter and off-gas system. Relevant conclusions include the following:

- Testing successfully demonstrated that the Hg DF of the lead column was greater than the required 450 for all the sample pairs. Measured DF values ranged from 486 to 13,423, with all but the first sampling having DF values greater than 2700.
- Mercury was typically about 95% elemental at the column and prefilter inlets, while mercury at the column outlets was typically only 10% to 35% elemental. This difference may be attributable to the Kombisorb BAT-37 having a much higher removal efficiency for elemental mercury than ionic or particulate mercury.
- Over 99.9% of the mercury detected in the carbon media was present in the first 10 inches of media in the lead bed. No mercury was detected in three of the samples from the lag bed and the virgin carbon sample. The concentration of mercury in the first 3 inches of media exceeds the 1.04 wt% minimum loading capacity requirement for the Kombisorb BAT-37 media.
- The speciation of mercury in exhaust streams as elemental, ionic, or particulate mercury is greatly influenced by the composition and conditions of the exhaust stream. The speciation of mercury in turn influences the effectiveness of unit operations to remove mercury.

Finally, in separate follow-on testing of iodine abatement behavior using Kombisorb BAT-37, the material was not able to sustain high levels of I capture as observed earlier (Matlack et al. 2020). A more detailed discussion of these results from Matlack et al (2020) and the impacts to the downstream flowsheet are provided in Section 1.1.

### 3.5 Existing Waste Form and Disposition Planning for Spent Media

Disposal of the Carbon Adsorber media, currently AC-S, requires consideration of non-debris mixed low-level waste for both its radiological ( $^{99}\text{Tc}$  and  $^{129}\text{I}$ ) and Resource Conservation and Recovery Act (RCRA)-metal (e.g., Hg) content. These containment levels will dictate treatment levels needed to meet LDR requirements in the IDF or alternate off-site disposal facilities.

Flach et al. (2016) generated a data package supporting a performance assessment of the IDF by addressing the planned disposition of four key secondary solid waste (SSW) streams in the IDF. Specific cementitious formulations were not provided to encapsulate or solidify the SSW, but recommendations for waste form physical and chemical properties were provided. However, since the issuance of the SSW data package, several efforts have been made to provide site- and material-specific information on the SSW and grouts themselves, including maturing new high-performance grout formulations for improved waste form performance (Asmussen et al. 2021b). The four SSW waste streams included HEPA filters, ion exchange resins, carbon adsorber beds, and Ag-mordenite, with a baseline assumption that HEPA filters will be macro-encapsulated and the other three stabilized (microencapsulated) in engineered containers using a cementitious slurry matrix. These processes are regularly performed in the nuclear industry and are considered a mature waste form technology. The conceptual plan is for the spent Carbon Adsorber beds to be transported to a local offsite treatment facility where they would be repackaged and stabilized for RCRA metals and Category 3 radioactive waste using a regulatory compliant and Hanford-approved grout formulation. Other waste form approaches for many of the materials presented here have been tested or hypothesized and are summarized elsewhere (Reiser et al. 2022).

The two dominant radionuclide sources impacting the near-surface disposal of low-level waste and SSW are  $^{99}\text{Tc}$  and  $^{129}\text{I}$  (WRPS and INTERA 2018). IDF performance assessment modeling results presented by Lee et al. (2018) illustrated that for SSW types,  $^{129}\text{I}$  release rates, highest to lowest, follow HEPA, AC /Ag-mordenite, and ion exchange resin while also assuming AC/Ag-mordenite materials retain their sorptive properties for  $^{129}\text{I}$  and other contaminants. However, follow-on testing of site-specific grout formulations and representative materials has shown that the AC does not provide additional retention capacity for iodine (Asmussen et al. 2020). Therefore, the stabilization of Carbon Adsorber media/materials as an acceptable waste form is an important consideration when selecting a replacement material at Hanford.

## 4.0 State of Gas-Phase Mercury Sorbent Technology

The objective of this discussion is to identify and summarize the broad diversity of material types that could be or have previously been applied to the specific application of adsorbing/absorbing elemental mercury ( $\text{Hg}^0$ ) from gas-phase conditions. The viability and propensity for the various materials to be applied for management of Hg emissions is also discussed, which can serve as a long-term guide to DOE-EM and other entities. At the Hanford Site, the specific application focuses on Hg abatement in the WTP LAW and HLW facilities' secondary off-gas systems that are treating emissions from the associated vitrification of nuclear wastes.

Many different classes of materials have been considered for Hg capture from the gaseous state, including porous inorganic crystalline matrices (e.g., zeolites), inorganic aerogels, inorganic sulfides, porous organic polymers (POPs), metal organic frameworks (MOFs), covalent organic frameworks (COFs), carbon-based sorbents, and metal-impregnated compounds. A non-exhaustive summary of Hg sorbents is provided in Table 4.1 with citations to the original works in the literature. Some of these materials are commercially available, but most are not. The TRL ratings of the materials in this list vary extensively, from very-low to very-high technical maturity and demonstrations.

Subsequent subsections address the individual material types for gas-phase sorption of Hg and describe the relevant attributes and performance under their associated test conditions.

Table 4.1. Overview of mercury capture material types and commercial availabilities.

Material Type	Specific Material	Reference	Commercially Available?
Zeolites	Ag-zeolite 4A	Sun et al. 2018	No
	$\text{FeCl}_3$ -faujasite	Qi et al. 2015	No
	Mn-MCM-22	Ma et al. 2021	No
	Mn-ITQ-2	Ma et al. 2022	No
Chalcogel	K-Pt-S chalcogels	Oh et al. 2012	No
Sulfides	CuS	Liu et al. 2019	No
	ZnS	Li et al. 2016	No
	$\text{H}_2\text{S}/\text{Fe}_2\text{O}_3$	Wu et al. 2021	No <sup>(b)</sup>
Metal particles	Ag	Johnson et al. 2008	Yes
	Cu	Johnson et al. 2008	Yes
	Se	Johnson et al. 2008	No
MOFs	MIL-101-Cr, UiO-66-(Br, Ag), Cu-BTC	Cavka et al. 2008; Zhang et al. 2016; D Chen et al. 2018; Zhao et al. 2018a,b; Dong et al. 2019; Zhao et al. 2021	No
COF	$\text{Cu}_2\text{WS}_4$ -COF-LZU1	Wang et al. 2022	No <sup>(b)</sup>
POP	POP-SH <sup>(a)</sup>	Aguila et al. 2017	No
Carbon	BAT-37, BAT-37 II, Desorex K43J/HGD, Chemsorb 701G	Reddy et al. 2014; Vidic and Siler 2001; Y Chen et al. 2018; Hutson et al. 2007; Cheng et al. 2020; Huggins et al. 1999; Rungrim et al. 2016; Khunphonoi et al. 2015; Feng et al. 2006; Kartaza 2011; Luo et al. 2010	Yes

(a) The term "SH" in the material description denotes that the material is thiolated.

(b) The base materials are commercially available, but the functional groups, metals, or compounds were added through additional processes in the laboratory.

MOFs = metal organic frameworks; COF = covalent organic framework; POP = porous organic polymer

## 4.1 Porous Inorganic Crystalline Matrices (e.g., Zeolites)

Zeolites are porous crystalline materials with moderate specific surface area (SSA) values. Zeolites are typically composed of aluminosilicate frameworks (other chemistries are possible) that are formed by a variety of different interconnected negatively charged structures of channels and cages linked through  $\text{SiO}_4^{4-}$  and  $\text{AlO}_4^{5-}$  tetrahedra that are charge-balanced by cations (e.g.,  $\text{Na}^+$ ,  $\text{Ca}^{2+}$ ,  $\text{H}^+$ ). These cations can be ion exchanged to functionalize the zeolites for various applications. Different zeolites have unique structures. Zeolite A (Linde type A) is mainly composed of  $\beta$ -cages, whereas zeolite X (faujasite) contains  $\alpha$ -cages and  $\beta$ -cages. The HZSM-5 (hydrogen Zeolite Socony Mobil-5) zeolite has a channel structure of MFI (Mobil-5) framework, and MCM-22 (Mobil Composition of Matter-22) has a layer structure with 10-membered rings and cages. Studies on the  $\text{Hg}^0$  removal efficiencies of zeolite A, zeolite X, HZSM-5, and MCM-22 are discussed below.

Two types of Ag-loaded zeolite 4A sorbents and raw zeolite 4A were evaluated for  $\text{Hg}^0$  removal at a temperature range of 30–110 °C using  $\text{CH}_4$  as a carrier gas (Sun et al. 2018). The Ag-loaded zeolite 4A, synthesized with stearic acid (C-AgNPs/4A-zeolite), showed >96%  $\text{Hg}^0$  removal efficiency at 30 °C after 200 min (Figure 4.1), but the removal efficiency dropped to ~50% at 110 °C. The  $\text{Hg}^0$  adsorption capacity was 5.985 mg/g at 30 °C. Formation of an Ag-Hg amalgam was observed at lower temperature (<70 °C).

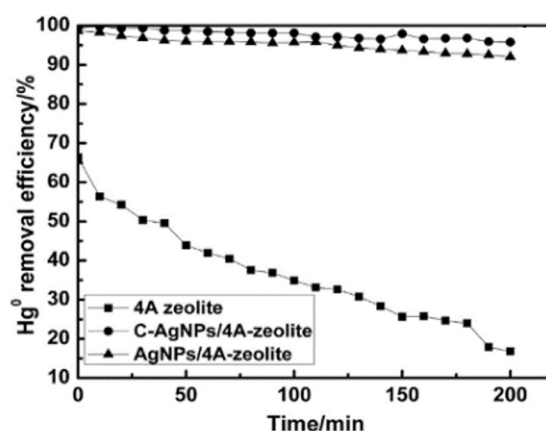


Figure 4.1.  $\text{Hg}^0$  removal efficiency of Ag-loaded zeolite 4A and raw zeolite 4A (Sun et al. 2018).

Three zeolites (NaA, NaX, HZSM-5) modified with the impregnation of  $\text{FeCl}_3$  were investigated for  $\text{Hg}^0$  removal by Qi et al. (2015). Among these zeolites, 5% $\text{FeCl}_3$ -HZSM-5 showed the highest  $\text{Hg}^0$  removal efficiency of 95% at 120 °C for 180 min under an  $\text{Hg}^0$  concentration of  $40.7 \pm 0.3 \mu\text{g}/\text{m}^3$  while 5%  $\text{FeCl}_3$ -NaA and 5%  $\text{FeCl}_3$ -NaX only had 3 mass% and 65 mass% removal efficiencies, respectively. The active Cl species on the zeolites were effective oxidants to convert  $\text{Hg}^0$  to  $\text{Hg}^{2+}$ , forming  $\text{HgCl}_2$ . The lower  $\text{Hg}^0$  removal efficiency of NaA and NaX was possibly due to fewer Cl species as NaCl crystals being formed during ion substitution processes. Temperature programmed desorption analysis showed that Hg was mainly present as  $\text{HgCl}_2$  in HZSM-5, whereas the main Hg species was  $\text{HgO}$  in NaA and NaX zeolites.

Two ITQ-2 zeolites modified with Mn and Co-Mn were investigated for  $\text{Hg}^0$  capture by Ma et al. (2022). The  $\text{Hg}^0$  adsorption capacity of 5%Mn/ITQ-2 zeolite was 2.04 mg/g at 300 °C and maintained a removal efficiency of 97 mass% at 300 °C after a 10-h loading. However, the  $\text{Hg}^0$  removal efficiency decreased to 53% while in the presence of 1000 ppm  $\text{SO}_2$ . The addition of Co to 5%Mn/ITQ-2 improved the  $\text{Hg}^0$  adsorption capacity in the presence of  $\text{SO}_2$ . The  $\text{Hg}^0$  adsorption mechanism was driven by the catalytic oxidation of  $\text{MnO}_x$  resulting in the formation of  $\text{HgO}$ .



The Mn-modified layered MCM-22 zeolites (Mn/MCM-22) with 2–10 mass% of Mn were evaluated for  $\text{Hg}^0$  capture by Ma et al. (2021). The 5% Mn/MCM-22 material showed an  $\text{Hg}^0$  adsorption capacity of 0.32 mg/g and a removal efficiency of 92% at 300 °C under an  $\text{Hg}^0$  concentration of 300  $\mu\text{g}/\text{m}^3$  and 5%  $\text{O}_2$ . Gaseous  $\text{Hg}^0$  was oxidized to  $\text{Hg}^{2+}$  at the  $\text{Mn}^{4+}$  sites, and  $\text{Mn}^{4+}$  was reduced to  $\text{Mn}^{3+}$  while  $\text{HgO}$  was formed and absorbed in the pores of Mn/MCM-22. The capture of  $\text{Hg}^0$  involved both physisorption and chemisorption. The  $\text{Hg}^0$  removal efficiency over the temperature range of 100–400 °C indicated that  $\text{Hg}^0$  was mainly physisorbed at 100–200 °C and chemisorbed at higher temperatures. The presence of  $\text{H}_2\text{O}$  and  $\text{SO}_2$  in the gas stream had a negative effect on  $\text{Hg}^0$  removal (Figure 4.2).

An Ag-exchanged zeolite, IONEX 900, was included in small-scale testing for Hg (DF of 137 in Hg only tests) and I (DF of 45 in iodine only tests) when tested individually, but improved removal of both Hg and I when tested simultaneously (DFs of 203 and 220, respectively).

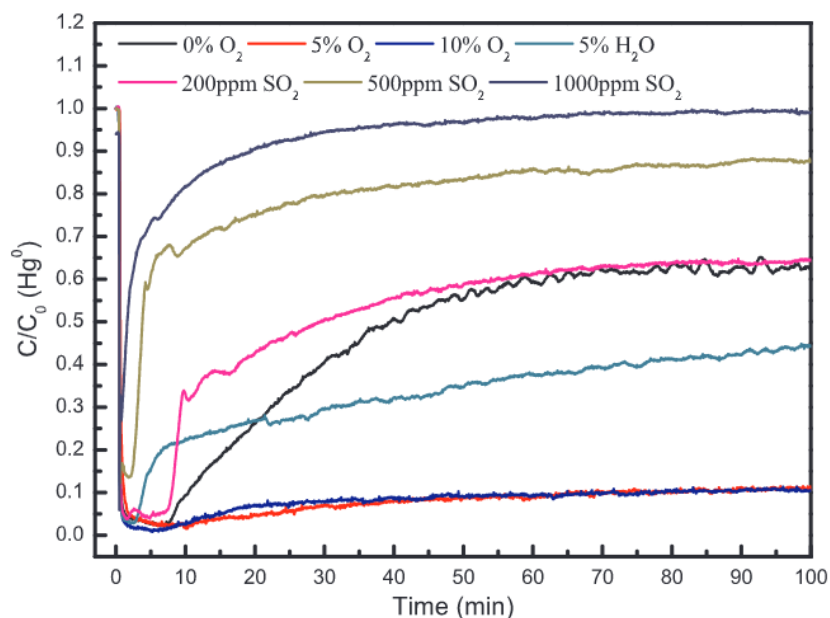


Figure 4.2. Effect of gas composition on  $\text{Hg}^0$  removal efficiency for Mn-modified layered MCM-22 zeolites under different atmospheric conditions (Ma et al. 2021).

In general, these types of materials are well suited for gaseous capture. They are attractive due to the commercial availability of base zeolite materials, but require additional functionalizations to be optimized for Hg capture. The material costs are likely much higher compared to other options like carbon-based materials due to the elements used for functionalization (e.g., Ag) and substrate preparation costs. The Hg loading capacities for these are low to moderate and no waste form has been demonstrated for these materials following Hg-loading.

## 4.2 Inorganic Aerogels

Aerogels are highly porous substrates (with moderate-to-high SSA values) that are generally produced through one of four separate processes: (1) hydrolysis and polycondensation reactions using metal alkoxides, (2) thiolysis reactions with metal alkoxides, (3) aggregation of nanoparticles, or (4) metathesis reactions where the overall goal is to convert molecular reactants or nanometer-sized materials into scaffolds by creating chemical linkages between the target species (Riley and Chong 2020). These porous materials can either be synthesized directly and functionalized after production or purchased commercially

and then functionalized for use in the capture of contaminants. While aerogels can be produced that are similar in chemistry to zeolites, the distinct difference is that they tend to be amorphous (non-crystalline) in structure.

Inorganic aerogels have been developed for  $\text{Hg}^0$  and  $\text{Hg}^{2+}$  capture. Recent studies have shown that metal-chalcogenide aerogels (called chalcogels) can be used for  $\text{I}_{2(\text{g})}$  capture (Riley et al. 2011, 2013; Subrahmanyam et al. 2015) and Hg vapor capture (Oh et al. 2012). Molybdenum sulfide-impregnated porous chalcogels (i.e.,  $\text{MoS}_x$ ) were demonstrated to chemisorb  $\text{Hg}^0$  vapor to form  $\text{HgS}$  with high Hg uptake of  $2.0 \times 10^6 \mu\text{g/g}$  at  $140^\circ\text{C}$  for a 24-h loading. The chalcogels containing  $\text{Pt}^{2+}$  and polysulfide clusters ( $[\text{S}_x]^{2-}$ ,  $x = 3-6$ , i.e., K-Pt- $\text{S}_x$ ) have thermal stability up to  $200^\circ\text{C}$  and showed high Hg vapor loading capacity  $(0.43-5.45) \times 10^6 \mu\text{g/g}$  at  $140^\circ\text{C}$  for 24 h (Oh et al. 2012).  $\text{Zn}_2\text{Sn}_x\text{S}_{2x+2}$  ( $x = 1, 2, 4$ ) chalcogels (referred to as ZTS-cg chalcogels) have high SSA values ( $363-520 \text{ m}^2/\text{g}$ ) and pore volumes ( $1.1-1.5 \text{ cm}^3/\text{g}$ ), and showed  $\text{Hg}^{2+}$  loading capacities of  $1.40-1.69 \text{ mmol/g}$  and  $\text{Hg}^{2+}$  removal efficiencies of  $99.2-99.9\%$ , as given in Table 4.2. The  $\text{Hg}^{2+}$  ion was chemisorbed by the ZTS-cg chalcogel forming  $\text{Hg}_2\text{Sn}_2\text{S}_6$  through an ion-exchange reaction ( $2 \text{Hg}^{2+} + \text{Zn}_2\text{Sn}_2\text{S}_6 \rightarrow \text{Hg}_2\text{Sn}_2\text{S}_6 + 2 \text{Zn}^{2+}$ ) (Oh et al. 2011).

In summary, inorganic aerogels have low technical maturity for Hg capture, but demonstrated examples do have promising capacity. However, emerging examples of inorganic aerogels utilize thiol (sulfur)-based linkages, and these groups could have a high affinity for Hg, providing dual functional capture of Hg and I. The cost of these materials will be driven by any elements used in functionalization (e.g., Ag or Pt). Some inorganic aerogels are known to be friable and may need improvement in physical stability. Waste forms have not been demonstrated for inorganic aerogels loaded with Hg but have been demonstrated at bench scale for I-loaded materials.

Table 4.2. Summary of properties and  $\text{Hg}^{2+}$  removal of ZTS chalcogel (Oh et al. 2011).

Material	SSA ( $\text{m}^2/\text{g}$ ) <sup>(a)</sup>	PV ( $\text{cm}^3/\text{g}$ ) <sup>(b)</sup>	$\text{Hg}^{2+}$ Removal (%)	$\text{Hg}^{2+}$ Loading ( $\text{mmol/g}$ )
ZTS-cg1	503-520	1.5-1.6	99.4	1.40
ZTS-cg2	413-415	1.1-1.3	99.2	1.69
ZTS-cg3	363-393	1.3-1.4	99.9	1.69

SSA = specific surface area (from BET); PV = total pore volume

In general, inorganic aerogels have low technical maturity for Hg capture, but demonstrated examples do have very promising capacities. Emerging examples of inorganic aerogels utilize thiol (sulfur)-based linkages, and these groups could have a high affinity for Hg, providing dual functional capture of Hg and I. The cost of these materials will be driven by any elements used in functionalization (e.g., Ag or Pt). Some inorganic aerogels are known to be friable and may need improvement in physical stability. Waste forms have not been demonstrated for inorganic aerogels loaded with Hg but have been demonstrated at bench scale for similar base materials loaded with I.

### 4.3 Inorganic Sulfide Materials

Based on documented examples of sulfur-based materials that are known to capture Hg, a separate section on sulfur-based materials is included in this report. Inorganic sulfides include a variety of metal sulfides, sulfide-based materials (e.g., chalcogels), or pure sulfur. From the perspective of metal sulfides, a wide range of materials exist in the literature for a diverse set of applications, including  $\text{Ag}_2\text{S}$ ,  $\text{Bi}_2\text{S}_3$ ,  $\text{CuS}$ ,  $\text{Cu}_2\text{S}$ ,  $\text{FeS}_x$ ,  $\text{MnS}$ ,  $\text{SnS}$ ,  $\text{SnS}_2$ , and  $\text{ZnS}$ .

CuS material was evaluated for its ability to capture  $\text{Hg}^0$  vapor in the presence of  $\text{O}_2$ ,  $\text{SO}_2$ ,  $\text{H}_2\text{O}$ , and/or  $\text{SO}_3$  within the temperature range of 25–175 °C for 180 min (Liu et al. 2019). The  $\text{Hg}^0$  removal efficiency of CuS was compared with different metal sulfides, and the removal efficiency order was  $\text{CuS} > \text{MnS} > \text{SnS} > \text{ZnS} > \text{CdS}$ , where CuS showed an  $\text{Hg}^0$  removal efficiency of ~75% after 3 h (Figure 4.3a). The loading capacity of  $\text{Hg}^0$  capture was 17.05 mg/g at 50 °C with 5%  $\text{O}_2$  and the loading values were similar, in the range of 25–100 °C under the same condition but decreased to 7.07 mg/g at 150 °C (Figure 4.3b). The effects of  $\text{O}_2$ ,  $\text{H}_2\text{O}$ , and  $\text{SO}_2$  on the  $\text{Hg}^0$  loading capacity were not significant, but the  $\text{Hg}^0$  removal efficiency of CuS decreased to 40% after exposure to  $\text{SO}_3$ .

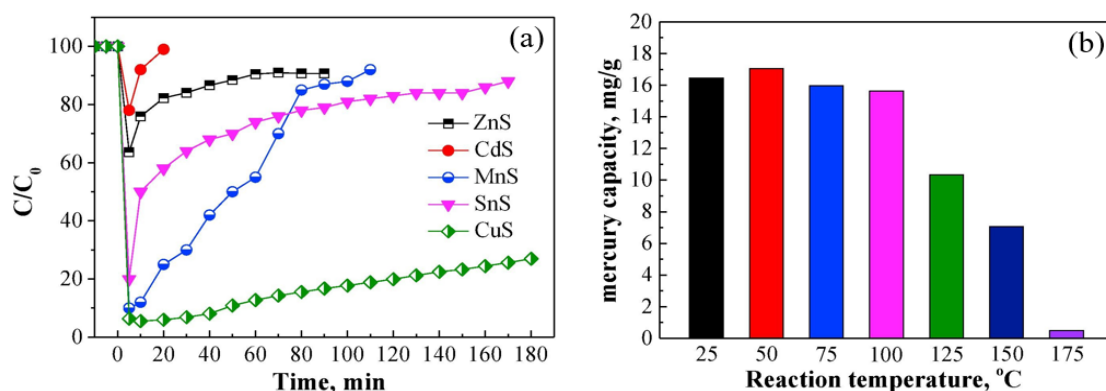


Figure 4.3. (a) Mercury removal efficiency of different sulfides and (b) the effect of temperature on CuS materials (Liu et al. 2019).

Zinc sulfide with a high SSA (called Nano-ZnS) was evaluated for  $\text{Hg}^0$  vapor removal (Li et al. 2016). The Nano-ZnS was synthesized with a liquid-phase precipitation method to augment the SSA and was compared with commercial ZnS as well as other synthesized ZnS that had different SSAs. The highest  $\text{Hg}^0$  removal was observed on the synthesized Nano-ZnS with a surface area of 196.1  $\text{m}^2/\text{g}$ , as shown in Figure 4.4. The  $\text{Hg}^0$  adsorption capacities (98.6 and 110.9  $\mu\text{g}/\text{g}$ ) of the synthesized nano-ZnS materials at 140 °C and 180 °C for 6 h were much higher than commercial ACs used in this study, as shown in Figure 4.5. Here, the  $\text{Hg}^0$  was chemisorbed by ZnS and mainly formed  $\text{HgS}$  on the Nano-ZnS.

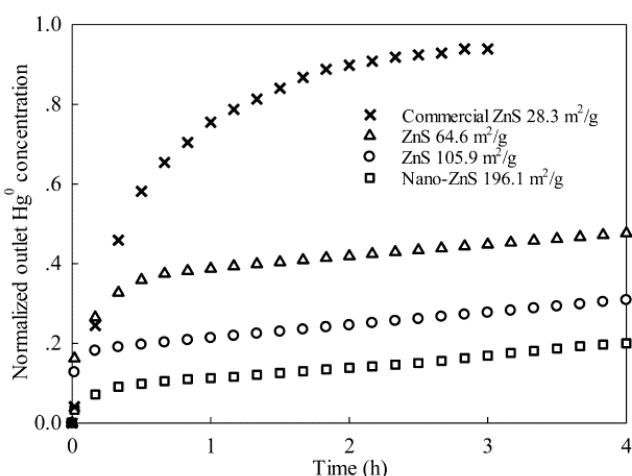


Figure 4.4. Normalized  $\text{Hg}^0$  outlet concentration mercury removal efficiency for ZnS sorbents with different surface areas (Li et al. 2016).

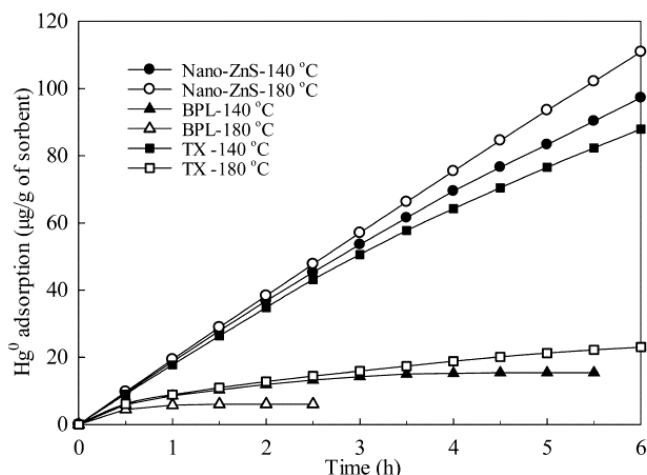


Figure 4.5. Comparison of mercury adsorption capacity on Nano-ZnS and commercial activated carbons (Li et al. 2016).

In a study by Wu et al. (2021),  $\text{H}_2\text{S}$ -modified  $\text{Fe}_2\text{O}_3$  adsorbents were developed to improve the  $\text{Hg}^0$  adsorption performance of the  $\text{Fe}_2\text{O}_3$  sorbent. The  $\text{Fe}_2\text{O}_3$  was modified by varying vulcanization temperature (50–250 °C) and dwell time (1–3 h). The adsorption capacity of  $\text{Hg}^0$  was increased from 7.2 µg/g at 50 °C to 45.1 µg/g at 200 °C with 2 h of vulcanization. At the constant vulcanization temperature of 200 °C, the  $\text{Hg}^0$  adsorption capacities were increased from 31.5 µg/g for the 1-h vulcanized sample to 45.1 µg/g for the 2-h vulcanized sample, but decreased to 43.1 µg/g for the 3-h vulcanization treatment (Figure 4.6a). The  $\text{Hg}^0$  loading capacity decreased when the vulcanization temperature exceeded 200 °C and the vulcanization time extended past 2 h (Figure 4.6b). The highest  $\text{Hg}^0$  adsorption capacity (51.6 µg/g) was observed at the lowest adsorption temperature (50 °C) (Figure 4.6c). The  $\text{Hg}^0$  vapor was chemisorbed by  $\text{H}_2\text{S}/\text{Fe}_2\text{O}_3$  and formed  $\text{HgS}$  (Figure 4.7).

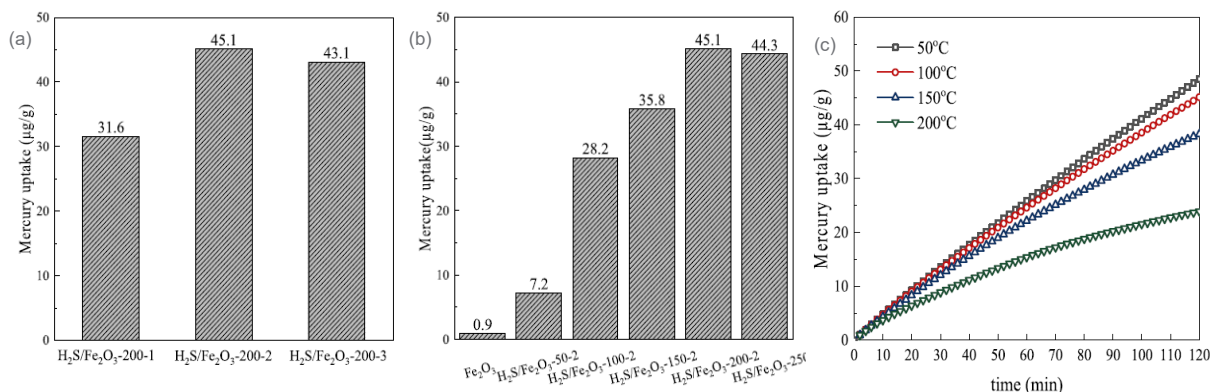


Figure 4.6. Effect of (a) vulcanization temperature, (b) vulcanization time, and (c) adsorption temperature on the adsorption capacity of  $\text{Hg}^0$  on  $\text{H}_2\text{S}/\text{Fe}_2\text{O}_3$  (Wu et al. 2021).

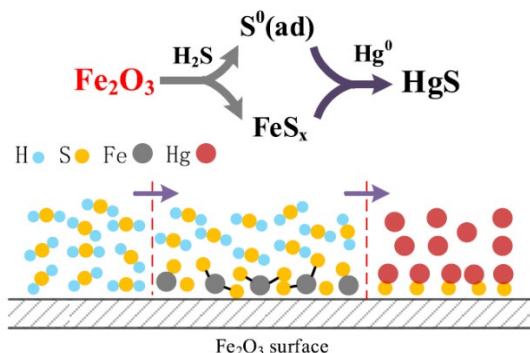


Figure 4.7. Mercury removal mechanism on  $\text{H}_2\text{S}/\text{Fe}_2\text{O}_3$  material (Wu et al. 2021).

The primary benefit for inorganic sulfide materials is the inclusion of S, whereby reactions with Hg can result in the formation of HgS. It is not clear if inorganic sulfide sorbents are commercially available. The costs of these materials range from low to moderate depending on the metals utilized. The capacities range from low to moderate, and they appear to be stable thermally and chemically with robust forms. However, no waste form options have been realized for the Hg-loaded materials in this category.

## 4.4 Porous Organic Materials

Porous organic materials are different from porous inorganic materials due to the organic building blocks used in fabrication of the former. The types of porous organic materials described in this section include MOFs, COFs, and POPs. For gaseous Hg capture, different organic materials including MOFs (Cavka et al. 2008; Zhang et al. 2016; D Chen et al. 2018; Zhao et al. 2018a,b; Dong et al. 2019, Zhao et al. 2021) (see Section 4.4.1), COFs (Wang et al. 2022) (see Section 4.4.2), and POPs (Aguila et al. 2017) (see Section 4.4.3) have been investigated and are summarized in this section. These materials have high SSAs and good thermal stability, and different functional getters can be inserted into the structure using an ion substitution process for specific applications. However, the costs of COFs are generally high, and grafting functional groups into the structure requires laboratory work (i.e., aqueous synthesis, hydrothermal processing). In particular, hydrothermal synthesis at scaled fabrication would have potential safety and cost concerns, making these materials less viable as an option to support WTP efforts.

In general, porous organic materials tend to have moderate-to-high Hg loadings, but the deployment will likely be hindered by the limitation (or lack) of commercially available materials that are not in a fine particle form, which is often the synthesis product form for these materials. The as-made materials are often characterized as being chemically and thermally stable. Also, no known final waste forms exist to date for these materials after Hg-loading.

### 4.4.1 Metal Organic Frameworks

The MOF class of porous organic materials is unique in that MOFs are 3D materials made by linking metal ions or clusters with organic ligands. The MOF materials have a wide range of applications, as various metal atoms or clusters can be inserted for specific applications. Three different MOFs, including MIL-101-Cr, UiO-66 with different functional groups, and Cu-BTC, were selected for brief discussion relating to  $\text{Hg}^0$  capture. Some Ag- or Cu-containing MOFs developed for  $\text{Hg}^0$  capture are attractive material sorbents because they could potentially be used for capturing both Hg and I, as different studies have shown that gaseous I reacts with Ag and Cu to form AgI and CuI, respectively (Riley et al. 2021; Chong et al. 2021, 2022).

The MIL-101-Cr MOF has an SSA of  $\sim 2400 \text{ m}^2/\text{g}$ , a decomposition temperature of  $\sim 300 \text{ }^\circ\text{C}$ , and good catalytic activity with the presence of Cr (Dong et al. 2019). The  $\text{Hg}^0$  equilibrium adsorption capacity of MIL-101-Cr was  $25.7 \text{ mg/g}$  at  $200 \text{ }^\circ\text{C}$  under the inlet  $\text{Hg}^0$  concentration of  $\sim 200 \text{ }\mu\text{g}/\text{m}^3$ , and the  $\text{Hg}^0$  removal efficiency was  $>70 \text{ mass}\%$  (Figure 4.8) (Dong et al. 2019). The addition of NO and/or  $\text{O}_2$  to  $\text{Hg}^0$  gas increased  $\text{Hg}^0$  adsorption, whereas adding  $\text{SO}_2$  generally decreased the adsorption due to the reaction between  $\text{SO}_2$  and  $\text{Hg}^0$  and sulfation of the material (Dong et al. 2019). Gaseous  $\text{Hg}^0$  was chemisorbed by reacting with  $\text{Cr}^{3+}$ , oxygen species, and C=O groups in MIL-101-Cr (Dong et al. 2019). Another study on MIL-101-Cr showed  $\text{Hg}^0$  loading of  $0.25 \text{ mg/g}$  at  $100 \text{ }^\circ\text{C}$  for 1 h (Zhao et al. 2018a). The  $\text{Hg}^0$  removal efficiency was tested on four different materials, including MIL-101-Cr MOF, UiO-66 MOF, Cu-BTC MOF, and AC, based on the concentration change curves of Hg passing through the materials, and the results showed that MIL-101-Cr was the most efficient capture material, but Hg-loading values were not provided (Zhao et al. 2018a).

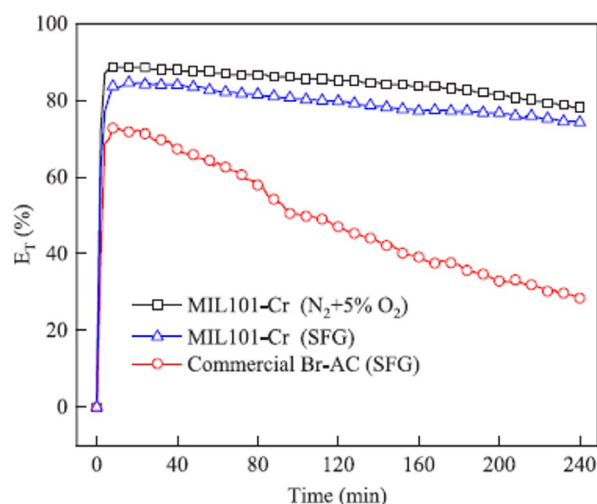


Figure 4.8.  $\text{Hg}^0$  removal efficiency of MIL-101-Cr. SFG denotes simulated flue gas (Dong et al. 2019).

The UiO-66 MOF with  $\text{Zr}_6\text{O}_4(\text{OH})_4(\text{CO}_2)_{12}$  clusters has high thermal stability with a decomposition temperature of  $540 \text{ }^\circ\text{C}$ , and modified UiO-66 MOFs have been studied for Hg capture (Cavka et al. 2008). The Ag particle doped UiO-66 (UiO-66-Ag) showed an  $\text{Hg}^0$  loading of  $3.7 \text{ mg/g}$  at  $50 \text{ }^\circ\text{C}$  and  $3.5 \text{ mg/g}$  at  $200 \text{ }^\circ\text{C}$  for 10 h loading with the  $\text{Hg}^0$  concentration of  $250 \text{ }\mu\text{g}/\text{m}^3$  (Zhao et al. 2018b). The gaseous  $\text{Hg}^0$  was chemisorbed by UiO-66-Ag, forming a Hg-Ag amalgam at  $50 \text{ }^\circ\text{C}$  and  $\text{Hg}^{2+}$  species with Zr and carboxyl or ester groups at  $200 \text{ }^\circ\text{C}$  (Zhao et al. 2018b). UiO-66-Ag is an attractive material because it has the potential to capture both Hg and I.

A study on UiO-66 MOF grafted with Br,  $\text{NO}_2$ , or  $\text{NH}_2$  and organic functional groups showed that the addition of Br significantly improved the  $\text{Hg}^0$  loading capacity compared to raw UiO-66, whereas the addition of  $\text{NO}_2$  or  $\text{NH}_2$  did not notably affect performance (Zhao et al. 2021); see Figure 4.9. The  $\text{Hg}^0$  loading capacity of UiO-66-Br was  $2.2 \text{ mg/g}$  at  $300 \text{ }^\circ\text{C}$  for 400 min, whereas the raw UiO-66 showed  $0.75 \text{ mg/g}$  under the same condition (Figure 4.9c). The  $\text{Hg}^0$  loading capacity of UiO-66-Br increased from  $\sim 0.9 \text{ mg/g}$  to  $\sim 2.5 \text{ mg/g}$  as the temperature increased from  $200 \text{ }^\circ\text{C}$  to  $350 \text{ }^\circ\text{C}$  (Figure 4.9d) (Zhao et al. 2021). For possible adsorption steps of  $\text{Hg}^0$ , the authors proposed that  $\text{Hg}^0$  was oxidized to HgO and then HgO was attached to the bromine functional group or stayed in the pore structure.

A previous study on the phenyl bromine-appended UiO-66 (2Br-UiO-66) MOF by the same group showed  $\text{Hg}^0$  loading of  $0.302 \text{ mg/g}$  after loading at  $200 \text{ }^\circ\text{C}$  for 48 h (Zhang et al. 2016). The benzene-HgBr complex



was formed on the 2Br-UiO-66 surface as an electron was transferred from  $\text{Hg}^0$  to the carbon-bromine bond (Zhang et al. 2016).

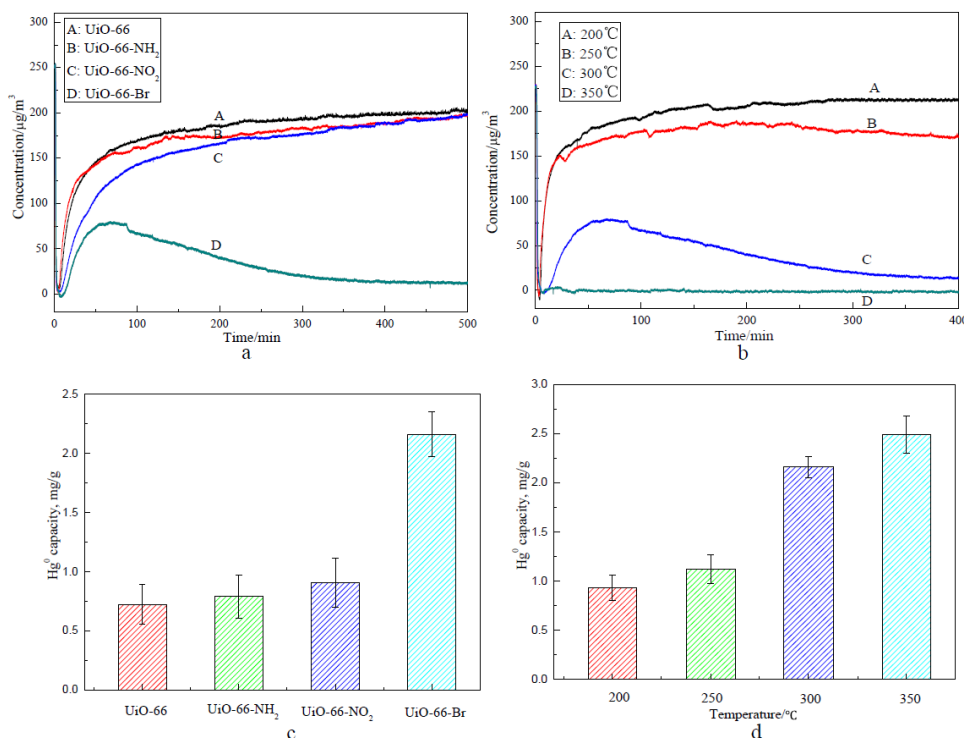


Figure 4.9.  $\text{Hg}^0$  concentration changes for (a) different MOFs at 300 °C and (b) UiO-66-Br at different temperatures;  $\text{Hg}^0$  loading capacities of (c) four types of UiO-66 MOFs and (d) UiO-66-Br at different temperatures (Zhao et al. 2021).

The  $\text{Hg}^0$  loading capacity of the Cu-BTC MOF was 0.08 mg/g at 150 °C for 2 h but increased to 1.7 mg/g when 15 ppm of HCl was added to  $\text{Hg}^0$  gas for 5 min (D Chen et al. 2018). Additional  $\text{Hg}^0$  loading tests with  $\text{SO}_2$ ,  $\text{H}_2\text{O}$ , and NO were performed, and the results showed that  $\text{SO}_2$  had an inhibitive effect on  $\text{Hg}^0$  capture whereas NO promoted  $\text{Hg}^0$  capture;  $\text{H}_2\text{O}$  had nearly no effect. The Cu-BTC MOF can be a good candidate as a dual-capture material for Hg and I since Cu reacts with I to form CuI when exposed gaseous I.

#### 4.4.2 Covalent Organic Frameworks

The COF class of porous organic materials is characterized as 2D or 3D organic solids composed of light elements (i.e., B, C, H, N, O) (Ding and Wang 2012). Defect-rich  $\text{Cu}_2\text{WS}_4$  nano-homojunctions on COF-LZU1 ( $\text{Cu}_2\text{WS}_4$ -COF) showed an  $\text{Hg}^0$  adsorption capacity of 21.6 mg/g at 80 °C for 3 h (Wang et al. 2022). The  $\text{Hg}^0$  adsorption capacity of  $\text{Cu}_2\text{WS}_4$ -COF was nine times higher than crystalline  $\text{Cu}_2\text{WS}_4$  due to more active S sites exposed in the COF composite. During adsorption,  $\text{Hg}^0$  was oxidized to form  $\text{Hg}^{2+}$  while the reduction of  $\text{S}^{1-}$  to  $\text{S}^{2-}$  and  $\text{Cu}^{2+}$  to  $\text{Cu}^+$  occurred, and  $\beta$ -HgS was formed as the coupling interaction between  $\text{Cu}_2\text{WS}_4$  nano-homojunctions and the COF promoted the charge separation and transportation. The  $\text{Cu}_2\text{WS}_4$ -COF composite hydrothermally synthesized with lower temperatures and shorter reaction times in the tested range (120–200 °C and 6–72 h) showed higher  $\text{Hg}^0$  adsorption capacities. Injection of  $\text{SO}_2$  into  $\text{Hg}^0$  gas had an inhibitory effect on  $\text{Hg}^0$  capture, while NO or  $\text{O}_2$  showed a negligible effect.

#### 4.4.3 Porous Organic Polymers

The POP class of porous organic materials consists of multi-dimensional porous materials with strong covalent bonds across organic moieties resulting in a range of geometries and topologies. The thiol-functionalized porous organic polymer (POP-SH) showed airborne ( $\text{Hg}^0$ ) and aqueous ( $\text{Hg}^{2+}$ ) mercury uptake capacities of 630 mg/g and 1216 mg/g, respectively (Aguila et al. 2017). For the  $\text{Hg}^0$  capture experiment, the POP-SH material was placed in a sealed container with  $\text{Hg}^0$  and heated to 140 °C for 8 d. The Hg-loading capacity obtained was 630 mg/g, which was much higher than thiol-functionalized MOF (83.6 mg/g) or AC (47 mg/g) under the same conditions. Formation of Hg-S bonds on the POP-SH material was observed, and the presence of  $\text{HgO}$  was negligible based on characterization analyses performed on the Hg-loaded samples.

### 4.5 Carbon-Based Sorbents

Activated carbons, the general trade name used for carbonaceous sorbents, are non-hazardous, high internal surface area materials used for the capture of a wide range of target compounds, primarily by physisorption (Fan et al. 2016). ACs are a coarse granular structure that have a ramified pore system containing mesopores (2-50 nm), micropores (0.4–2 nm), and submicropores (<0.4 nm) that branch off of macropores (>50 nm). A range of low-cost materials can be used in the fabrication of ACs, including charcoal, spent coal (Zhou et al. 2014), and abundant organic waste material (e.g., bamboo) (Huve et al. 2018). While ACs are widely used industrially, specific targets require impregnation of the AC to improve efficiency and cost-effectiveness (Henning and Schafer 1993; Vidic and Siler 2001; Hutson et al. 2007; Y Chen et al. 2018). Impregnation involves loading the internal surface of the AC with a suitable chemical, which is utilized to improve or change the capture mechanism.

Native AC can sequester Hg via chemisorption, but that performance can be substantially improved through impregnation in both vapor and liquid phase capture (Wajima and Sugawara 2011). Sulfur impregnation commonly gives a high degree of improvement for Hg capture along with thermal stability (Henning and Schafer 1993; Korpiel and Vidic 1997; Hsi et al. 2001; Lee and Park 2003; Rashid et al. 2013; N Li et al. 2018; Liu et al. 2020), and a full review is available elsewhere (Reddy et al. 2014). The impregnated sulfur does not react stoichiometrically with Hg (Otani et al. 1988). The presence of lactonic and carbonyl functional groups promotes Hg sorption onto ACs (Reddy et al. 2014). Impregnation with halides (e.g., I) also improves Hg capture (Cheng et al. 2020). Iodide impregnation has been shown to give the largest improvement in Hg capture when compared with other halides (Runnim et al. 2016; Cheng et al. 2020). The impregnated AC can then capture the Hg through physisorption, via interaction with the oxygen functional groups or chemisorption of a stable species (e.g.,  $\text{HgS}$ ,  $\text{HgI}_2$ ) (Huggins et al. 1999; Runnim et al. 2016) or, in the case of Ag-containing sorbents, form an amalgam ( $\text{HgAg}$ ) (Khunphonoi et al. 2015). Impregnation can also be used to improve chemical stability toward humidity, temperature, and competing species.

With their extensive history, ACs are the most widely used sorbent for Hg capture in the vapor phase (Liu et al. 2020). This wide use also leads to a market with relatively low costs due to the nature of the carbonaceous substrate and impregnation chemicals used. (Note that some impregnation chemicals can have significant costs, such as Ag.) During sorption, heat can be generated from the AC, leading to temperature increases, as was seen with the initial testing of a Kombisorb BAT-37 material for use at the WTP LAW Facility (Matlack et al. 2005). The inclusion of an inert zeolite with the AC can largely mitigate such temperature increases during operation. The impacts of any decomposition products from the AC (e.g., sulfuric acid) on the operating system need to be considered. Minor concerns around dust production also exist with ACs.



Capacities for AC capture of Hg range from 1 µg/g of material up to 1000 mg/g material, with variations induced by method of sulfur impregnation (Rashid et al. 2013; Korpiel and Vidic 1997), temperature of impregnation (Reddy et al. 2014), form of sulfur (Feng et al. 2006), additional additives (e.g., Ag) (Karatza et al. 2011), and substrate used (e.g., nanotubes) (Luo et al. 2010; Khunphonoi et al. 2015).

Once contaminated, AC particulates can be stabilized for disposal using a cementitious matrix. The AC can be microencapsulated (blended) into the cementitious waste form. Prior work has shown limited interaction between spent AC and various encapsulation matrices (Fujii Yamagata et al. 2022). However, it is unknown if the AC improves Hg retention within the cementitious matrix.

In summary, ACs are commercially available, tailorable solutions for off-gas management applications. With the varied impregnation options and applications globally, a range of these materials are available that could meet the needs for capture of Hg in the WTP with high capacity and desirable stability. While some challenges do exist for ACs under the WTP off-gas conditions (humidity, heat, NO<sub>x</sub>), an idealized solution can be attained as combinations of ACs. Waste forms are available through solidification in grout.

## 4.6 Metal Substrates and Other Materials

Metal particles are commercially available with different particle sizes and can be used for Hg capture, and the metal particles can be mixed with other compounds by coating or hydrothermal process. Different metals (Ag, Cu, Ni, S, Se, Zn), sulfides (MoS<sub>2</sub>, WS<sub>2</sub>), copper oxide, and carbon sorbents were evaluated for Hg vapor capture in a static environment with 60 µg/m<sup>3</sup> Hg vapor at 20 °C for >24 h (Johnson et al. 2008). Table 4.3 summarizes the Hg loading capacities and surface areas of tested materials. Among the tested materials, Nano-Se and nano-Ag particles showed relatively high Hg<sup>0</sup> loading capacities of 188 mg/g and 8.5 mg/g, respectively, compared to ACs (0.02–2.6 mg/g) and other materials.

Table 4.3. Summary of low-temperature Hg vapor capture materials (Johnson et al. 2008).

Sorbents	Hg loading (mg/g) <sup>(a)</sup>	SSA (m <sup>2</sup> /g)	Particle Size
Micro-sulfur (Sigma Aldrich)	2.6×10 <sup>-5</sup>	0.3	~10 µm
Sulfur nanotubes	6.2×10 <sup>-4</sup>	30	~200 µm
Micro-zinc (Sigma Aldrich)	5.0×10 <sup>-6</sup>	0.2	4.2 µm
Nano-zinc (Sigma Aldrich)	8.0×10 <sup>-5</sup>	3.7	0.23 µm
Micro-nickel (Sigma Aldrich)	4.0×10 <sup>-5</sup>	0.5	1.5 µm
Nano-nickel (Alfa Aesar)	1.5×10 <sup>-3</sup>	15.9	43 nm
Micro-copper (Sigma Aldrich)	2.5×10 <sup>-3</sup>	0.4	1.7 µm
Nano-copper (Alfa Aesar)	3.18×10 <sup>-2</sup>	13.5	50 nm
Aged nano-copper	7.13×10 <sup>-2</sup>	-	-
Nano-copper-oxide	4.3×10 <sup>-3</sup>	-	-
Nano-silver (Inframat Advanced Materials)	8.51	-	50–100 nm
Nano-silver, 500°C vacuum annealed	2.28	-	100–500 nm
Micro-MoS <sub>2</sub> (Sigma-Aldrich)	7.0×10 <sup>-3</sup>	-	<2 µm
Micro-WS <sub>2</sub> (Sigma-Aldrich)	2.5×10 <sup>-2</sup>	-	<2 µm
Nano-WS <sub>2</sub> (Nanostructured & Amorphous Materials Inc.)	2.7×10 <sup>-2</sup>	30	100–500 nm
Carbon black (Cabot M120)	4.5×10 <sup>-4</sup>	38	75 nm
Mesoporous carbon	1.25×10 <sup>-3</sup>	144	-
Activated carbon 1, undoped	2.0×10 <sup>-2</sup>	900 <sup>b</sup>	-
Activated carbon 2, undoped	1.15×10 <sup>-1</sup>	550 <sup>b</sup>	-
Activated carbon 3, S-impregnated (HgR, Calgon Carbon Corp.)	2.6	1000–1100	-
Micro-Se (commercial, ground, amorphous)	>5	0.03	10–200 µm
BSA-stabilized amorphous nano-Se	6.16×10 <sup>-1</sup>	65	6–59 nm
Unstabilized amorphous nano-Se	188	9	12–615 nm

(a) Inlet gas stream at 20 °C, 60 µg/m<sup>3</sup> Hg  
(b) Data provided by manufacturer

Metal sorbents composed of 2–9 mass% of Pt or Pd supported on alumina were tested for  $\text{Hg}^0$  capture at 204 °C, 288 °C, and 371 °C (Poulston et al. 2007). The synthetic gas with 45% CO, 35%  $\text{H}_2$ , 15%  $\text{N}_2$ , and 5%  $\text{CO}_2$  was passed through an Hg permeation tube. A metal sorbent with 8.5 mass% of Pd (8.5 Pd) showed the highest  $\text{Hg}^0$  loading of 2.7 mass% at 204 °C, whereas a sorbent with 8.9 mass% of Pt had 0.61 mass% of Hg. The  $\text{Hg}^0$  loading capacity increased with higher metal loading in the sorbent and decreased with increasing temperature.

The adsorption capacity of sulfur-abundant S/ $\text{FeS}_2$  was 2.73 mg/g at 80 °C under  $\text{N}_2$  atmosphere after 50 h when the normalized  $\text{Hg}^0$  concentration reached 50% (H Li et al. 2018). Note that the equilibrium  $\text{Hg}^0$  adsorption capacity is higher, but it was not reported in this study. The effect of 50–150 ppm  $\text{SO}_2$  on the adsorption capacity was negligible. The  $\text{Hg}^0$  removal efficiency of 88.6% was obtained when the simulated flue gas with 150 ppm  $\text{SO}_2$ , 75 ppm NO, 8%  $\text{H}_2\text{O}$ , and 4%  $\text{O}_2$  was used (Figure 4.10). Both elemental sulfur and sulfide from  $\text{FeS}_2$  were the active sites for  $\text{Hg}^0$  adsorption and formed  $\beta\text{-HgS}$ .

Metal sorbents range from commercially available to moderately available when engineered forms are required to be made from commercially available materials. The material and fabrication costs can be moderate to high depending on the selected material, and some of the materials discussed in this section are hazardous (e.g., Se), adding safety concerns. The Hg-loading capacities range from medium to high, with medium-to-high thermal stabilities and chemical stabilities. These materials can often be procured in powder or granular forms.

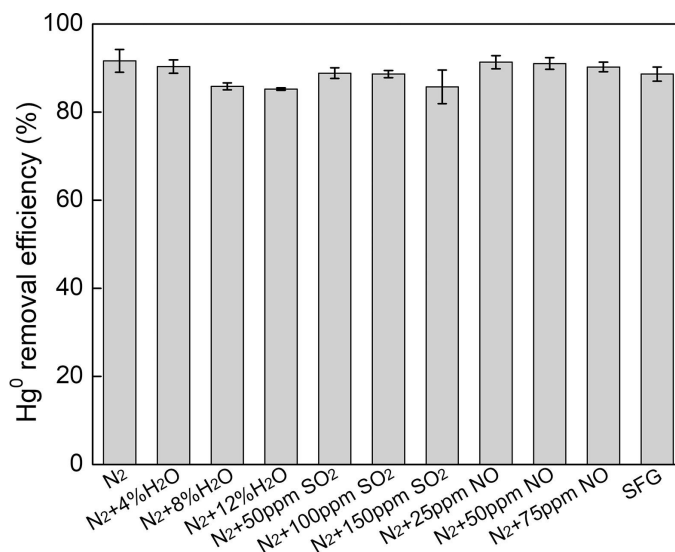


Figure 4.10. Effect of flue gas composition on the  $\text{Hg}^0$  removal efficiency for S/ $\text{FeS}_2$  material (H Li et al. 2018).

## 5.0 State of Gas-Phase Iodine Sorbent Technology

The discussion that follows identifies and summarizes the broad diversity of material types that could be or have been previously applied to the specific application of adsorbing/adsorbing I from gas-phase conditions. The viability of and propensity for the various materials to be applied for management of  $^{129}\text{I}$  emissions is also discussed. The focus here is on  $^{129}\text{I}$  abatement in the WTP LAW and HLW facilities' secondary off-gas systems, but the results have application across the DOE-EM complex and other entities. In the nuclear energy industry (funded by the DOE Office of Nuclear Energy), materials for effective I capture (including  $\text{I}_{2(\text{g})}$ ,  $\text{CH}_3\text{I}$ , and others) have been investigated for over 50 years from reprocessing of used nuclear fuel and capture of  $^{129}\text{I}$  released from nuclear accidents.

Many different classes of materials have been evaluated for I capture from the gaseous state, including porous inorganic crystalline matrices (e.g., zeolites), inorganic aerogels, inorganic xerogels, porous organic structures, AC, and non-porous metal substrates (e.g., metal particles, metal wires). A non-exhaustive summary of I sorbents is provided in Table 5.1, with citations to the original works in the literature. Some of these materials are commercially available, whereas many are under a lower level of technical maturity and have limited demonstration data for this application.

Subsequent subsections address the individual material classes for gas-phase sorption of I and relevant attributes and performance under their associated test conditions.

Table 5.1. Overview of iodine capture material types and commercial availabilities.

Material type	Specific Material <sup>(a)</sup>	Reference	Commercially available? <sup>(b)</sup>
Zeolite	Ag-faujasite (AgX)	Riley et al. (2022)	Yes
	Ag-mordenite (AgZ)	Riley et al. (2017)	Yes
Chalcogel	NiMoS <sub>4</sub> , CoMoS <sub>4</sub> , Sb <sub>4</sub> Sn <sub>3</sub> S <sub>12</sub> , Zn <sub>2</sub> Sn <sub>2</sub> S <sub>6</sub> , KCoS <sub>x</sub> , Pt <sub>2</sub> Ge <sub>5</sub> S <sub>10</sub> , Sn <sub>2</sub> S <sub>3</sub>	Subrahmanyam et al. (2015); Riley et al. (2011, 2013, 2014, 2015)	No
Silica aerogel	Ag <sup>0</sup> -S-SiO <sub>2</sub> aero	Strachan et al. (2010)	No
Aluminosilicate aerogels	AgAlSiO <sub>4</sub> aero; S-AgAlSiO <sub>4</sub> aero	Riley et al. (2017); Chong et al. (2020)	No
Aluminosilicate xerogels	AgAlSiO <sub>4</sub> xero; S-AgAlSiO <sub>4</sub> xero	Riley et al. (2022)	No
Metal wires	Ag, Cu, In, Sn	Riley et al. (2021)	Yes
Metal-PAN composites	Ag, Bi, Cu, Sn	Chong et al. (2022)	No
Metal foams	Ag(Ni), Bi(Ni)	Tian et al. (2021)	No
MOFs	ZIF-8, Cu-BTC	Sava et al. (2011, 2013)	Yes
COFs	COF-TAPT; TPB-DMTP; TTA-TTB; ETTA-TPA	Xie et al. (2022); Wang et al. (2018)	No
PAF	P-DPDA; P-TPB; P-PC; PAF-23; PAF-24; PAF-25	Wang et al. (2021); Yan et al. (2015)	No
POPs/CMPs	POP-1; POP-2; HCMP-1; HCMP-2; HCMP-3; HCMP-4	Qian et al. (2017); Liao et al. (2016)	No
Carbon	Bi-carbon foam; activated carbon	Baskaran et al. (2022); Wren et al. (1999)	Yes/no

(a) The term "S" in the material description denotes that the sorbent is thiolated (i.e., it contains –S– groups).

(b) Example commercially available materials include: AgZ is IONEX Ag-900; AgX is IONEX Ag-400; ZIF-8 is BASF Basolite Z1200 and Cu-BTC is BASF Basolite C300 (both available from Sigma Aldrich).

PAN = polyacrylonitrile; MOF = metal organic framework; COF = covalent organic framework; PAF = porous aromatic framework; POP = porous organic polymer.

## 5.1 Porous Inorganic Crystalline Matrices (e.g., Zeolites)

Porous inorganic crystalline matrices (e.g., zeolites) were introduced in Section 4.1. Several types of porous crystalline matrices have been evaluated for iodine capture within the literature for more than 50 years. The majority of I capture studies in this category include metal-exchanged zeolites, with the overwhelming amount of studies being done on various forms of Ag-mordenite (AgZ) and Ag-faujasite (AgX). Both AgZ and AgX are available commercially through IONEX as Ag-900 and Ag-400, respectively. Several studies were published in the 1970s and 1980s on Zeolon products from Norton Company, and it is unclear from various sources whether or not Zeolon 900 is related to the IONEX Ag-900 mordenite despite Oak Ridge National Laboratory (ORNL) reports claiming they are the same sorbent (Jubin and Bruffey 2015).<sup>3,4</sup> The Ag-mordenite sorbent (generally referred to as AgZ) was said to have superior acid resistance (Holladay 1979) over other zeolites, including X-type and Y-type faujasite zeolites, and this is attributed to the higher fraction of SiO<sub>2</sub> present in mordenites over other zeolite types (see Figure 5.1).

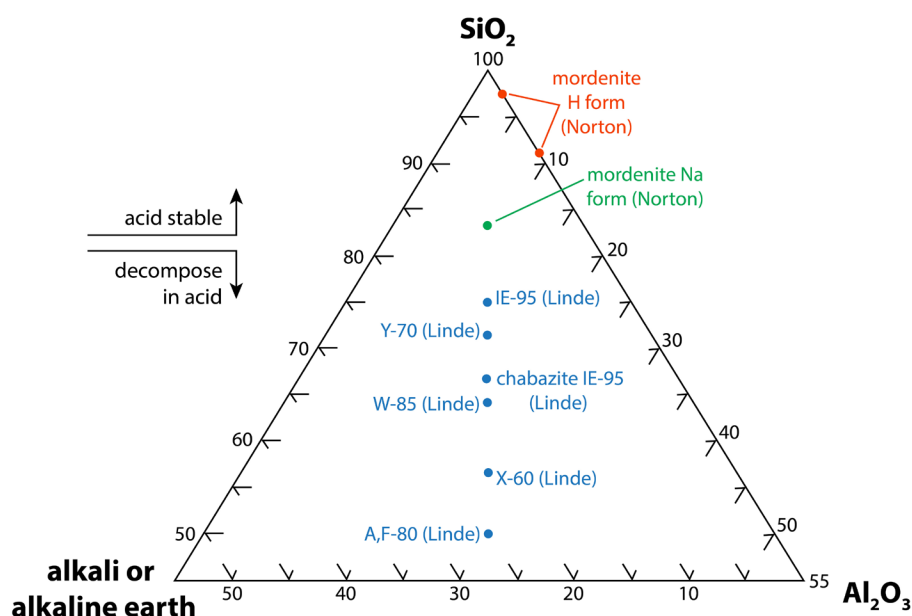


Figure 5.1. SiO<sub>2</sub>-Al<sub>2</sub>O<sub>3</sub>-(alkali or alkaline earth) ternary diagram for zeolite minerals that shows the acid stability (Jubin 1988)<sup>5</sup> (modified from ORNL drawing 78-15097).

While mordenite, X-faujasite, and Y-faujasite are all zeolites, they differ in composition (i.e., Si:Al molar ratios) and crystal structure (see Figure 5.2). In general, the Si:Al molar ratio found in mordenite is typically 5:1, while the different faujasite zeolites are characterized by lower ratios: Si/Al < 2 for zeolite X and Si/Al > 2 for zeolite Y. The aluminosilicate zeolites contain negatively charged frameworks built from AlO<sub>4</sub><sup>5-</sup> and SiO<sub>4</sub><sup>4-</sup> tetrahedra, and the charge balance is provided by a variety of metal cations (or H<sup>+</sup>), often including alkalis and alkaline earths. It is these charge balancing cations that can be exchanged for active getters such as Ag<sup>+</sup> for applications in radionuclide scavenging (e.g., I or Hg capture). Several experimental and

<sup>3</sup> According to researchers at the IONEX Research Corporation, Norton's products were large-pore mordenites while the Ag-900 from Douglas Porrey (CEO) at IONEX Research Corporation is a small-pore mordenite.

<sup>4</sup> According to Norton Company Bulletin Z-51, "Zeolon Acid Resistant Molecular Sieves," the clay binder in Norton Zeolon-900 is what helped provide acid resistance in this sorbent. IONEX Research Corporation claims that IONEX Ag-900 mordenite does not contain a binder (is self-binding), so this is another difference.

<sup>5</sup> The information for this figure is derived from Norton Company, Chemical Process Products Division, 1976. "Zeolon Acid Resistant Molecular Sieves," Bulletin Z-51, 1976, Akron, Ohio.

modeling (conceptual) studies have included data on I capture for different metal-exchanged zeolites to find the optimum base zeolite structure, Si:Al molar ratio, metal getter (e.g., Ag, Cd, Pb), and metal getter loading (Maeck and Pence 1970; Pence et al. 1972; Thomas et al. 1977; Holladay 1979; Bruffey and Jubin 2015; Bruffey et al. 2016; Chibani et al. 2016; Ayadi et al. 2022).

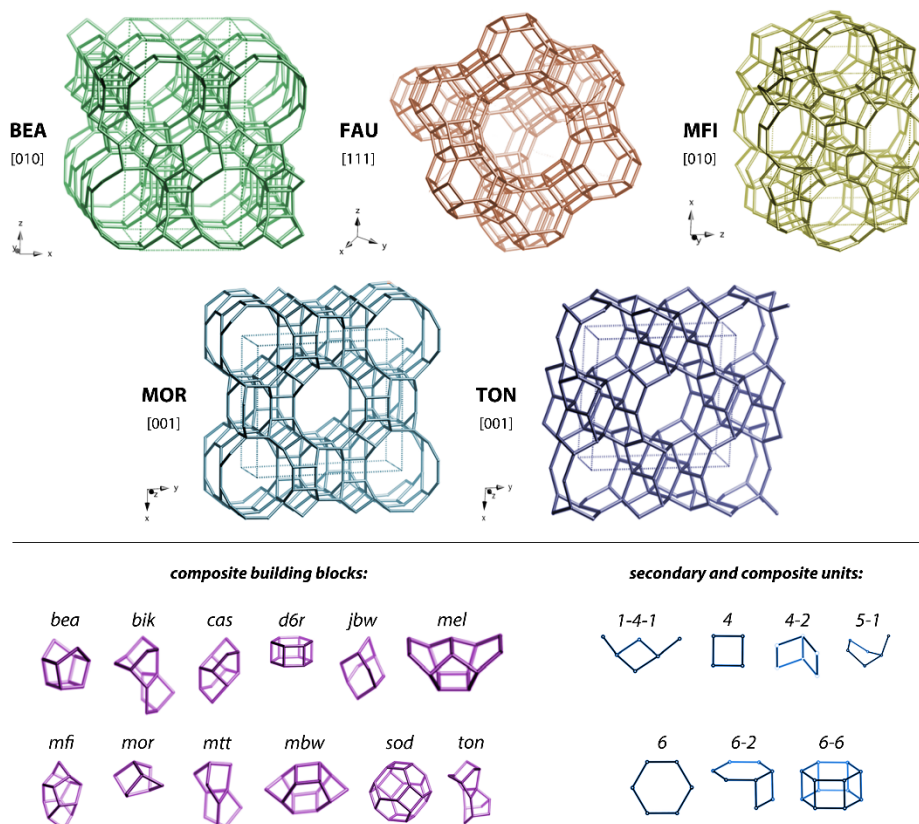


Figure 5.2. General summary of zeolite structures, including BEA, FAU (faujasite), MFI, MOR (mordenite), and TON, including the crystal structures on top and the building blocks below (modified from Baerlocher et al. 2007).

While Ag-exchanged zeolites are commercially available, they tend to have low I capacities and are not completely stable in oxidizing conditions. For example, aging studies on AgZ (IONEX Ag-900) performed by Bruffey et al. (2015b) at ORNL in 1% NO for 2 months showed an 80% loss of I capacity. They also tend to be rather expensive to procure commercially (e.g., Sigma Aldrich, Molecular Products, IONEX Research Corporation). These materials are chemically stable in air at moderate temperatures (>400 °C) and are mechanically stable with high mechanical integrity.

The capture mechanism for Ag-based zeolites is chemisorption, whereby Ag in the zeolites reacts to form AgI crystals through chemisorption mechanisms, which are environmentally stable with low release rates. Waste forms have been demonstrated using hot isostatic pressing or spark plasma sintering (Bruffey et al. 2016, 2017a,b).<sup>6</sup> In comparisons between IONEX Ag-900 (AgZ) and Ag-400 (AgX), the I-loading capacities of AgX are much higher at ~333 mg/g compared to AgZ at ~131 mg/g. The Ag utilization, which is the molar ratio of I:Ag, tends to be much higher in the AgZ (85%–92%) compared to AgX (33%–60%)

<sup>6</sup> Spark plasma sintering data on iodine-loaded zeolites includes unpublished work from PNNL.

(Holladay 1979), and it is unclear why so little of the Ag is utilized for AgX compared to that of AgZ.<sup>7</sup> This difference, which includes the expense of added Ag (a precious metal) that is not being used, coupled with the presumed lower acid resistance of AgX based on previous literature data (Holladay 1979), suggests that AgX would not fare as well as AgZ in these conditions. However, AgX has remained relatively untested in the recent past for these types of applications compared to the way that AgZ has been tested in aging environments, in oxidizing gas conditions, and with competing species (Bruffey et al. 2014, 2015a; Holladay 1979). Ag-impregnated titania has also shown proficiency for I uptake with up to 25 mass% in static humid conditions (Wu et al. 2014).

In general, these types of sorbents are available commercially; for example, AgX (IONEX Ag-400) and AgZ (IONEX Ag-900) are both manufactured in bulk forms of different granular types, including cylindrical pellets and/or spherical beads. The primary getter utilized in these materials is Ag, and disposal of Ag-containing materials is controlled by the U.S. Environmental Protection Agency through the RCRA, so these materials add a regulatory concern. The chemical and mechanical stabilities of Ag-zeolites are generally good, but the I-loading capacities decrease under oxidizing conditions.

## 5.2 Inorganic Aerogels

Inorganic aerogels were initially discussed in Section 4.2. Several inorganic aerogels have been evaluated for I capture, including silica-based, aluminosilicate-based, and chalcogen (S,Se)-based materials (called chalcogels). Oxide-based aerogels are produced by combining metal alkoxides (e.g., tetraethyl orthosilicate, aluminum tri-*sec*-butoxide, sodium ethoxide) through hydrolysis and polycondensation reactions in a common solvent including water, often alcohols, and some type of acidic (e.g., CH<sub>3</sub>COOH) or basic (e.g., NH<sub>4</sub>OH) catalyst (Brinker and Scherer 1990). For chalcogel synthesis, the base materials are produced through alkoxide thiolation, nanoparticle aggregation, or metathesis reactions of chalcogen-containing complexes (Riley and Chong 2020). For all gels, the base hydrogel gel (after gelation) is converted to an alcogel through the removal of the solvent after gelation with a pure alcohol (e.g., ethanol), and then the alcohol can be removed with a critical point dryer using a supercritical fluid (e.g., CO<sub>2</sub>). The critical point drying process requires a pressure chamber, and the sample throughput volume is directly proportional to the vessel size. This process is tedious and utilizes a large volume of liquid CO<sub>2</sub>.

A lot of off-gas testing under different environmental conditions has been done with the silver-functionalized silica aerogel (SFSA) sorbent developed at PNNL (Matyáš et al. 2011; Strachan et al. 2010); Figure 5.3 provides a schematic of the synthesis process for making SFSA sorbents. These materials are produced by removing trimethylsilyl surface groups from commercially available silica aerogels through a heat treatment at 750 °C, followed by thiolation with (3-mercaptopropyl) trimethoxysilane in supercritical CO<sub>2</sub> at 150 °C, Ag loading in AgNO<sub>3</sub> solution, and Ag reduction to Ag<sup>0</sup> in an H<sub>2</sub>/Ar atmosphere. These sorbents have been evaluated under a variety of conditions, including saturated I, 4.2 ppm I in air, and under various oxidizing conditions containing I to simulate aging. Aging studies, including some I loading tests after aging for this material, were performed at ORNL by Bruffey et al. (2012, 2013, 2015a,b), Jubin et al. (2014) and Matyáš et al. (2016, 2018). In these aging studies, samples of the SFSA provided by PNNL were subjected to humidity, 2% NO<sub>2</sub>, and 1% NO for extended periods. Aging in 2% NO<sub>2</sub> for up to 2 months showed a 15% loss in I capacity, and 1% NO at 150 °C for 2 months showed a 43% loss in I capacity. Iodine reactions for these materials are based on chemisorption of AgI formation and are very stable upon formation.

<sup>7</sup> Some of these values are based on unpublished data acquired at PNNL comparing Ag-400 with Ag-900.

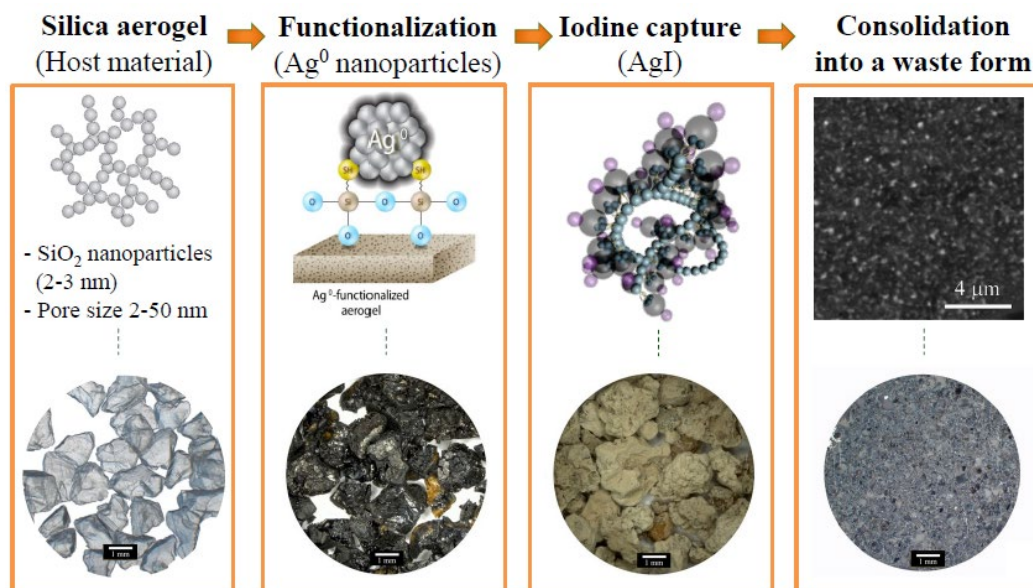


Figure 5.3. Pathway for producing SFSA iodine sorbents and subsequent waste forms (after iodine loading) showing the various synthesis stages, including the host material, the Ag-functionalization process, the iodine capture process, and the final waste form.

Researchers at PNNL are working on aluminosilicate aerogels that can be ion exchanged with different metal getters (see Figure 5.4). These materials are produced with target compositions of NaAlSiO<sub>4</sub>, and the Na<sup>+</sup> ions are ion exchanged out of the gel for metals like Ag<sup>+</sup>, Cu<sup>+</sup>, Sn<sup>2+</sup>, and Sn<sup>4+</sup> (Riley et al. 2017, 2020). These materials have only been tested in saturated I conditions, and the technical maturity is low, but some of these materials have high I loadings, including 553 mg/g for NAS-12a-SH-AgI (Riley et al. 2017) and 881 mg/g for 12bA-Sn<sup>4+</sup>+I (Riley et al. 2020). These materials can be produced in powdered or granular forms that have low-to-moderate mechanical integrity but can be further strengthened through heat-treatment processes. Synthesis of these aerogels is limited to volume of the critical point dryer. Some of the more promising materials require the utilization of toxic elements (e.g., Ag) or toxic solvents (e.g., ethanol, formamide) to prepare the base materials for the ion exchange process.



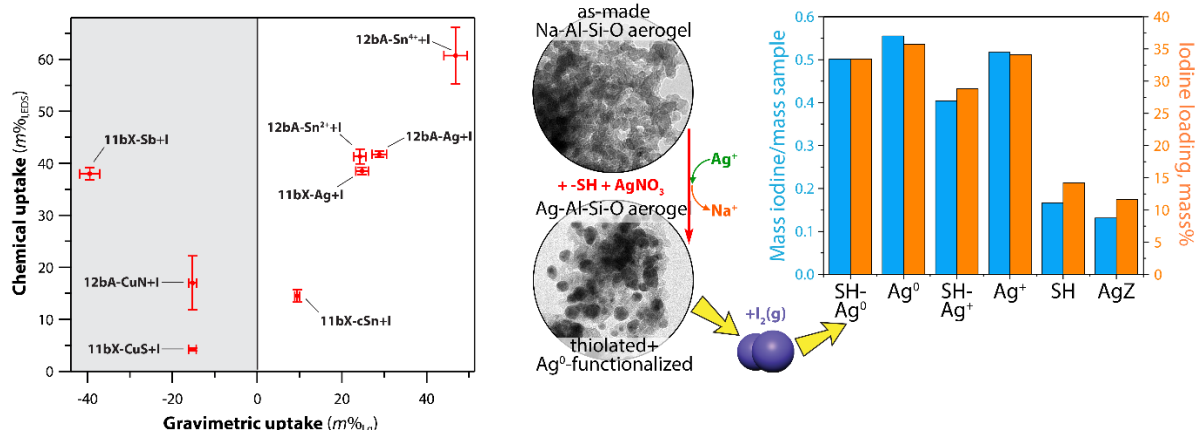


Figure 5.4. (left) Chemical uptake (measured with energy dispersive X-ray spectroscopy) vs. gravimetric uptake (measured by mass change during uptake experiment) of various aluminosilicate aerogels and xerogels loaded with different metal getters (Riley et al. 2020). (right) Summary of iodine loadings in terms of iodine loadings (g/g) as well as mass% iodine in the final materials, including thiolated Ag<sup>0</sup>AlSiO<sub>4</sub> aerogels (SH-Ag<sup>0</sup>), Ag<sup>0</sup>AlSiO<sub>4</sub> aerogels (Ag<sup>0</sup>), thiolated Ag<sup>+</sup>AlSiO<sub>4</sub> aerogels (SH-Ag<sup>+</sup>), Ag<sup>+</sup>AlSiO<sub>4</sub> aerogels (Ag<sup>+</sup>), thiolated NaAlSiO<sub>4</sub> aerogels (before Ag exchange), and silver mordenite (AgZ) for comparison (Riley et al. 2017).

Additional inorganic aerogel work at PNNL included research on sulfide-based aerogels referred to as chalcogels. These materials were produced through the combination of chalcogenide clusters and metal linkers to create combinations including NiMoS<sub>4</sub> (2250 mg/g), CoMoS<sub>4</sub> (2000 mg/g), Sb<sub>4</sub>Sn<sub>3</sub>S<sub>12</sub> (2000 mg/g), Zn<sub>2</sub>Sn<sub>2</sub>S<sub>6</sub> (2250 mg/g), KCoS<sub>x</sub> (1600 mg/g), Pt<sub>2</sub>Ge<sub>5</sub>S<sub>10</sub> (>2000 mg/g), and Sn<sub>2</sub>S<sub>3</sub> (~2000 mg/g), with maximum I loadings under saturated conditions listed in parentheses (*q<sub>e</sub>* in terms of milligrams I loading per gram of sorbent) (Subrahmanyam et al. 2015; Riley et al. 2011, 2013, 2014, 2015). These materials have very high maximum I loadings in saturated conditions, and the ones that have been tested in 4.2 ppm iodine concentrations in air (including Pt<sub>2</sub>Ge<sub>5</sub>S<sub>10</sub>, Co<sub>0.5</sub>Ni<sub>0.5</sub>MoS<sub>4</sub>, and Sn<sub>2</sub>S<sub>3</sub>) show high I removal in these low-concentration I streams (Riley et al. 2013); see Figure 5.5. These materials appear to utilize a mixture of chemisorption and physisorption capture mechanisms based on the X-ray diffraction (XRD) data that sometimes show crystalline iodide complexes in the loaded materials [e.g., SnI<sub>4</sub>, SbI<sub>3</sub>, KI, SnI<sub>4</sub>(S<sub>8</sub>)<sub>2</sub>] (Subrahmanyam et al. 2015; Riley et al. 2015), but often do not show any crystalline diffraction. These sorbents are not commercially available and can be quite expensive to synthesize. Also, many of the required precursors are not commercially available and require synthesis in the laboratory, e.g., Na<sub>4</sub>Sn<sub>2</sub>S<sub>6</sub>·14H<sub>2</sub>O, [(CH<sub>3</sub>)<sub>4</sub>N]<sub>4</sub>Ge<sub>4</sub>Se<sub>10</sub>, [(CH<sub>3</sub>)<sub>4</sub>N]<sub>4</sub>Ge<sub>4</sub>Se<sub>10</sub>, [(C<sub>2</sub>H<sub>5</sub>)<sub>4</sub>N]<sub>4</sub>Ge<sub>4</sub>Se<sub>10</sub> (Bag et al. 2007; Riley et al. 2011, 2015; Subrahmanyam et al. 2015). Several of these reactants are also quite toxic to handle.



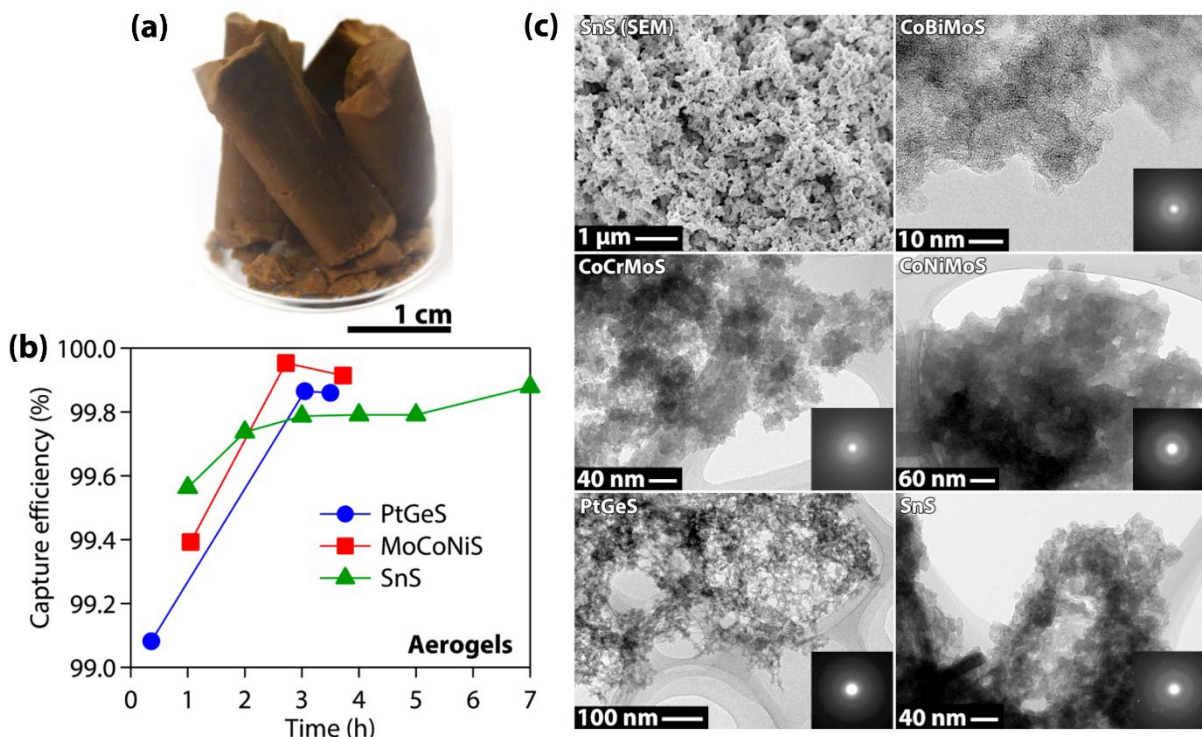


Figure 5.5. (a) Picture of Pt<sub>2</sub>Ge<sub>5</sub>S<sub>10</sub> chalcogels (Riley et al. 2011). (b) Summary of iodine capture with chalcogels in a 4.2-ppm iodine stream over different times, including Pt<sub>2</sub>Ge<sub>5</sub>S<sub>10</sub>, Co<sub>0.5</sub>Ni<sub>0.5</sub>MoS<sub>4</sub>, and Sn<sub>2</sub>S<sub>3</sub> aerogels (Riley et al. 2013). (c) Scanning electron and transmission electron micrographs of different chalcogels (Riley et al. 2013).

The chemical stabilities of these sorbents are unknown, and they have low mechanical stability. In general, the high costs to produce chalcogels and the difficulties in scaling up production volumes make them less attractive. Waste form demonstrations have been very limited (Riley et al. 2015). These materials tend to have low mechanical stability as well with friable and fragile surfaces.

### 5.3 Inorganic Sulfide Materials

Some initial information about inorganic sulfide sorbents is included in Section 4.3. Recent studies were done on inorganic sulfide-polymer composite structures that show promise. In particular, Bi<sub>2</sub>S<sub>3</sub> (Yu et al. 2020) and SnS<sub>2</sub> (Yu et al. 2021) were embedded into polyacrylonitrile (PAN) composites at various loading values (Figure 5.6). Due to the high sulfur (S) content in both of these composite sorbent materials and, due to the fact that S is freed up from the initial metal (i.e., Bi<sub>2</sub>S<sub>3</sub> + 3 I<sub>2</sub> → 2 BiI<sub>3</sub> + 3 S and SnS<sub>2</sub> + 2 I<sub>2</sub> → SnI<sub>4</sub> + 2 S), it is likely that the residual S after I capture could be used as a getter for Hg vapors for the given application. For both sets of sulfide-PAN composites, these were produced by suspending flower-like sulfides in a mixture of PAN dissolved in dimethyl sulfoxide (DMSO), followed by precipitation of sphere-like beads in a water bath. For the Bi<sub>2</sub>S<sub>3</sub>-PAN composites, Bi<sub>2</sub>S<sub>3</sub> loadings (in PAN) were varied from 30% to 90% by mass, where I loadings varied within these materials from 490 mg/g to 1203 mg/g with the phase formed being BiI<sub>3</sub> (Yu et al. 2020). For the SnS<sub>2</sub>-PAN composites, beads were made with SnS<sub>2</sub> loadings (in PAN) of 10% to 90%, and maximum I loadings of up to 2727 mg/g were noted with the phase formed being SnI<sub>4</sub> (Yu et al. 2021). The costs to produce these types of composite materials are moderate based on the costs of the sulfide compounds (i.e., Bi<sub>2</sub>S<sub>3</sub> and SnS<sub>2</sub>), whereas PAN is very affordable. To produce these materials, toxic solvents (DMSO) are required. The iodine loading process produced metal iodides through chemisorption processes. The mechanical integrity is high as the PAN matrix allows for some springback.

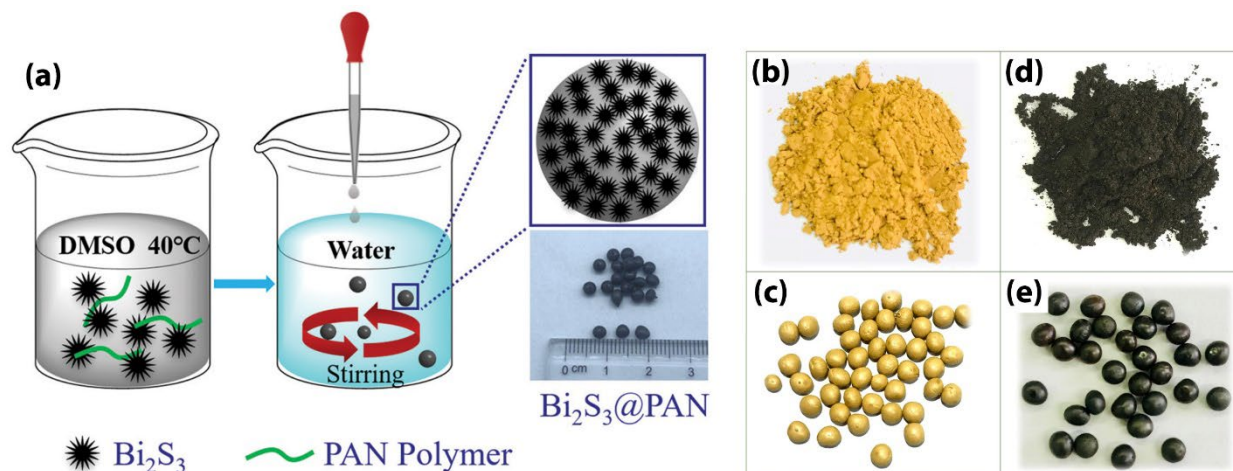


Figure 5.6. (a) Summary of PAN-Bi<sub>2</sub>S<sub>3</sub> composite synthesis process (Yu et al. 2020). SnS<sub>2</sub> study for iodine capture including pure SnS<sub>2</sub> powder (b) before and (d) after iodine loading as well as SnS<sub>2</sub>-PAN composites (c) before and (e) after iodine loading (Yu et al. 2021).

It is unclear how well the polymer matrix would withstand the harsh environmental conditions expected in the WTP off-gas system. To date, the only viable waste form concepts for PAN composite sorbents is to grout them into a monolithic form.

## 5.4 Inorganic Xerogels

In addition to aluminosilicate aerogels, PNNL is also developing AgAlSiO<sub>4</sub> xerogels (Chong et al. 2020, 2021; Riley et al. 2020, 2022). These xerogels use feedstock materials similar to those used by the aerogels discussed previously, but are instead dried using an ambient temperature process instead of requiring a critical point dryer with supercritical CO<sub>2</sub> used to produce aerogels. Thus, xerogels should be significantly cheaper to manufacture at larger volumes than equivalent aerogels. While both aerogel and xerogels tend to have moderate SSA values, aerogels often have higher SSA values than xerogel equivalents, but this is not always the case, especially after subsequent treatments following synthesis (e.g., Ag<sup>+</sup> exchange) (Chong et al. 2020).

Xerogels have high maximum I loadings that are directly tied to the Ag loadings in these sorbents. They also have much higher mechanical integrity compared to the equivalent AgAlSiO<sub>4</sub> aerogel sorbents with similar I loadings of up to 522 mg/g for heat-treated-thiolated-Ag<sup>0</sup> xerogels (HTX-S-Ag<sup>0</sup>) and 497 mg/g heat-treated-unthiolated Ag<sup>0</sup> xerogels (HTX-Ag<sup>0</sup>) (Riley et al. 2022). An evaluation with dynamic mechanical analysis testing comparing the heat-treated NaAlSiO<sub>4</sub> aerogels with equivalent heat-treated NaAlSiO<sub>4</sub> xerogels showed that the xerogels had 163-fold higher hardness (Chong et al. 2021), as shown in Figure 5.7, so the xerogels have a notably more robust structure than the aerogels. The thiolation process for the heat-treated xerogels was much less damaging to the pore structure of the base sorbent, where the SSA value of thiolated heat-treated xerogels was 294 m<sup>2</sup>/g compared to ~30 m<sup>2</sup>/g for the equivalent thiolated aerogel materials. After Ag exchange (i.e., Na<sup>+</sup>AlSiO<sub>4</sub> → Ag<sup>+</sup>AlSiO<sub>4</sub>), the xerogels (HTX-S-Ag<sup>+</sup>) had an SSA value of 118 m<sup>2</sup>/g whereas the aerogel equivalent (HTA-S-Ag<sup>+</sup>) was around 30 m<sup>2</sup>/g (Riley et al. 2017, 2022). This shows that the xerogel starting materials are more robust and fare better during subsequent treatments. Details are provided in Table 5.1 for the overview of the properties of this class of materials. In general, this class of materials is more mechanically stable than aerogels and should be cheaper to produce. The usage of Ag is a problem from an RCRA disposal restrictions standpoint, but it is plausible that other metals could be used in place of Ag, such as Cu or Sn, based on other work (Riley et al. 2020). Very limited waste form work has been conducted to date.

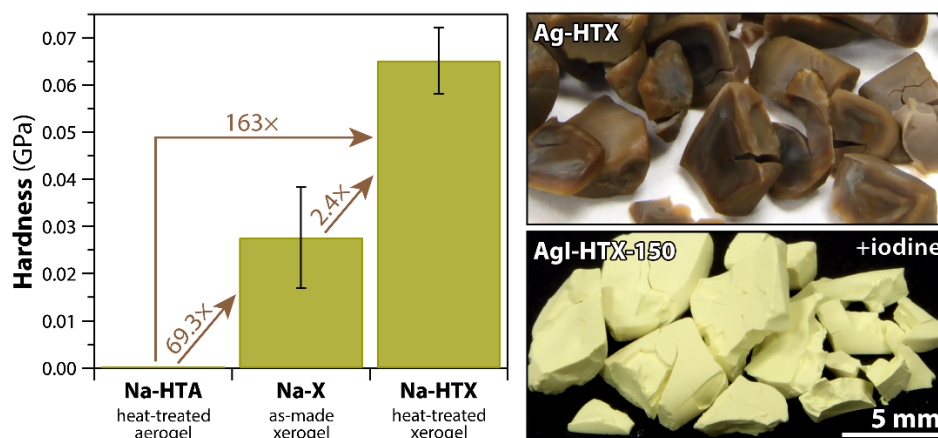


Figure 5.7. (left) Hardness comparison between heat-treated NaAlSiO<sub>4</sub> aerogels (Na-HTA), as-made NaAlSiO<sub>4</sub> xerogels (Na-X), and heat-treated NaAlSiO<sub>4</sub> xerogels (Na-HTX) prior to Ag-loading (i.e., AgAlSiO<sub>4</sub> shown in the top right as Ag-HTX) and iodine loading (AgAlSiO<sub>4</sub>+I shown in the bottom right as AgI-HTX-150) (Chong et al. 2021).

## 5.5 Porous Organic Sorbents

Porous organic sorbents were introduced in Section 4.4. Iodine capture has been demonstrated in a number of different porous organic structures, including MOFs (see Section 5.5.1) (Valizadeh et al. 2018; Sava et al. 2011, 2013), COFs (see Section 5.5.2) (Wang et al. 2018; Zhang et al. 2021; Xie et al. 2022), porous aromatic frameworks (PAFs; see Section 5.5.3) (Yan et al. 2015; Wang et al. 2021), and POPs (see Section 5.5.4) (Qian et al. 2017; Xie et al. 2019), which also include conjugated microporous polymers (CMPs) (Liao et al. 2016; Wang et al. 2019). These types of materials are highly tailorable with a wide range of chemistries. The main limitations of these types of materials are that (1) they are often not available commercially and thus have to be produced; (2) the materials that are commercially available are often very expensive; (3) production often requires high-pressure processes (e.g., autoclaves) at small volume scales, which can limit scale-up; and (4) these materials are often produced in very small particle sizes, making implementation in an off-gas system difficult. These materials are very rarely available commercially, but show a lot of promise in terms of iodine capacities, which can often be >4,000 mg/g. They also tend to capture iodine based solely on physisorption-based processes, so the iodine capture process can be reversible if desired for sorbent recycle. The path to an environmentally stable waste form for these materials following I loading is unclear.

### 5.5.1 Metal Organic Frameworks

More information about MOFs is provided in Section 4.4.1. Two MOFs that have been evaluated for I capture include ZIF-8 (Sava et al. 2011) and Cu-BTC (Sava et al. 2013). The ZIF-8 showed I loadings of up to 1250 mg/g under loading conditions of 350 K (~77 °C) air and I vapor pressures of 0.014 atm, and maximum loadings were achieved within 5–12 h. The Cu-BTC showed I-loading values of 1750 mg/g. A third MOF is HKUST-1, where the MOF was loaded into different polymers, including polyacrylamide (PAM) as well as three hydrophobic polymers of polyethersulfone (PES), polyetherimide (PEI), and polyvinyl difluoride (PVDF) (Valizadeh et al. 2018). The HKUST-1 was loaded into these polymer matrices at a 70 mass% loading. The iodine capture performance varied among these different composite sorbents, where HKUST-1@PVDF, HKUST-1@PES (see Figure 5.8), and HKUST-1@PEI showed maximum iodine sorption values of 225 mg/g, 348 mg/g, and 498 mg/g, respectively. While these values are lower than desired, these materials do have the ability for regeneration. The MOF sorbents tend to perform well at the 70–80 °C temperature range, but it is unclear how well these materials would perform



in off-gas conditions where species are competing for binding sites [e.g.,  $\text{Cl}_{2(g)}$ ] or oxidizers (e.g.,  $\text{NO}_x$ ). In a separate study, He et al. (2021) demonstrated that a nitrogen-rich MOF had a high capacity for iodine (6 g I/g sorbent) and methyl iodide (1.45 g/g) in simple gases under dynamic conditions, showing the promise of MOF with the correct functionality.

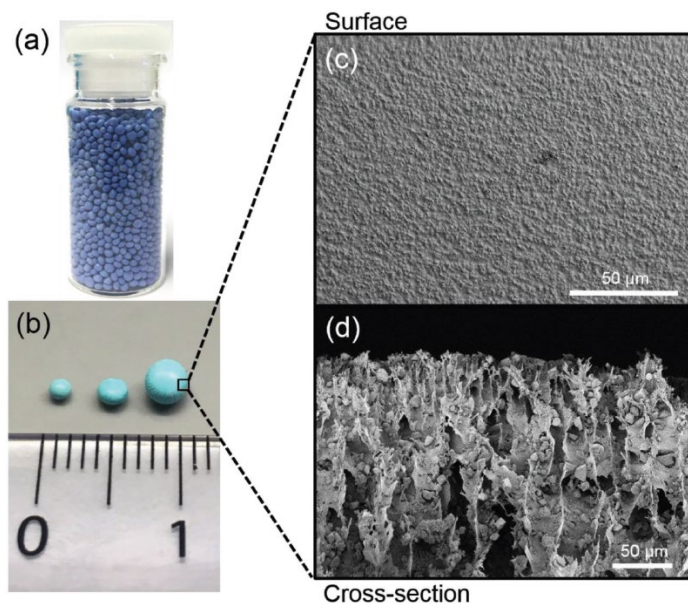


Figure 5.8. (a) Picture of activated HKUST-1@PES composite sorbent beads, (b) pictures of these beads at different sizes, (c) picture of the surface of a bead, and (d) a scanning electron microscopy (SEM) micrograph of the cross-sectional view of the outside of a bead. (Taken from Valizadeh et al. 2018).

### 5.5.2 Covalent Organic Frameworks

More information about COFs is provided in Section 4.4.2. COFs are 2- or 3-dimensional materials synthesized with organic precursors and have strong covalent bonds. These materials have a demonstrated ability to capture  $\text{I}_{2(g)}$  as well as  $\text{CH}_3\text{I}$  with very high capacities and demonstrated regeneration options in some cases. In a study by Xie et al. (2022), the COF called COF-TAPT [TAPT is an abbreviation for 2,4,6-tri(4-aminophenyl)-1,3,5-triazine] was shown to capture both  $\text{I}_2$  and  $\text{CH}_3\text{I}$  at low concentrations. This material also was demonstrated to capture up to 1530 mg/g  $\text{CH}_3\text{I}$  at 25 °C. In a mixed-gas experiment with 150 ppm  $\text{I}_2$  and 50 ppm of  $\text{CH}_3\text{I}$ , this material captured 1510 mg/g total mixed iodine. In a study by Wang et al. (2018), COFs were produced with extremely high iodine loadings and the ability to be regenerated. The highest iodine loadings in this study were achieved with TPB-DMTP (6300 mg/g; triphenylbenzene dimethoxyterephthaldehyde), TTA-TTB (5000 mg/g), and ETTA-TPA (1,4-terephthaldicarbaldehyde) (4700 mg/g) after loading at ~77 °C (350 K); see Figure 5.9. The TPB-DMTP and TTA-TTB [4,4',4''-(1,3,5-triazine-2,4,6-triyl)trianiline 4,4',4''-(1,3,5-triazine-2,4,6-triyl)tribenzaldehyde] COFs are thermally stable in nitrogen up to 400 °C and 500 °C, respectively, and both are also stable in pH 14 NaOH solutions.

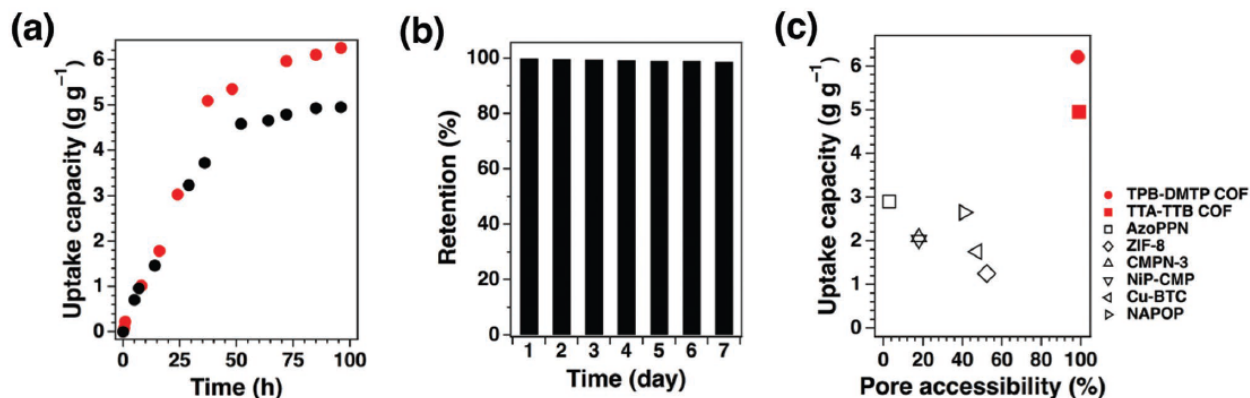


Figure 5.9. (a) Summary of iodine uptake of the TPB-DMTP (red) and TTA-TTB (black) COFs during iodine exposure time at  $\sim 77^\circ\text{C}$  (350 K). (b) Iodine retention after exposure to  $25^\circ\text{C}$  in air. (c) Iodine capacities of different porous organic sorbents, including various COFs and MOFs. (Taken from Wang et al. 2018.)

Two COFs produced in a study by Zhang et al. (2021) had very high iodine capacities of 5885 mg/g (TJNU-203) and 5335 mg/g (TJNU-204). These materials were produced through condensation reactions between 1,3,5-trimethyl-2,4,6-tris(4-aminophenyl)benzene (called TMTAPB) and terephthalaldehyde (TPA) [or 2,5-dihydroxy-1,4-benzenedicarboxaldehyde (DHA)] in a 50/50 (vol/vol) solvent mixture of 1,2-dichlorobenzene and n-butanol. These reactions were performed in the presence of aqueous 3M acetic acid at  $120^\circ\text{C}$  over the course of 3 days. Iodine loading experiments were conducted on these materials at a temperature of 350 K ( $77^\circ\text{C}$ ) in air using iodine sublimation. The capture kinetics show extremely fast capture in very short times (Figure 5.10). Recycling potential for these sorbents was also demonstrated by heating iodine-loaded sorbents to  $150^\circ\text{C}$  under vacuum, where TJNU-203 and TJNU-304 revealed iodine loading values of 4162 mg/g and 2876 mg/g, respectively, even after five regeneration cycles.

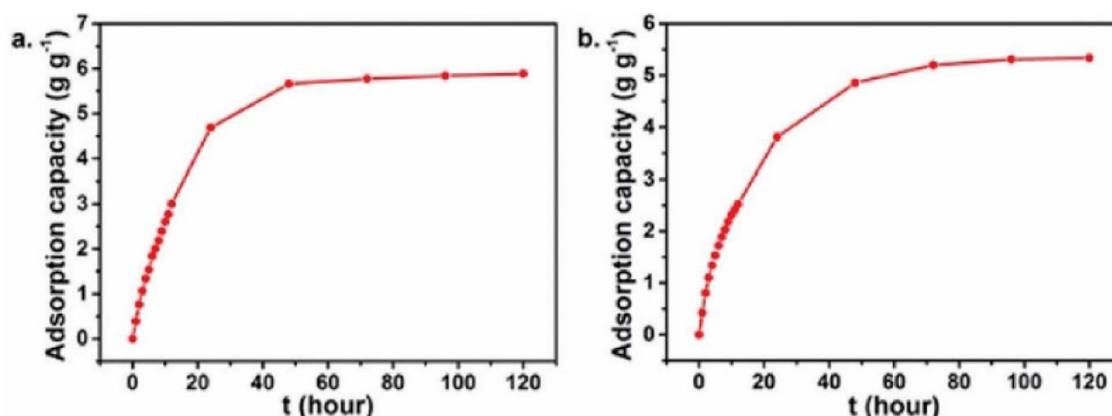


Figure 5.10. Summary of  $\text{I}_{2(g)}$  mass loadings for COFs (a) TJNU-203 and (b) TJNU-204 over time at  $77^\circ\text{C}$  in air (Zhang et al. 2021).

### 5.5.3 Porous Aromatic Frameworks

PAFs are high-SSA solids produced through bonding (C–C) and interlinking of aromatic units, and some of these materials have SSA values of  $>5000\text{ m}^2/\text{g}$  (Tian and Zhu 2020). In a study by Wang et al. (2021), PAFs of P-DPDA, P-TPB, and P-PC were shown to have iodine capacities of 4080 mg/g, 3350 mg/g, and 2680 mg/g, respectively, after loading at 348 K ( $75^\circ\text{C}$ ) in air (see Figure 5.11). In a study by Yan et al.

(2015), PAFs including PAF-23, PAF-24, and PAF-25 were shown to capture very large quantities of iodine (2710 mg/g, 2760 mg/g, and 2600 mg/g, respectively) at 75 °C. They demonstrated elution of the adsorbed iodine by soaking the iodine-loaded PAFs in ethanol solutions, suggesting that they could be regenerated if needed.

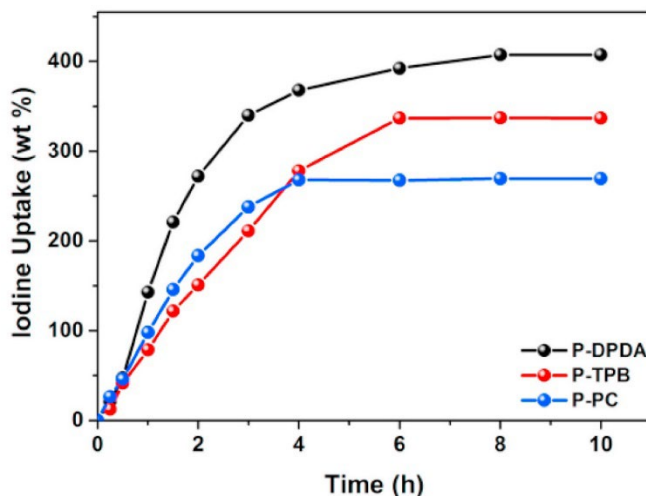


Figure 5.11. Summary of iodine loading kinetics for PAFs P-DPDA, P-TPB, and P-PC in saturated conditions at 75 °C (Wang et al. 2021).

#### 5.5.4 Porous Organic Polymers

More information about POPs is provided in Section 4.4.3. POPs are porous materials that have high SSAs and good physical and chemical stabilities (Qian et al. 2017). In a study by Qian et al. (2017), POP-1 and POP-2 (see SEM micrographs in Figure 5.12a) were developed for gaseous  $I_2(g)$  capture as well as capture of iodine dissolved in cyclohexane. The iodine loadings for POP-1 and POP-2 were 3570 mg/g and 3820 mg/g, respectively (Figure 5.12b).

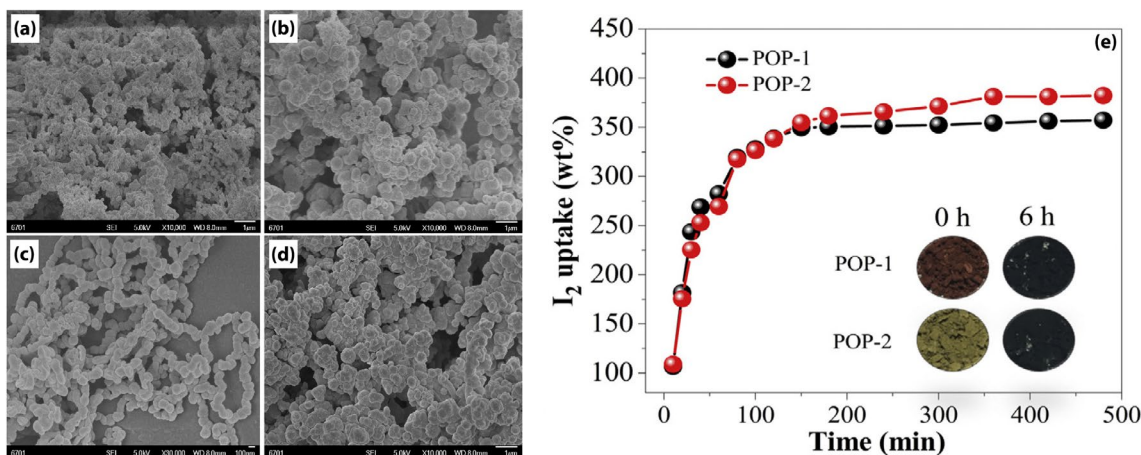


Figure 5.12. SEM images of (a,c) POP-1 and (b,d) POP-2 and (e) iodine loading over time (Qian et al. 2017).

CMPs are a class of POP materials that are often built with light elements, including C, N, O, H, and B, so they have lower densities than zeolites and MOFs. In a study by Liao et al. (2016), the CMP compounds of HCMP-1, HCMP-2, HCMP-3, and HCMP-4 were produced through various reactions involving a range of

organic solvents. These products had SSA values of up to 430 m<sup>2</sup>/g with I capacities up to 3160 mg/g and up to 3360 mg/g if they were reduced in hydrazine before the capture experiments (experiments were performed at 85 °C).

## 5.6 Carbon-Based Sorbents

See Section 4.5 for background on AC and its performance in Hg capture. Iodine interaction with ACs is well known, best evidenced by the use of an iodine number to determine the porosity of ACs [ASTM Method D4607-14(2021) *Standard Test Method for Determination of Iodine Number of Activated Carbon*]. Iodine can physisorb to the AC, and the mass change can be used to determine porosity. However, impregnation and the presence of functional groups change the interaction mechanism of I, and this can impact the effectiveness of the technique. As such, I capture by carbon substrates can be improved through impregnation or functionalization but can be hindered in the presence of competition for physisorption sites (e.g., water). Capacities for AC capture of I can range up to 1000 mg/g material, where in cases of impregnation the capacity can be dictated by the amount of impregnated element (e.g., Ag).

The capture of <sup>129</sup>I by ACs has been studied since the origin of nuclear reprocessing (Huve et al. 2018). In many nuclear environments, high temperatures, humidity, and competing species are present and specific functionalization/impregnation is required for I capture. The most widely studied impregnation chemical is triethylenediamine (TEDA, also known as 1,4-diazabicyclo[2.2.2]octane, DABCO) (Wren et al. 1999). TEDA doping up to 10 wt% can increase I-capture capacity, but increased loading increases the risk of porosity clogging due to the formation of clusters (González-García et al. 2013). TEDA-impregnated AC is also capable of capturing methyl iodine through physisorption with the AC and interaction with the TEDA via an S<sub>N</sub>2 reaction, where an ionic product with the iodide is generated (González-García et al. 2011; Herdes et al. 2013; Aneheim et al. 2018; Ho et al. 2019). Prior testing has shown TEDA-impregnated AC to capture both Hg and I, with the capture of I increasing the capacity of Hg (Chemsorb 701 G). However, the Hg capacity of TEDA-impregnated AC was lower than that of S/KI-impregnated AC (BAT- 37) (Abramowitz et al. 2019a). An additional advantage of TEDA-impregnated AC is its interaction with water converting it to a hydroxide, making more sites accessible for physisorption and improving overall uptake of I in humid conditions (Ho et al. 2019).

Iodine impregnation of AC can also improve I capture, mainly through isotope dilution with the iodide present in the material (Deitz 1987). However, unlike TEDA-impregnated AC, there is no beneficial interaction with water. Kombisorb BAT-37 is sulfur and iodide impregnated and has been shown to capture both Hg and I (Abramowitz et al. 2019a). A combination of TEDA and KI-impregnation has been shown to improve I capture over KI-impregnated AC (Kitani et al. 1972; Deitz 1987). Other impregnations such as NaOH have been shown to improve I capture by up to 2 mass% loading (Gourani et al. 2014), and ZnCl<sub>2</sub> impregnation of a walnut shell AC showed high I capacity in dynamic conditions (Yang et al. 2023). Ag-impregnated ACs are also available commercially, but their performance has been primarily focused on removal of liquid streams (Hoskins et al. 2002; Asmussen et al. 2016). Alternate carbon substrates have been developed for I capture (but not shown for Hg capture), including Bi-decorated electrospinning carbon nanofibers (Chee et al. 2020) and busofite-type carbon fibers (Ampellogova et al. 2002).

Prior work has shown limited deleterious interaction between spent AC and various encapsulation matrices (Fujii Yamagata et al. 2022); however, no improvement in I retention was observed with a sulfur-impregnated and KI-impregnated AC. Ag-impregnated AC has shown improvement in I retention, especially in slag-free grout formulations (Li et al. 2019).

In addition to AC-based sorbents, a new type of carbon-based sorbent was recently discovered, which is a Bi-functionalized carbon foam produced from carbonizing a melamine foam and then functionalizing it with Bi using electrodeposition (Baskaran et al. 2022). In this study, different bismuth electrodeposition

times were utilized, including 5 min, 15 min, 30 min, and 60 min, with a 1 V direct current potential. After iodine loading and after 24 h of desorption to remove loosely physisorbed iodine, the maximum iodine loading achieved was 799.5 mg/g (BCF-15 with 15 min electrodeposition time).

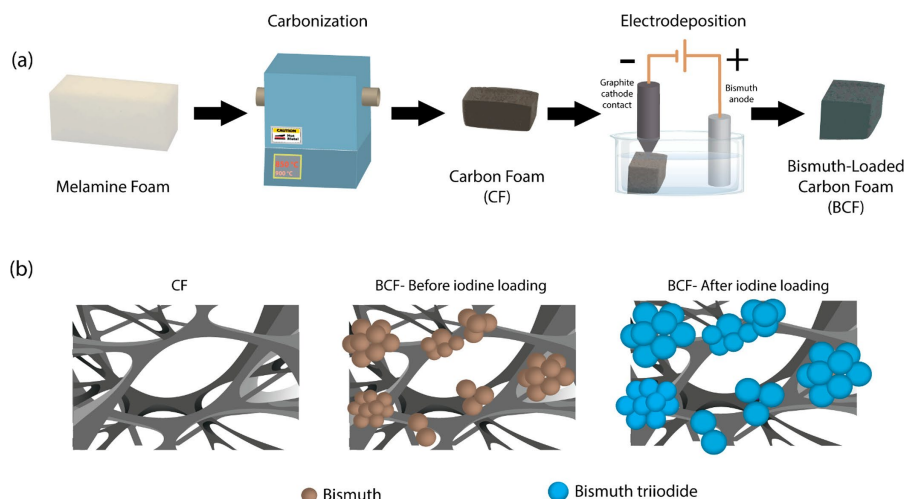


Figure 5.13. (a) Summary of the production process for making Bi-functionalized carbon foams along with (b) schematics showing the structure of the carbon foam followed by bismuth functionalization of the carbon foam without and with iodine loading (from Baskaran et al. 2022).

In general, ACs have a similar level of maturity for I capture as they do for Hg capture, with similar challenges and benefits as discussed in Section 4.5. Carbon-based materials, in general, have a high commercial availability, are low-cost, and tend to have good stabilities. One drawback is that they can be flammable, and some contain toxic elements (e.g., Ag).

## 5.7 Metal Substrates (e.g., Metal Particles, Metal Wires)

In a 2021 study, 0.5-mm-diameter metal wires were evaluated for I capture in saturated I conditions at temperatures of 100, 121, and 139 °C, including metals of Al, Ag, Cu, In, Mo, Nb, Ni, Pd, Pt, Sn, and Ta (Riley et al 2021). In this study, the highest performing materials were Cu, Al, In, Ag, and Sn, where all of these showed loadings of >400 mg/g and some up to 4370 mg/g (Sn-100 °C). The relationships between reactivity (I loading) and temperature also varied, with the different metals showing favorable loadings; for example, as the experimental temperature was increased, the I-loadings for Al and Sn metals decreased while they increased for Ag, Cu, and In metals. While metals like Al and In showed favorable reactions with I, the resulting metal-iodide compounds (i.e.,  $AlI_3$ , and  $InI_3$ , respectively) are water soluble and thus are not ideal products from an environmental remediation perspective. This study shows that pure metals could potentially be used to adsorb I, but it is unclear how an approach like that could be implemented in an off-gas capture facility. Full-scale deployment of pure metals could be more difficult to arrange in a cartridge or pour into the existing Carbon Adsorber units; pressure drop may increase and it is unclear how the metals would perform in the presence of other competing species (e.g., chloride-based compounds, oxidizing gases). However, it might also be cheaper to implement something like this, where engineered materials are not needed (e.g., metal-exchanged zeolites) in the off-gas capture process. In one scenario, it is possible that metal shot could be utilized, whereby air could still travel between the shot through the Carbon Absorber units.



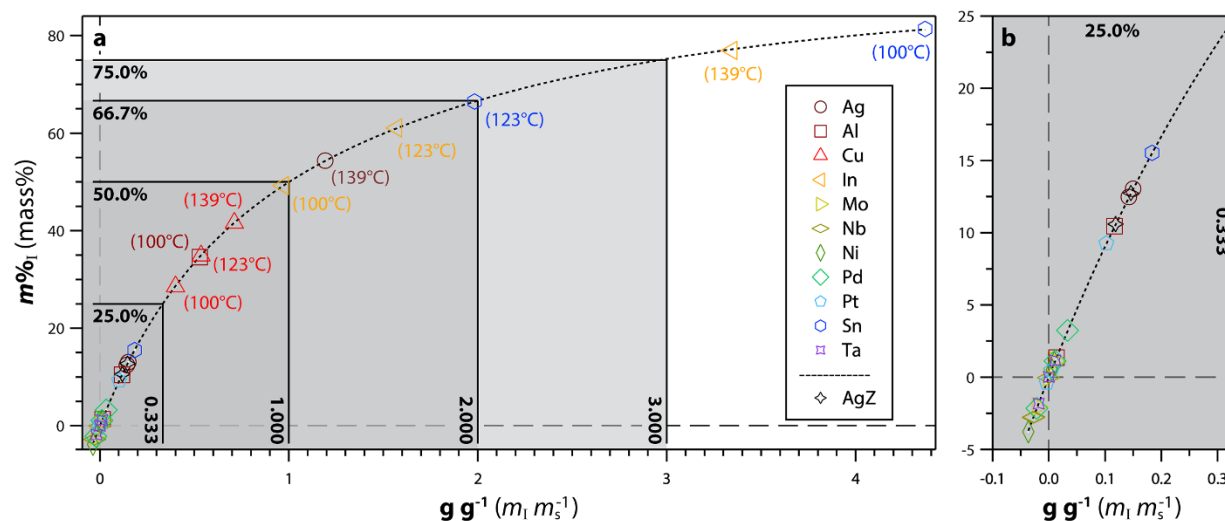


Figure 5.14. (a) A summary of the iodine capture performance of pure metal wires in saturated iodine environments and (b) a magnified version of the lower left corner in (a) (Riley et al. 2021).

In a follow-up study to the metal wire study discussed above, metal particles were embedded in PAN composites at 75 mass% metal loadings, including  $\text{Ag}^0$ ,  $\text{Bi}^0$ ,  $\text{Cu}^0$ , and  $\text{Sn}^0$  (Chong et al. 2022); see Figure 5.15 for more details about the process required to manufacture these PAN composites. These metal-PAN composites worked very well at providing an engineered form of the active metal sites where the Ag-PAN, Bi-PAN, Cu-PAN, and Sn-PAN showed maximum I capture values of 753 mg/g ( $\text{AgI}$ ), 474 mg/g ( $\text{BiI}_3$ ), 1457 mg/g ( $\text{CuI}$ ), and 1669 mg/g ( $\text{SnI}_4$ ) after 48 h at 120 °C within saturated I conditions in air. Parallel experiments were conducted on the metal particles for comparison with the metal-PAN composites, and for Ag, Bi, and Sn, the particles showed higher I loadings while the Cu-PAN composites showed higher loadings than the Cu particles alone. For both particles and metal-PAN composites, the Bi materials required 72-h heat treatments to fully convert from  $\text{Bi}^0$  to  $\text{BiI}_3$ . The sizes of the metal-PAN composites did not change noticeably between the base sizes and after I-loading of the sorbents, suggesting that the PAN matrix allows for volume expansion while maintaining the original shape and structure.

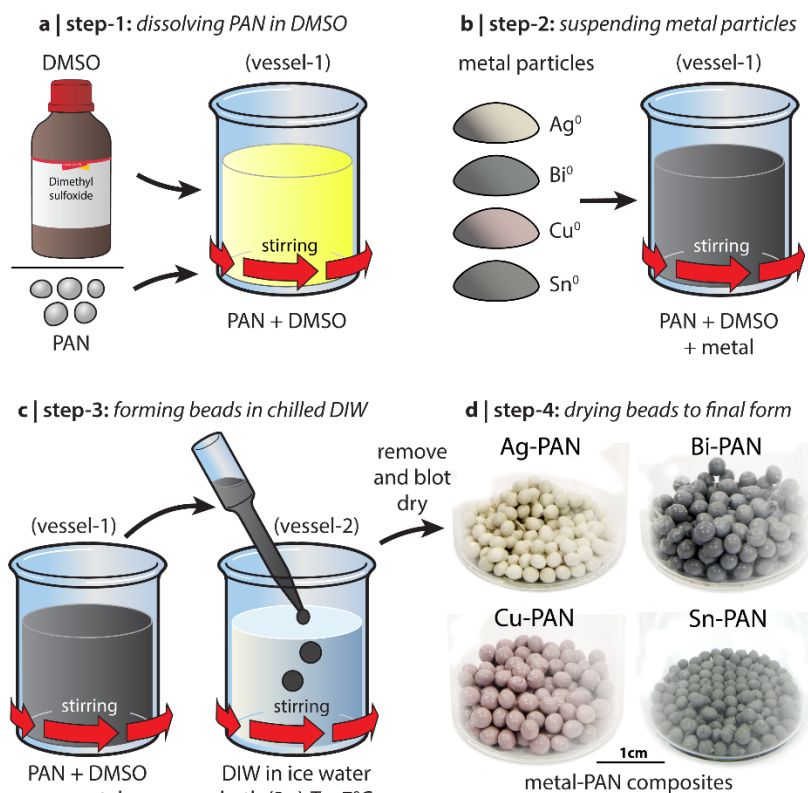


Figure 5.15. Process for making metal-PAN composites, including (a) dissolving PAN in dimethyl sulfoxide (DMSO), (b) suspending metal particles in the PAN+DMSO mixture, (c) dropping the PAN+DMSO+metal mixture into water to create spheres, and (d) drying the spheres into the final product (Chong et al. 2022).

In a study by Tian et al. (2021), nickel metal foams were functionalized with either Bi or Ag to create Bi-Ni or Ag-Ni substrates (see Figure 5.16). The functionalization process to add Bi or Ag to the nickel foams was done using solvothermal processes including ethylene glycol, ethanol, and either Bi(NO<sub>3</sub>)<sub>3</sub>·5H<sub>2</sub>O or AgNO<sub>3</sub> in a Teflon autoclave at 200 °C for 12 h. The metal-functionalized Bi-Ni and Ag-Ni foams contained Bi<sup>0</sup> and Ag<sup>0</sup> (in addition to Ni<sup>0</sup>) during XRD analysis. The I loading experiments were performed at 200 °C. Iodine-loading capacities of the Bi-Ni and Ag-Ni foams were 618.9 mg/g and 442.4 mg/g, respectively, but the I-loading rate was much faster for the Ag-Ni foam compared with the Bi-Ni foam. Since the metal functionalization process can be used to coat the structure of the Ni foam substrate, different sizes and shapes could be made using these templates.

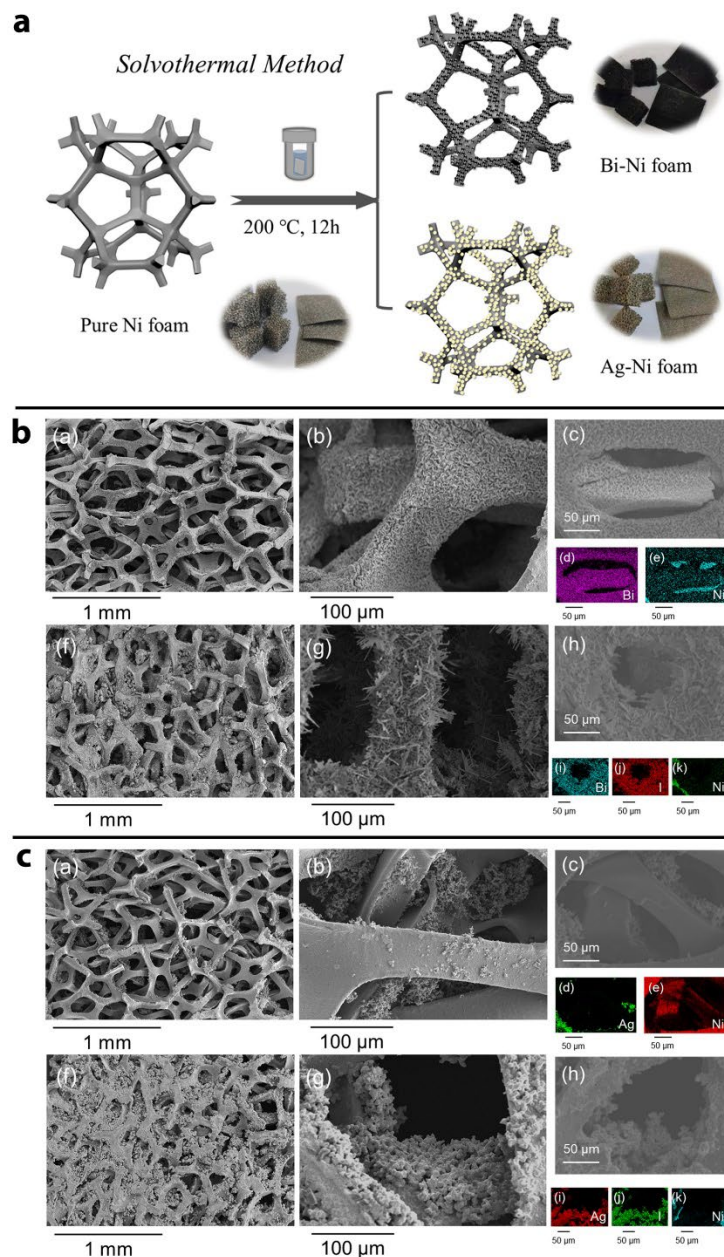


Figure 5.16. (a) Process by which metal-functionalized Ni foams are produced. (b) SEM and energy-dispersive X-ray spectroscopy (EDS) results of Bi-Ni foam before iodine loading and Bi-Ni foam loaded with iodine. (c) SEM and EDS results of Ag-Ni foam before iodine loading and Ag-Ni foam loaded with iodine. This data is from Tian et al. (2021).

In general, the cost to purchase pure metals commercially ranges from expensive (e.g., Ag) to inexpensive (e.g., Bi, Cu, Sn). The costs to produce the metal-polymer composites are higher and involve hazardous chemicals (i.e., DMSO). Functionalizing metal foams would probably be even more expensive, but would provide a more rigid support framework. Since this type of sorbent approach is to utilize full chemisorption of a metal transitioning to a metal-iodide complex, the metal loading in the composite forms will directly correspond to the maximum I capacity (which varies by metal and metal oxidation state in the resulting metal iodide). For instance, the common metal-iodides for Ag, Bi, Cu, and Sn after I loading are AgI ( $\text{Ag}^+$ ),  $\text{BiI}_3$  ( $\text{Bi}^{3+}$ ),  $\text{CuI}$  ( $\text{Cu}^+$ ), and  $\text{SnI}_4$  ( $\text{Sn}^{4+}$ ), which correspond to maximum I capacities of 1176 mg/g,

1822 mg/g, 1997 mg/g, and 4276 mg/g, respectively. These values assume no oxide conversion of the pure metal substrates prior to reaction with I to produce metal iodides. With such high I loadings, it is unclear how mechanically stable these types of substrates would be, and it is likely that metal iodides could flake off. It is also possible that the process of iodine loading could result in embrittlement of the sorbent due to the volume expansion because of the reaction.

## 6.0 Sorbent Screening and Evaluation

### 6.1 Criteria for Material Evaluation

A literature review and industrial canvassing effort was performed to identify and screen candidate materials for Hg-capture, I-capture, or simultaneous capture of both. A second screening was then applied to segregate (or bin) materials for likely near-term (e.g., 1–3 years) implementation potential (i.e., commercially available) vs. longer-term (e.g., 3–7 years) implementation (i.e., development needed), giving priority to near-term commercial materials but not disregarding and removing potential development material candidates for longer-term implementation. In either case, the goal was to guide material selection and required testing to facilitate time-sensitive decisions and subsequent vendor actions for incorporating these potential abatement materials into the mission life of both the WTP LAW and HLW facilities. These two initial screening criteria are defined by:

#### *Literature/Commercial Material Screening:*

- a. *(Yes-keep) Material has been demonstrated for I and/or Hg capture from off-gas or vapor-phase environments.*
- b. *(No-remove) Material has not been demonstrated for I and/or Hg capture from off-gas or vapor-phase environments.<sup>8</sup>*

#### *Commercial vs. Development Material Binning:*

- a. *(Yes-commercial) Material is commercially available and demonstrated for iodine and/or mercury off-gas capture.*
- b. *(No-developmental) Material is not commercially available and would require further development. Material shows promise for iodine and/or mercury off-gas capture and its synthesis production can be scaled up to meet needs.*

Candidate materials passing the screening criteria were given a brief description of their candidacy and further evaluated by a more detailed set of seven distinguishing attributes, described below. The focus of the evaluation was to guide decision-making on materials for testing to support the replacement for Kombisorb BAT-37 (or BAT-37 II) with a material that can sustain abatement of both Hg and I in the WTP LAW and HLW facilities' secondary off-gas systems. The set of evaluation criteria were weighted in order of perceived importance by the review team and then applied to assess the materials' potential for success when used in the WTP LAW Facility off-gas system. This list of criteria is presented below in order of priority and was applied to both the commercial (i.e., near-term) and development (i.e., longer-term) material implementation candidates. A predominantly qualitative ranking (i.e., positive to negative assessment marker) for each evaluation criterion was established, with item (a), or in the case of material cost, item (i), always being the most positive rank marker in the text below. The colors displayed beside each assessment level correspond to the visuals in Table 6.1 and Table 6.2.

- 1) **Material Cost:** Directly quantifiable cost bases were identified as challenging to obtain due to proprietary information for commercial materials and extrapolations for developmental materials. This criterion was established as a qualitative attribute and separated by the two binned material types, i.e., commercial or development. The primary cost assessment in this criterion was the perceived cost per mass basis of material components (e.g., Ag use leads to high cost, a substrate that must be purchased carrying a significant cost given a medium cost).

---

<sup>8</sup> Materials screened out at this stage also included organic and hybrid resins that would not survive at the temperatures in service.

- a. **Commercial Material Cost:**
    - i. Low – commercially available with no components carrying significant costs (green)
    - ii. Medium – contains a component that is perceived to be a moderate or higher cost item than low-cost materials (e.g., organic substrates) (yellow)
    - iii. High – contains a significant amount of a high-cost material such as precious metals (e.g., Ag) (red)
  - b. **Development Material Cost:**
    - i. Low – components can be prepared without significant costs and an identified path to scale up exists (green)
    - ii. Medium – contains a component that is perceived to be a moderate or higher cost item than low-cost materials (e.g., organic substrates) and an identified pathway to scale up exists (yellow)
    - iii. High – contains a significant amount of a high-cost material such as precious metals (e.g., Ag) and/or no identifiable path to scale up (red)
- 2) **Safety Risks:** This criterion is focused on safety-related issues (e.g., flammability, toxicity, dust) that could create risk to implementation into operations. As it is a risk with the existing AC bed material, flammability must be considered for any replacement material. Toxicity is relevant to manufacturer and operations/worker handling, potential stack emission from the bed, and for disposal. Dust generation from explosion is a risk when handling during transport, bed filling, and draining, where granular material would be preferred over powders. If no data was available, the assessment was marked as such. This is a qualitative criterion described as one of three:
- a. None – no identified safety risks for handling and at WTP-relevant conditions (green)
  - b. Some – some safety risks could be present when handling and near WTP-relevant conditions (yellow)
  - c. Significant – multiple or significant safety risks exist for handling and use of the material (red)
- 3) **Mercury/Iodine Loading Capacity:** The sorption performances for Hg and/or I were identified from available literature and reported using the presented value (mass loading in mg/g, percent mass loading converted to mg/g or a DF). The test conditions for the material are critical to assessing the loading capacities for each, and rankings were assigned based on test conditions. This evaluation criterion will be important in relation to waste classification prior to disposal based on the projected loadings of <sup>129</sup>I or Hg (RCRA metal) that are feasible to ensure LDR can be met for disposal of the eventual waste form. A quantitative value is presented; if no data was available for Hg or I (or both), it was given a low ranking for that element. As sorbent performance can be directly influenced by test conditions, the test conditions providing the performance are also listed.
- a. High – highest priority given to materials showing loading capacity (>0.01 mass%) in dynamic test conditions (i.e., flow-through testing) (green)
  - b. Moderate – materials showing moderate loading capacity (<0.01 mass%) in dynamic test conditions or excellent capacity (>0.01 mass%) in partially dynamic conditions, such as regeneration of a static test or low flow rates with long residence times (yellow)
  - c. Low – materials showing low capacity (<0.001 mass%) in dynamic conditions or excellent capacity in static conditions (red)
- 4) **Test Conditions Relevant to WTP LAW Facility:** The test conditions for Hg/I capture were evaluated against the projected operating conditions at the WTP LAW Facility (e.g., high flow rates, complex off-gas composition, and sorption temperature of ~75 °C) in order of rank materials. The target operating conditions are provided in Sweeney (2020). Unique to this criterion, four ranking levels are provided that vary based on assessment of flow, gas composition, and temperature conditions for the data available to date:



- a. *High – data exists in representative test conditions for all three areas* (green)
  - b. *Moderate – data exists in two of the three identified conditions* (yellow)
  - c. *Partial – data exists in one of the three identified conditions* (orange)
  - d. *Low – data only available in non-relevant conditions* (red)
- 5) **Thermal and Chemical Stability in Service:** This criterion is based on evidence of material stability under conditions similar to those expected in the WTP LAW Facility. Thermal stability was evaluated (i.e., fines generation, temperature breakdown at WTP conditions), and chemical stability was evaluated with respect to humidity/water, NO<sub>x</sub>/oxidizing conditions, and organics exposure at temperatures (around 75 °C). If no data was available, the assessment was marked as such. This is a qualitative criterion where the material is classified as follows.:
- a. *Stable – experimental data is available in relevant conditions showing stability in all thermal/chemical variables* (green)
  - b. *Partially stable – experimental data is available in some condition(s) but no data is available for other conditions, some data is available in one or more thermal/chemical variables, or some deterioration has been identified in one or more conditions* (yellow)
  - c. *Unstable – experimental data shows significant thermal/chemical induced degradation of material under the relevant condition(s)* (red)
- 6) **Mechanical Stability and Physical Form:** This criterion is intended to assess the physical form of the material to gauge its mechanical stability in the WTP LAW off-gas configuration as well as its amenability to the existing infrastructure and downstream systems. Compressive strength and friability are examples of this criterion.
- a. *Ready – Engineered form that is mechanically stable for both transport and operations, conducive to current dimensions and configurations of the WTP LAW and HLW facilities' Carbon Adsorber units and no further development or design required. Material has known mechanical stability and has known (or perceived suitable) pressure drop and flowability behavior* (green)
  - b. *Alter – A mostly mechanically stable form that may require some modification or further development and design to be conducive to current dimensions and configurations of the WTP LAW and HLW facilities' Carbon Adsorber units. A material lacking mechanical stability may fracture or fail during transport and loading, pressure drop and flowability may be suitable in existing form but requires testing* (yellow)
  - c. *Raw – Raw powder form and major modification to current dimensions and configurations of the WTP LAW and HLW facilities' Carbon Adsorber units would be needed to accommodate current form. Raw powder cannot be used due to high bed pressure drop and poor flowability* (red)
- 7) **Waste Form Demonstration:** The final disposition of the Hg/I-loaded material must be considered, and any demonstration of waste form from the material is noted. This is a qualitative criterion with the waste form class listed.
- a. *Full-scale – fabrication of waste form demonstrated at full-scale or performed commercially (minimum 55-gallon drum)* (green)
  - b. *Bench – fabrication of waste form demonstrated at bench-scale* (yellow)
  - c. *None – no fabrication of waste form demonstrated at any scale* (red)

## 6.2 Sorbent Screening, Evaluation, and Ranking Analysis

Utilizing the evaluation criteria, the various material types were assessed against one another using a representative material. In nearly all cases, the representative material selected was one with the highest capacity for Hg/I or the one with the most data. Detailed material screening, evaluation, and ranking tables are presented in Appendix A for reference. A visual summary of the rankings is given in Table 6.1 for

commercially available materials and Table 6.2 for the developmental materials. In each table, the order of the material classes presented is based on the evaluations and is used to guide the candidacy testing goals in Section 7.0. Materials ranking higher are perceived to have a larger return on investment in maturing the material to be ready for deployment in the WTP, whether near-term or long-term. The most significant gap or unknown is listed for each material class that should be pursued in bench-scale testing. Also listed are any significant challenges that may require extensive R&D to overcome that were not directly captured when applying the evaluation criteria. The final table column lists testing/information gaps that also need to be filled before the material is fully matured for full-scale implementation into the WTP. This final column can be thought of as a checklist guiding future testing. Grouped material types are discussed below, providing evaluation ranking results illustrated by the tables, highlighting some of the evaluation team's reasoning, and documenting other notable observations.

## 6.2.1 Commercially Available

*Carbon-Based Sorbents* – Among the commercially available materials, the carbon-based sorbents (ACs) scored the highest due to their low cost, demonstrated capture of both Hg and I (although minimal data from the same test and dependent on the specific AC), test data of some ACs in WTP-like conditions, and wide availability from an array of different chemical supply vendors. A disposal pathway for ACs exists due to its demonstration as a grouted waste form at full scale. The ACs (four types listed) all compare well to the new baseline material (Kombisorb BAT-37 II), although the stability challenges of BAT-37 II remain similar to those of the original BAT-37. The Ag-impregnated ACs scored lower due to their higher cost (relative to baseline BAT-37 II) and lack of data for I and Hg at WTP-relevant conditions, but ranked just above porous inorganic crystalline matrix materials (mordenite and faujasite) due to an expected enhanced stability. The largest opportunity for ACs is the capture performance of mixtures of carbon types to maximize both Hg and I capture. In this case, implementation of two (or more) carbon types in the Carbon Absorber would be used: either a mixed-type material bed within both the guard and primary beds or one type in the guard bed and one in the primary bed.

*Porous Inorganic Crystalline Matrices* – While commercially available and used in off-gas management for I capture, the porous inorganic crystalline matrices were ranked lower than all the carbon-based materials, primarily due to their high cost (most contain Ag) and lack of a waste form demonstration at full scale. While mordenite has been demonstrated to capture both Hg and I simultaneously in dynamic conditions (Abramowitz et al. 2019a), its known deterioration in NO<sub>x</sub>/oxidizing off-gas conditions was a significant detraction. Faujasite was ranked higher as its stability in NO<sub>x</sub> substrates is only inferred in dated literature, while showing promise for capture of Hg and I. Demonstration of the stability of Ag-faujasite in NO<sub>x</sub> was identified as the highest priority testing need, while both mordenite and faujasite could be pursued as regenerative sorbents as a means to lower cost. In a regeneration process the AgI or HgAg would be converted to another cation form (e.g., NaI) that can be freed from the sorbent and the Ag returned to service (Yadav et al. 2022).

*Inorganic Sulfide Sorbents* – As sulfur impregnation enhances the capture of Hg for ACs, a pure metal-sulfide sorbent from a commercially available simple compound (e.g., CuS, Ag<sub>2</sub>S) could be used whereby the metal and sulfur components are chosen to capture iodine and mercury, respectively. However, this option scored low due to the limited data and lack of a physically stable form (i.e., currently produced only as raw powders) for operations. To mature these sulfide sorbents, which contain low-cost metal cations, they should first be demonstrated for simultaneous Hg and I capture, followed by development of engineered forms/scaffold for deployment, and then scaled testing at WTP-relevant conditions.

*Metal Substrates* – All candidates within this grouping had a negative evaluation due to the limited data available and questions around having a thermal/chemical and mechanical stable form for deployment.



These materials could warrant maturation if they can show effective and sustained capture of both Hg and I.

## 6.2.2 Developmental

The evaluation criteria remained the same for developmental materials as they were for the commercial materials, which generated a partial bias due to the inherent lower technological maturity of developmental materials. However, with the long-term mission needs of WTP, many of these developmental materials could warrant maturation for deployment by providing better capture than commercial materials available now, improved safety and operational stability, and reduced long-term mission cost (e.g., relative to silver mordenite in the WTP HLW Facility).

*Inorganic Aerogels (Aerogel)* – A broad category of stable, high-SSA materials that have emerged as the most promising candidates to date for improved off-gas capture in various applications. This class of materials has been matured significantly for I capture in reprocessing off-gas conditions, and as such, has shown capacity for I uptake in dynamic conditions with many of the competing species similar to the WTP off-gas conditions (e.g., NO<sub>x</sub>). A highly durable waste form has also been demonstrated at the bench scale. The cost of an Ag-containing material may be a detriment without regeneration of the material. With the thiol-linkage (sulfur) present in the material, it could have significant capacity for Hg capture, although this has not been demonstrated to date. Herein lies the next logical step for maturation, which includes testing of Ag-functionalized silica-aerogel to demonstrate simultaneous Hg and I capture in dynamic conditions.

*Inorganic Aerogels (Xerogel)* – These materials are less mature than their aerogel counterparts but possess many of the same potentially beneficial properties and have much higher hardness values with similar SSA values, giving increased structural stability without compromising on the functionality of the material performance. Iodine capture has been demonstrated in static conditions. Like aerogels, the cost of an Ag-containing material may be a detriment without a regeneration pathway for Ag recycle. With the thiol-linkage (sulfur) optionally added to these materials, they could have a similar capacity for Hg capture as the Ag-functionalized silica aerogels, although this has not been demonstrated to date. Similar to aerogels, the most significant gap to resolve would be to demonstrate simultaneous Hg and I capture in dynamic conditions.

*Engineered Membranes* – This is an emerging group of materials where the foam substrates provide a high surface area for sorption. The Bi-functionalization could provide an economical alternative to Ag, and their candidacy is strengthened by demonstrated I capture in static conditions. Further maturation would be required for mechanical and chemical stability and waste form demonstration. The ability of these materials to capture both Hg and I needs to be evaluated first to improve their candidacy, but that work is ongoing.

*Inorganic Aerogels (Chalcogels)* – Using the evaluation criteria, the chalcogels, specifically a Mo-S chalcogel, ranked the highest due to demonstrated simultaneous capture of both Hg and I. However, they lack maturity from a safety, deployment form, and disposal standpoint. While the criteria ranking gave precedence to the chalcogels, these materials present a significant challenge in their synthesis – and low-cost pathway to large-scale production quantities – even with several developments in the past decade. Until better and more cost-effective synthesis approaches are available, research into chalcogels for Hg and I capture should not proceed.

*Improving Existing Substrates through Functionalization* – This item was included as an opportunity to take existing or emerging high-SSA substrates and functionalize/impregnate them to be utilized as Hg and I sorbent. This is a purely developmental case, but from one which the inorganic aerogels emerged. A clear example of an opportunity here would be to add thiol groups to existing (and functionally demonstrated) I sorbents.

*Porous Organic Sorbents* – These materials have demonstrated high capacity for Hg and I, but they (currently) lack a path to full-scale production of the inorganic aerogels in the near term. As well, significant questions remain about viable and stable engineered forms that have the mechanical properties for deployment. If dual capture of Hg and I were to be demonstrated, then scaled development and mechanical integrity would be significant needs. Another limitation is the lack of data for both Hg and I on specific porous organic sorbents, where a large assortment (hundreds of thousands) of different possible materials exist; narrowing this down to a short list for study is not trivial.

*Titania Supported Sorbents* – Titanium dioxide is a very stable matrix for which there are only limited studies on off-gas capture in nuclear applications. It can be functionalized for other capture applications; for example, an Ag-TiO<sub>2</sub> has demonstrated a small capacity for Hg and would likely capture I as well. Overall technical maturity is low and simultaneous Hg and I capture would need to be demonstrated first at appreciable levels.

*Inorganic Sulfide Sorbents* – While having the sulfur functionality known to capture Hg and I, these powders have only shown limited Hg capacity in static conditions. Without a significant breakthrough in development and testing, these materials are unlikely to be successful in the WTP application.

Table 6.1. Summary of the material evaluations for commercially available materials.

Material	Representative Material	Cost	Safety	Hg	I	WTP Test	Stability	Form	Waste Form	Most Significant Gap/Question	Significant Challenge	Other Gaps/questions
Baseline	BAT-37 II									Performance under WTP conditions	Stability in Humid Conditions	Long-term service performance vs. BAT 37 (original)
Carbon Based: S-Impregnated	Desorex (K43J/HGD)									Combined deployment with other activated carbons	N/A	Testing in WTP conditions
Carbon Based: TEDA-Impregnated	Chemsorb 705G									Combined deployment with other activated carbons	N/A	Testing in WTP conditions
Carbon Based: KI-Impregnated	Oxorbion K 40J									Combined deployment with other activated carbons	N/A	Hg/I testing in WTP conditions
Carbon Based: Ag-Impregnated	AGC-50 CS-Si									Can it be a dual capture material? (Hg) or improve performance as a minor addition to a second AC?	Cost	Combination with other activated carbons, Testing in WTP conditions, service lifetime vs. cost, is regeneration of sorbent possible
Porous Inorganic Crystalline Matrices (Faujasite)	IONEX Ag-400									How is stability in NO <sub>x</sub> compared with mordenite?	Cost	Can it dual capture in WTP conditions? Is regeneration of sorbent possible? Waste form demonstration at full scale
Porous Inorganic Crystalline Matrices (Mordenite)	IONEX Ag-900									Is regeneration of sorbent possible?	Stability in NO <sub>x</sub> and cost	Can it stably dual capture in WTP conditions? Waste form demonstration at full scale
Inorganic Sulfide Sorbents	CuS									Can it be a dual capture material?	N/A	WTP conditions, engineered scaffold, does it capture both at same reported capacity, waste form, large scale synthesis/production route?
Metal Substrates and Other Sorbents (Non-metal)	Unstabilized Amorphous nano-Se									Can it be a dual capture material?	Stabilization of fine nano-sized powders	WTP conditions, needs an engineered form, does it capture both at same reported capacity, waste form, large scale synthesis/production route?
Metal Substrates and Other Sorbents (Metal)	Pure metal wires									Can they capture Hg?	N/A	Service lifetime, dynamic testing, metal-type for cost, pressure drop, possible volume expansion in capture, flowability into unit, combining different metals
Metal Substrates and Other Sorbents (Nano-metals)	Nano-Ag									Can it be a dual capture material?	Cost (dependent on metal)	WTP conditions, need engineered form, possible volume expansion, does it capture both at same reported capacity, waste form, large scale synthesis/production route?

Table 6.2. Summary of the material evaluations for developmental materials.

Material Group	Representative Material	Cost	Safety	Hg	I	WTP Test	Stability	Form	Waste Form	Most Significant Gap/Question	Significant Challenge	Other Gaps/Questions
Inorganic Aerogels (Aerogel)	Ag <sup>0</sup> -functionalized silica aerogel									Can it be a dual capture material? (Hg)	N/A	WTP conditions, stability in bed at large scale (may need scaffold), testing for dust generation, regeneration of Ag or use of Bi, large scale synthesis/production route
Inorganic Xerogels	Thiolated AgAlSiO <sub>4</sub> xerogel									Can it be a dual capture material? (Hg)	N/A	Dynamic condition testing, WTP conditions, stability in bed at large scale (may need scaffold), regeneration of Ag or use of Bi, large scale synthesis/production route
Engineered Membranes	Bi-loaded Carbon Foam									Can it be a dual capture material? (Hg) FY23 UNR scope	N/A	Dynamic condition testing, WTP conditions, deployable form/stability in bed at large scale (may need scaffold), large scale synthesis/production route
Inorganic Aerogels (Chalcogel)	Chalcogel (Mo-S)									Can this be synthesized successfully and incorporate updated knowledge?	Fabrication	Can it be a dual capture material simultaneously? Testing in WTP conditions, need engineered form, does it capture both at same reported capacity, waste form, large scale synthesis/production route?
Improving Existing Materials through Functionalization	Various	Exploratory concepts, no available data								What other available substrates that are stable in WTP conditions can be altered to meet needs?	N/A	N/A
Porous Organic Sorbents	Nitrogen Rich Organic Framework									Can a MOF-type sorbent be a dual capture material simultaneously?	Cost of MOF at large scale application	WTP conditions, needs an engineered form, does it capture both at same reported capacity, waste form, large scale synthesis/production route?
TiO <sub>2</sub> Support	15% Ag loaded-TiO <sub>2</sub>									Can it be a dual capture material?	N/A	Dynamic condition testing, WTP conditions, deployable form/stability in bed at large scale (may need scaffold), large scale synthesis/production route
Inorganic Sulfide Sorbents	Nanotubes/microS									Can it be a dual capture material?	Stabilization of sulfide	Dynamic condition testing, WTP conditions, needs an engineered form, does it capture both at same reported capacity, waste form, large scale synthesis/production route?

& indicates the material group was tested on a different material than cited in this class.

## 7.0 Testing and Material Development Priorities

The assessment of the various materials for Hg and I capture provides potential opportunities for improvement in both Hg and I capture for the Carbon Absorber units in the WTP LAW Facility. However, the methodology established in this evaluation can be leveraged and, with very little adaptation, applied to replace Hg and I capture materials currently planned for deployment in the WTP HLW Facility and those actively deployed in other DOE waste treatment sites (e.g., Savannah River Site) and/or within the nuclear industry (i.e., primarily iodine). The evaluation in this document supplies the approach for subsequent material maturation through bench-scale testing based on closure of identified information gaps to achieve further down-selection of the “best” materials for deployment. This section presents the suggested testing approach based on immediate, near-term solutions (e.g., 1–3 years) and long-term maturation (e.g., 3–7 years) of promising approaches. Following demonstration of key testing objectives (mainly sustained capture of Hg and I under WTP-relevant conditions), a deployment roadmap is presented in Section 8.0 that is a recommended process for maturing any material for use at WTP (and elsewhere). The proposed bench-scale testing of promising materials is composed of three components:

- Static testing for Hg and I capture may be used as a preliminary screening in cases where limited capture data exists to quickly screen out developmental material candidates.
- Simplified off-gas composition (i.e., only Hg and/or I in moist air without competitors) testing in dynamic flow conditions and prototypic bed residence time to screen materials prior to complex off-gas composition testing.
- Complex off-gas composition (i.e., additional chemistry including NO<sub>x</sub>, SO<sub>2</sub>, etc.) testing in dynamic conditions and prototypic bed residence time to select a limited material set for future scaled testing under full prototypic and representative WTP LAW Facility melter off-gas conditions.

### 7.1 Testing Priorities

#### 7.1.1 Near Term: Activated Carbons in Combination

Based on the material evaluation process conducted, it is likely that the implementation of alternate AC(s) or mixtures is the most efficient and effective near-term option for improving Carbon Adsorber abatement performance for Hg and I. As described previously, the BAT-37 (or BAT-37 II), while showing removal of Hg and I, is not an optimized AC for the WTP LAW Facility off-gas. The WTP LAW off-gas is somewhat similar to flue gas, where ACs are regularly applied for Hg capture, but the WTP-specific off-gas stream remains unique with its high NO<sub>x</sub> content (among other constituents). As such, no one specific AC has been directly designed to operate in the unique conditions of the WTP LAW Facility.

ACs stand out as low cost and stable sorbents that can capture both Hg and I, dependent on the specific functionalizations (i.e., active getter impregnation). The evaluation team communicated with several commercial vendors selling ACs, and each one recommended that no one carbon was likely to meet the WTP LAW off-gas conditions (described in Sweeney 2020), but that a combination of ACs would be the preferred approach with the unique opportunity to capture both Hg and I. As such, the evaluation team recommends the testing of these mixtures of ACs for Hg and I capture to compare against capture by an individual AC.

An example test set would be alternate carbons produced by Donau Carbon, the maker of BAT-37 and BAT-37 II. The Kombisorb BAT-37 II to be used at the WTP as a direct replacement for BAT-37 has a lower sulfur impregnation at 2 mass%. However, within the conditions of the WTP, a recommended combination would be a layer of Desorex HGD 4S for mercury removal (iodine removal may also be possible onto this material as continued uptake of Hg can lead to capture of I as shown by Abramowitz et

al. 2019a)) followed by a layer of Oxorbon K40J for I removal. Kombisorb BAS55 is a separate AC that uses a modified sulfur impregnation, which may be preferable for Hg capture in the WTP conditions.

With their low cost and commercial availability from several vendors, an AC-based approach could lead to a near-term solution for enhanced stability in the performance of the carbon bed and improved I capture. Several different AC combinations have been proposed in discussions with vendors and should be pursued as an idealized approach to remediate additional species in the carbon bed without impacting Hg removal.

### **7.1.2 Long Term: Inorganic Aerogels for Hg and I Capture**

Highlighted by their placement in the developmental materials evaluation binning, inorganic aerogels are the most prominent emerging technology for off-gas treatments in several areas. As such, this class of materials holds promise for use in Hg and I removal for two reasons: 1) known stability in oxidizing, competitive off-gas environments and 2) the promise of substituting/regenerating Ag in the sorbents to lower costs. While their costs are higher than ACs, the stability, enhanced capacity, and lower safety risk (albeit a cost risk, and toxicity concern) of inorganic aerogels make them a promising candidate for replacement of AC in the long-term.

The Ag-functionalized silica-based aerogels are the most mature of these materials for I capture. Their thiol-linkage (i.e., providing sulfur) could likely be utilized for Hg capture as well. A demonstration of dual Hg and I capture is recommended for the aerogels prior to proceeding with other testing.

Coupled with aerogels are the more physically durable xerogels that can be functionalized in a similar fashion to the aerogels. A similar demonstration of dual Hg and I capture is recommended for the xerogels prior to pursuit of any further testing.

If the materials demonstrate success for Hg and I, further testing would be required to show sustained capture in WTP conditions, including dynamic and melter conditions, demonstrating stability in transfers to the absorbed bed at large scale (as the materials may need an additional scaffold), testing for dust generation (aerogels), possible regeneration of Ag to lower cost or convert to the use of Bi, and finally a large-scale synthesis/production route from a commercial vendor.

The performance of aerogels and xerogels should be compared against their current commercially available and compositionally similar counterparts: Ag-mordenite and Ag-faujasite.

### **7.1.3 Long Term: Engineered Membranes (Carbon Foam)**

A recent sorbent development is the use of carbon foams; foams could combine desirable attributes of both a carbon-based substrate material (like AC) and bismuth-metal iodine getters (lower cost than Ag). While less mature than the aerogels and xerogels, development is continuing on carbon foams and, with a demonstration of simultaneous Hg and I capture, the ranking of these carbon foams would increase to be on par with aerogels and xerogels. If these carbon foams can be demonstrated for Hg and I capture, their next logical maturation step would be dynamic flow testing at bench-scale under WTP LAW relevant off-gas conditions, larger-scale testing under prototypic WTP conditions, definition of a deployable form, and definition of a large-scale synthesis/production route.

#### **7.1.4 Long Term: Development of Other Stable Sorbent Materials**

An opportunistic development of low-TRL materials that supports long-term improvements is impregnation/functionalization of emerging substrates for use in the WTP. An obvious example of this is to add sulfur (e.g., thiol-based) functional groups to existing and commercially available iodine sorbents. A similar development approach has previously led to the maturation of inorganic aerogels. This area could also involve designing better physical supports for currently impractical materials such as MOFs.

## 8.0 Material Deployment Roadmap

The objective of this evaluation methodology was to identify candidate materials (and material groups) that may efficiently and effectively abate Hg and I in the WTP LAW Facility secondary off-gas system through direct replacement of the Kombisorb BAT-37 media in the Carbon Adsorber units. Specific candidate materials, as well as material groups, were identified and ranked based on evaluation criteria assessing various parameters such as cost, stability, Hg and I abatement effectiveness, safety, physical form, and waste disposal. This evaluation effort directly informs material candidates for subsequent bench-scale testing under static conditions (bulk candidate screening of development materials) and dynamic conditions (down-selection of commercial and developmental materials for deployment maturation).

A test plan will be generated by PNNL that describes the testing methodology and conditions for proposed candidate materials testing with the objective of down-selecting materials and advancing the relevant Hg and I data on these identified materials and material groups. The first phase of bench-scale testing at PNNL will focus on determining the material's affinity for Hg or I, and then both constituents simultaneously in appropriate moisture air conditions reflective of the WTP LAW Facility off-gas MDS by Sweeney (2020). Many materials are expected to be screened out from candidacy from this work. In the second phase of bench-scale testing, select commercial and developmental materials will undergo dynamic Hg and I capture performance testing in a complex gas stream incorporating NO, NO<sub>2</sub>, N<sub>2</sub>O, SO<sub>2</sub>, and HCl in moist air to investigate potential physical and chemical deterioration in materials with time, as indicated by reduced capture performance and post-test forensic inspection with tools such as SEM, XRD, and EDS.

It is important to emphasize that the testing priorities listed in Section 7.1 are only a portion of the evaluation steps needed to reach a material development maturation for deployment in the WTP LAW Facility or elsewhere in the DOE complex. The conceptualized roadmap steps required for maturation and deployment are presented in chronological order in Figure 8.1. The deployment roadmap steps on the left are grouped as part of the "Candidacy Evaluation," which consists of activities completed in this report and subsequent material specific testing to ensure viability. If the candidacy evaluation succeeds, activity shifts to the right-hand roadmap steps, referred to as the "Deployment Assessment." In assessing deployment, regulatory and engineering studies (including testing) are required to directly inform and ensure performance in the full-scale facility. Additionally, there are important considerations relating to (1) the cost and capabilities to fabricate approximately 12,600 kg of sorbent material (i.e., based on two Carbon Adsorber units, each with two beds, each bed filled with 3153.7 kg of BAT-37 AC) every few years to replenish the spent Carbon Adsorber unit beds and (2) the secondary solid waste immobilization operations incorporating the spent material into an accepted waste form for permanent disposition. The consideration of these deployment roadmap steps by DOE and DOE subcontractors is essential to anticipating total budget, schedule, and risk impacts for replacing a sorbent material to abate constituent emissions for regulatory compliance in a radioactive melter off-gas stream.



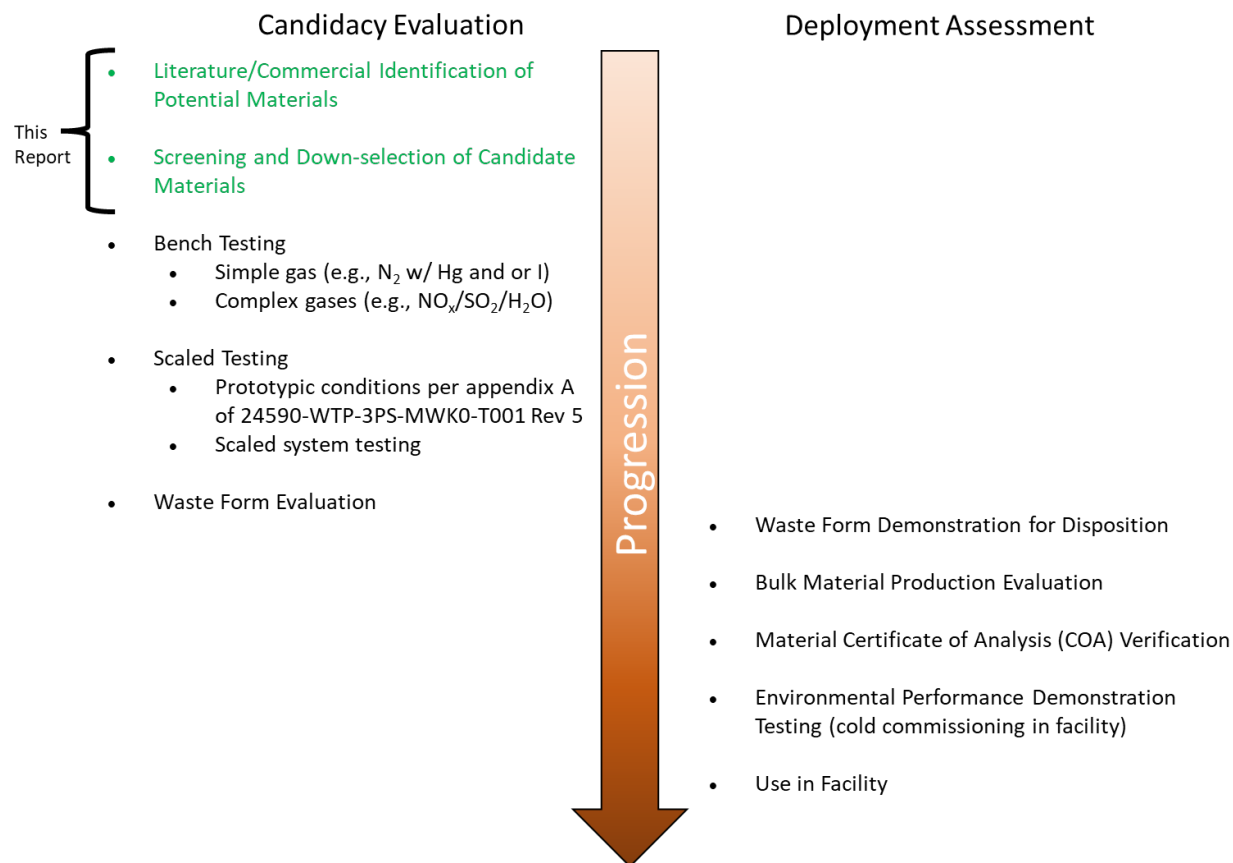


Figure 8.1. Deployment roadmap for maturation candidate materials for sustained Hg and I capture in WTP operations.

## 9.0 Conclusions

PNNL conducted a search of commercial and literature sources, developed an evaluation methodology, and then screened and evaluated potential candidate materials (both commercially available materials for near-term application and developmental materials for potential long-term integration) with the intent to rank and recommend materials for subsequent laboratory-scale testing for Hg and/or I abatement under dynamic simple gas conditions initially, followed by dynamic flow using complex gas conditions for the most promising materials.

A diverse array on materials were screened for gas-phase capture of Hg and I, and each material group was summarized under a commercially available (near-term replacements) or developmental (long-term replacements) binning and seven evaluation criteria.

Each criterion was given a qualitative measure to rank and prioritize these materials for potential use in the WTP LAW Facility off-gas application. Top priority materials were inherently biased to commercial candidates for near-term implementation, and the highest ranked materials were carbon-based, driven primarily by low-cost, but also maturity in safety, loading, and stability. Porous inorganic crystalline matrices and inorganic sulfide sorbents were deemed the next most promising commercially available binned materials. Developmental materials were also ranked and prioritized; these materials need more time for development and have a lower maturity, but that is counteracted by their significant potential to improve safety and operational stability and reduce long-term mission costs. The order of priority for the top three developmental materials is aerogels, xerogels, and engineered membranes, with multiple additional developmental material groups provided at lower ranking.

Laboratory-scale testing priorities were established based on the material rankings, and known near-term needs are believed to be best met through investigation of commercially available ACs for Hg and I abatement. Attractive materials for long-term implementation were identified, in priority order, as 1) inorganics aerogels, 2) engineered membranes (like carbon foam), and 3) development of new sorbents through modification (impregnate/functionalize) of emerging substrates. Planned laboratory testing to advance material candidacy will follow this evaluation work and be conducted in three phases: 1) static testing for Hg and I capture where limited capture data exists to quickly screen out material candidates, 2) simplified off-gas composition (i.e., only Hg and/or I in moist air without competitors) testing in dynamic flow conditions to screen materials prior to complex off-gas composition testing, and 3) complex off-gas composition (i.e., additional chemistry including NO<sub>x</sub>, SO<sub>2</sub>, etc.) testing in dynamic conditions to select a limited material set for future scaled testing under full prototypic and representative WTP LAW Facility melter off-gas conditions.

Finally, the testing priorities listed above are only a portion of the evaluation steps needed to reach a material development maturation for deployment in the WTP LAW Facility or elsewhere in the DOE complex. A conceptualized deployment roadmap (presented in Section 8.0) was derived that groups major activities by “candidacy evaluation” and “deployment assessment” to serve as a guide to DOE and DOE contractors for anticipating total budget, schedule, and risk impacts for replacing a sorbent material to abate constituent emissions for regulatory compliance in a radioactive melter off-gas stream.

## 10.0 References

Abramowitz H, KS Matlack, M Brandys, IL Pegg, GA Diener. 2018. Test Plan: Activated Carbon Media Small-Scale Testing. VSL-18T4530-1, Rev. 0; 24590-CM-HC4-MWK0-00002-01-00002, Rev. 00B. Vitreous State Laboratory, The Catholic University of America, Washington, District of Columbia.

Abramowitz H, KS Matlack, M Brandys, IL Pegg, GA Diener. 2019a. *Final Report: Activated Carbon Media Small-Scale Testing*. VSL-19R4530-1, Rev. 0; 24590-CM-HC4-MWK0-00002-02-00001, Rev. 00B. Vitreous State Laboratory, The Catholic University of America, Washington, District of Columbia.

Abramowitz H, KS Matlack, M Brandys, IL Pegg, GA Diener. 2019b. *Final Report: Activated Carbon Media Appendix M Testing*. VSL-19R4530-2, Rev. 0; 24590-CM-HC4-MWK0-00002-02-00002, Rev. 00B. Vitreous State Laboratory, The Catholic University of America, Washington, District of Columbia.

Aguila B, Q Sun, JA Perman, LD Earl, CW Abney, R Elzein, R Schlaf, and S Ma. 2017. “Efficient mercury capture using functionalized porous organic polymer.” *Advanced Materials* 29:1700665; <https://doi.org/10.1002/adma.201700665>.

Ampelogova NI, VG Kritskii, NI Krupennikova, AI Skvortsov. 2002. “Carbon-fiber adsorbent materials for removing radioactive iodine from gases.” *Atomic Energy* 92(4):336-340; <https://doi.org/10.1023/A:1016558127710>.

Aneheim E, D Bernin, MR Foreman. 2018. “Affinity of charcoals for different forms of radioactive organic iodine.” *Nuclear Engineering and Design* 328:228-240; <https://doi.org/10.1016/j.nucengdes.2018.01.007>.

Asmussen RM, EA Cordova, ALM Bourchy, ALF Yamagata, RC Daniel, NA Avalos, AC Moore, JR Stephenson, SA Saslow, GL Smith. 2021a. *The Removal of Iodine from Liquid Effluents Directed Toward the Effluent Treatment Facility*. PNNL-31794 Rev. 0; RPT-ITT-001 Rev. 0, Pacific Northwest National Laboratory, Richland, Washington.

Asmussen RM, SA Saslow, GL Smith, ALM Bourchy, JJ Neeway, AL Fujii Yamagata, R Nichols, CA Langton, R Mabrouki, J Bernards, RS Skeen, and DJ Swanberg. 2021b. *Evaluation of Degradation Mechanisms for Solid Secondary Waste Grout Waste Forms*. PNNL-32458. Pacific Northwest National Laboratory, Richland, Washington.

Asmussen RM, SA Saslow, JJ Neeway, AL Fujii Yamagata, ALM Bourchy, T Varga, KA Rod, CE Lonergan, BR Johnson. 2020. *Development and Characterization of Cementitious Waste Forms for Immobilization of Granular Activated Carbon, Silver Mordenite, and HEPA Filter Media Solid Secondary Waste*. PNNL-28545, Rev 1.0. Pacific Northwest National Laboratory, Richland, Washington.

Asmussen RM, JJ Neeway, AR Lawter, A Wilson, NP Qafoku. 2016. “Silver-based getters for 129I removal from low-activity waste.” *Radiochimica Acta* 104(12) 905-913; <https://doi.org/10.1515/ract-2016-2598>.

Ayadi T, M Madawi, L Cantrel, S Lebeque. 2022. “Rational approach for an optimized formulation of silver-exchanged zeolites for iodine capture from first-principles calculations.” *Molecular Systems Design & Engineering* 7(5)422-433; <https://doi.org/10.1039/d1me00149c>.

Baerlocher C, LB McCusker, DH Olson. 2007. *Atlas of Zeolite Framework Types*, 6<sup>th</sup> revised ed.; Elsevier: Oxford.

Bag S, PN Prikalitis, PJ Chupas, GS Armatas, MG Kanatzidis. 2007. “Porous semiconducting gels and aerogels from chalcogenide clusters,” *Science* 317(5837):490; <https://doi.org/10.1126/science.1142535>.

Barnes CM, DD Taylor, SC Ashworth, JB Bosley, and DR Haefner. 1999. *Technology Evaluations Related to Mercury, Technetium, and Chloride in Treatment of Wastes at the Idaho Nuclear Technology and Engineering Center of the Idaho National Engineering and Environmental Laboratory*. INEEL/EXT-99-00894, Idaho National Engineering and Environmental Laboratory, Idaho Falls, Idaho.

Baskaran K, M Ali, BJ Riley, I Zharov, K Carlson. 2022. "Evaluating the physisorption and chemisorption of iodine on bismuth-functionalized carbon foams." *ACS Materials Letters* 4(9):1780-1786; <https://doi.org/10.1021/acsmaterialslett.2c00466>.

Brandys M, KS Matlack, H Abramowitz, IL Pegg, and GA Diener. 2018. *Test Plan: Activated Carbon Media Testing*. VSL-17T4180-1, Rev. 0; 24590-CM-HC4-MWK0-00002-01-00001, Rev. 00C. Vitreous State Laboratory, The Catholic University of America, Washington, District of Columbia.

Brandys M, KS Matlack, H Abramowitz, IL Pegg, HK Pasiaka, and GA Diener. 2014. *Test Plan: Activated Carbon Media Testing*. VSL-13T3170-1, Rev. 0; 24590-CM-HC4-MWK0-00001-01-00001, Rev. 00C. Vitreous State Laboratory, The Catholic University of America, Washington, District of Columbia.

Brar N. 2019. *Emissions Study for the Hanford Tank Waste Treatment and Immobilization Plant*. 24590-WTP-ES-PE-17-001, Rev. 1. (Bechtel National, Inc.) River Protection Project Waste Treatment Plant, Richland, Washington.

Brinker CJ, GW Scherer. 1990. *Sol-Gel Science: The Physics and Chemistry of Sol-Gel Processing*, Academic Press, Inc. San Diego, California.

Brown R. 2012. *LAW Primary Bed Kombisorb Bat 37 Carbon Media Technical Data and MSDS*. 24590-QL-POA-MWK0-00001-08-00001, Rev. 00F. (Bechtel National, Inc.) River Protection Project Waste Treatment Plant, Richland, Washington.

Bruffey SH, JA Jordan, RT Jubin. 2017a. *Hot Isostatic Pressing of Engineered Forms of I-AgZ*. ORNL/SR-2017/707, NTRD-MRWFD-2017-000412, Oak Ridge National Laboratory, Oak Ridge, Tennessee.

Bruffey SH, JA Jordan, RT Jubin. 2017b. *Preparation of Hot Isostatically Pressed AgZ Waste Form Samples*. ORNL/SPR-2017/514, NTRD-MRWFD-2017-00210, Oak Ridge National Laboratory, Oak Ridge, Tennessee.

Bruffey SH, KK Anderson, JF Walker Jr, RT Jubin. 2013. *Humid Aging and Iodine Loading of Silver-Functionalized Aerogels*, FCRD-SWF-2013-000258, ORNL/LTR-2013-315, Oak Ridge National Laboratory, Oak Ridge, Tennessee.

Bruffey SH, KK Anderson, RT Jubin, JF Walker Jr. 2012. *Aging and Iodine Loading of Silver-Functionalized Aerogels*. FCRD-SWF-2012-000256, ORNL/LTR-2012/343, Oak Ridge National Laboratory, Oak Ridge, Tennessee.

Bruffey SH, KK Patton, JF Walker Jr., RT Jubin. 2015a. *Complete NO and NO<sub>2</sub> Aging Study for AgZ*, FCRD-MRWFD-2015-000631, Oak Ridge National Laboratory, Oak Ridge, Tennessee.

Bruffey SH, KK Patton, RT Jubin. 2015b. *Complete Iodine Loading of NO-Aged Ag<sup>0</sup>-Functionalized Silica Aerogel*, FCRD-MRWFD-2015-000419, Oak Ridge National Laboratory, Oak Ridge, Tennessee.

Bruffey SH, RT Jubin, JA Jordan. 2016. *Fundamental Aspects of Zeolite Waste Form Production by Hot Isostatic Pressing*, FCRD-MRWFD-2016-000267, ORNL/SR-2016/759, Oak Ridge National Laboratory, Oak Ridge, Tennessee.

Bruffey SH, RT Jubin, KK Anderson, JF Walker Jr. 2014. *Aging of Iodine-Loaded Silver Mordenite in NO<sub>2</sub>*. FCRD-SWF-2014-000465, ORNL/LTR-2014/153, Oak Ridge National Laboratory, Oak Ridge, Tennessee.

Bruffey SH, RT Jubin. 2015. *Recommend HIP Conditions for AgZ*, FCRD-MRWFD-2015-000423, ORNL/SPR-2015/503, Oak Ridge National Laboratory, Oak Ridge, Tennessee.

Cavka JH, S Jakobsen, U Olsbye, N Guillou, C Lamberti, S Bordiga, KP Lillerud. 2008 “A new zirconium inorganic building brick forming metal organic frameworks with exceptional stability.” *Journal of the American Chemical Society* **130**(42):13850-13851; <https://doi.org/10.1021/ja8057953>.

Chee T-S, Z Tian, X Zhang, L Lei, C Xiao. 2020. “Efficient capture of radioactive iodine by a new bismuth-decorated electrospinning carbon nanofiber.” *Journal of Nuclear Materials* **542**:152526; <https://doi.org/10.1016/j.jnucmat.2020.152526>.

Chen D, S Zhao, Z Qu, N Yan. 2018. “Cu-BTC as a novel material for elemental mercury removal from sintering gas.” *Fuel* **217**:297-305; <https://doi.org/10.1016/j.fuel.2017.12.086>.

Chen Y, X Guo, F Wu, Y Huang, Z Yin. 2018. “Applied Surface Science Experimental and theoretical studies for the mechanism of mercury oxidation over chlorine and cupric impregnated activated carbon.” *Applied Surface Science* **458**:790-799; <https://doi.org/10.1016/j.apsusc.2018.07.167>.

Cheng Y, K Shiota, T Kusakabe, K Oshita, M Takaoka. 2020. “Characterizing the mechanisms of gas-phase elemental mercury adsorption with iodine-impregnated activated carbons using Brunauer-Emmett-Teller analysis, X-ray diffraction, X-ray photoelectron spectroscopy, and X-ray absorption near-edge structure analysis,” *Chemical Engineering Journal* **402**:126225; <https://doi.org/10.1016/j.cej.2020.126225>.

Chibani S, M Chebbi, S Lebegue, L Cantrel, M Badawi. 2016. “Impact of the Si/Al ratio on the selective capture of iodine compounds in silver-mordenite: a periodic DFT study.” *Physical Chemistry Chemical Physics* **18**:25574; <https://doi.org/10.1039/c6cp05015h>.

Chong S, BJ Riley, JA Peterson, MJ Olszta, ZJ Nelson. 2020. “Gaseous iodine sorbents: A comparison between Ag-loaded aerogel and xerogel scaffolds,” *ACS Applied Materials & Interfaces* **12**(23):26127–26136; <https://doi.org/10.1021/acsami.0c02396>.

Chong S, BJ Riley, RM Asmussen, A Fujii Yamagata, J Marcial, S Lee, CA Burns. 2022. “Iodine capture with metal-functionalized polyacrylonitrile composite beads containing Ag<sup>0</sup>, Bi<sup>0</sup>, Cu<sup>0</sup>, or Sn<sup>0</sup> particles,” *ACS Applied Polymer Materials* **4**(12):9040-9051; <https://doi.org/10.1021/acsapm.2c01407>.

Chong S, BJ Riley, W Kuang, MJ Olszta. 2021. “Iodine capture with mechanically robust heat-treated Ag-Al-Si-O xerogel sorbents,” *ACS Omega* **6**(17):11628; <https://doi.org/10.1021/acsomega.1c00852>.

Deitz VR. 1987. “Interaction of radioactive iodine gaseous species with nuclear-grade activated carbons.” *Carbon* **25**(1):31–38; [https://doi.org/10.1016/0008-6223\(87\)90037-6](https://doi.org/10.1016/0008-6223(87)90037-6).

Deng Y, RC Chen, R Gimpel, B Slettene, MR Gross, K Jun, and R Fundak. 2016. *Flowsheet Bases, Assumptions, and Requirements*. 24590-WTP-RPT-PT-02-005, Rev. 8. (Bechtel National, Inc.) River Protection Project Waste Treatment Plant, Richland, Washington.

Ding S-Y, W Wang. 2013. “Covalent organic frameworks (COFs): From design to applications,” *Chemical Society Reviews* **42**:548-568; <https://doi.org/10.1039/c2cs35072f>.

Dong L, Y Huang, L Liu, C Liu, L Xu, J Zha, H Chen, H Liu. 2019. “Investigation of elemental mercury removal from coal-fired boiler flue gas over MIL101-Cr.” *Energy & Fuels* **33**(9):8864-8875; <https://doi.org/10.1021/acs.energyfuels.9b01355>.

Fan L, L Ling, B Wang, R Zhang. 2016. “The adsorption of mercury species and catalytic oxidation of Hg<sup>0</sup> on the metal-loaded activated carbon.” *Applied Catalysis A: General* **520**:13-23; <https://doi.org/10.1016/j.apcata.2016.03.036>.

Feng W, E Borguet, RD Vidic. 2006. “Sulfurization of a carbon surface for vapor phase mercury removal – II: Sulfur forms and mercury uptake.” *Carbon* **44**(14):2998-3004; <https://doi.org/10.1016/j.carbon.2006.05.053>.

Flach GP, DI Kaplan, RL Nichols, RR Seitz, and RJ Serne. 2016. *Solid Secondary Waste Data Package Supporting Hanford Integrated Disposal Facility Performance Assessment*. SRNL-STI-2016-00175, Rev. 0, Savannah River National Laboratory, Aiken, South Carolina.

Fountain MS to J Reynolds. 2020. *Electronic Transmittal of the final letter attachment, “Inorganic Iodine Speciation and Quantification of Hanford Tank Waste Samples from 241-AP-105, 241-AP-107, and 241-AN-102.”* LTR-OSIF-014, Pacific Northwest National Laboratory, Richland, Washington.

Fountain MS to L Cree. 2022. *Electronic Transmittal of the final letter attachment, “Evaluation of Glass Formulation and Waste Loading Impacts Due to Caustic Scrubber Stream Recycle to EMF for Iodine Risk Mitigation.”* LTR-OSIF-029, Pacific Northwest National Laboratory, Richland, Washington.

Fountain MS, TG Levitskaia, M Asmussen. 2019. *Iodine Speciation and Flowsheet Inventory Tracking Gaps at Hanford During DFLAW*. LTR-OSIF-007, Pacific Northwest National Laboratory, Richland, Washington.

Fujii Yamagata, AL, SA Saslow, JJ Neeway, T Varga, LR Reno, Z Zhu, KA Rod, BR Johnson, JA Silverstein, JH Westsik, GL Smith, RM Asmussen. 2022. “The behavior of iodine in stabilized granular activated carbon and silver mordenite in cementitious waste forms.” *Journal of Environmental Radioactivity* **244-245**:106824; <https://doi.org/10.1016/j.jenvrad.2022.106824>.

González-García CM, JF González, S Román. 2011. “Removal efficiency of radioactive methyl iodide on TEDA-impregnated activated carbons.” *Fuel Processing Technology* **92**(2):247-252; <https://doi.org/10.1016/j.fuproc.2010.04.014>.

González-García CM, S Román, JF González, E Sabio, B Ledesma. 2013. “Surface free energy analysis of adsorbents used for radioiodine adsorption.” *Applied Surface Science* **282**:714-717; <https://doi.org/10.1016/j.apsusc.2013.06.040>.

Gourani M, A Sadighzadeh, F Mizani. 2014. “Effect of impregnating materials in activated carbon on Iodine-131 (<sup>131</sup>I) removal efficiency.” *Radiation Protection and Environment* **37**(3):179-183; <https://doi.org/10.4103/0972-0464.154882>.

Haggard R. 2019. *Radioactive Air Emissions Notice of Construction Operating License Application for the WTP LAW, LAB, and EMF*. 24590-WTP-RPT-ENV-18-002, Rev. 1. (Bechtel National, Inc.) River Protection Project Waste Treatment Plant, Richland, Washington.



He L, L Chen, X Dong, S Zhang, M Zhang, X Dai, X Liu, P Lin, K Li, C Chen, T Pan, F Ma, J Chen, M Yuan, Y Zhang, L Chen, R Zhou, Y Han, Z Chai, S Wang. 2021. "A nitrogen-rich covalent organic framework for simultaneous dynamic capture of iodine and methyl iodide." *Chem* 7(4): 699-714.

Henning KD, S Schafer. 1993. "Impregnated Activated Carbon for Environmental Protection." *Gas Separation & Purification* 7(4):235-240; [https://doi.org/10.1016/0950-4214\(93\)80023-P](https://doi.org/10.1016/0950-4214(93)80023-P).

Herdes C, C Prosenjak, S Román, EA Müller. 2013 "Fundamental studies of methyl iodide adsorption in DABCO impregnated activated carbons." *Langmuir* 29(23):6849-6855; <https://doi.org/10.1021/la401334d>.

Ho K, S Moon, HC Lee, YK Hwang, C-H Lee. 2019. "Adsorptive removal of gaseous methyl iodide by triethylenediamine (TEDA)-metal impregnated activated carbons under humid conditions." *Journal of Hazardous Materials* 368:550-559; <https://doi.org/10.1016/j.jhazmat.2019.01.078>.

Holladay DW. 1979. *A literature Survey: Methods for the Removal of Iodine Species from Off-Gases and Liquid Waste Streams of Nuclear Power and Nuclear Fuel Reprocessing Plants, with Emphasis on Solid Sorbents*, ORNL/TM-6350, Oak Ridge National Laboratory, Oak Ridge, Tennessee.

Hoskins JS, T Karanfil, SM Serkiz. 2002. "Removal and sequestration of iodide using silver-impregnated activated carbon." *Environmental Science & Technology* 36(4):784-789; <https://doi.org/10.1021/es010972m>.

Hsi H-C, MJ Rood, M Rostam-Abadi, S Chen, R Chang. 2001. "Effects of sulfur impregnation temperature on the properties and mercury adsorption capacities of activated carbon fibers (ACFs)." *Environmental Science & Technology* 35(13):2785-2791; <https://doi.org/10.1021/es001794k>.

Huggins FE, GP Huffman, GE Dunham, CL Senior. 1999. "XAFS examination of mercury sorption on three activated carbons." *Energy & Fuels* 13(1):114-121; <https://doi.org/10.1021/ef9801322>.

Hutson ND, BC Attwood, KG Scheckel. 2007. "XAS and XPS characterization of mercury binding on brominated activated carbon." *Environmental Science & Technology* 41(5):1747-1752, <https://doi.org/10.1021/es062121q>.

Huve J, A Ryzhikov, H Nouali, V Lalia, G Augé, TJ Daou. 2018. "Porous sorbents for the capture of radioactive iodine compounds: A review." *RSC Advances* 8:29248-29273; <https://doi.org/10.1039/C8RA04775H>.

Johnson NC, S Manchester, L Sarin, Y Gao, I Kulaots, RH. Hurt. 2008. "Mercury vapor release from broken compact fluorescent lamps and in situ capture by new nanomaterial sorbents." *Environ. Sci. Technol.* 42(15):5772-5778; <https://doi.org/10.1002/adma.201700665>.

Jubin RT, SH Bruffey, KK Patton. 2014. *Humid Aging and Iodine Loading of Silver-Functionalized Aerogels*, FCRD-SWF-2014-000594, Oak Ridge National Laboratory, Oak Ridge, Tennessee.

Jubin RT, SH Bruffey. 2015. "Initial evaluation of a hot isostatic pressed waste form from iodine-loaded silver-exchanged mordenite." In *Proceedings of GLOBAL 2015*; pp1393-1402.

Jubin RT. 1988. *Airborne Waste Management Technology Applicable for Use in Reprocessing Plants for Control of Iodine and Other Off-Gas Constituents*, ORNL/TM-10477, Oak Ridge National Laboratory, Oak Ridge, Tennessee.

Karatza D, M Prisciandaro, A Lancia, D Musmarra. 2011. “Silver impregnated carbon for adsorption and desorption of elemental mercury vapors.” *Journal of Environmental Sciences* **23**(9):1578-1584; [https://doi.org/10.1016/S1001-0742\(10\)60528-1](https://doi.org/10.1016/S1001-0742(10)60528-1).

Khunphonoi R, P Khamdagsag, S Chiarakorn, N Grisdanurak, A Paerungruang, S Predapitakkun. 2015. “Enhancement of elemental mercury adsorption by silver supported material.” *Journal of Environmental Sciences* **32**:207-216; <https://doi.org/10.1016/j.jes.2015.01.008>.

Kitani S, T Noro, T Kohara. 1972. “Removal of methyl iodide by impregnated charcoals from flowing air under humid condition.” *Journal of Nuclear Science and Technology* **9**(4):197–202; <https://doi.org/10.1080/18811248.1972.9734831>.

Korpiel JA, RD Vidic. 1997. “Effect of sulfur impregnation method on activated carbon uptake of gas-phase mercury.” *Environmental Science & Technology* **31**(8):2319-2325; <https://doi.org/10.1021/es9609260>.

Kulyukhin SA. 2012. “Fundamental and applied aspects of the chemistry of radioactive iodine in gas and aqueous media.” *Russian Chemical Reviews* **81**(10):960-982; <https://doi.org/10.1070/RC2012v081n10ABEH004269>.

WRPS and INTERA. 2018. *Performance Assessment for the Integrated Disposal Facility, Hanford, Site, Washington*. RPP-RPT-59958, Rev. 1. Washington River Protection Solutions, LLC. Richland, Washington.

Lee S-H, Y-O Park. 2003. “Gas-phase mercury removal by carbon-based sorbents.” *Fuel Processing Technology* **84**(1-3):197-206; [https://doi.org/10.1016/S0378-3820\(03\)00055-9](https://doi.org/10.1016/S0378-3820(03)00055-9).

Li D, DI Kaplan, KA Price, JC Seaman, K Roberts, C Xu, P Lin, W Xing, K Schwehr, PH Santschi. 2019. “Iodine immobilization by silver-impregnated granular activated carbon in cementitious systems.” *Journal of Environmental Radioactivity* **208-209**:106017; <https://doi.org/10.1016/j.jenvrad.2019.106017>.

Li H, L Zhu, J Wang, L Li, and K Shih. 2016. “Development of nano-sulfide sorbent for efficient removal of elemental mercury from coal combustion fuel gas.” *Environmental science & technology* **50**(17): 9551-9555; <https://doi.org/10.1021/acs.est.6b02115>.

Li H, W Zhu, J Yang, M Zhang, J Zhao, W Qu. 2018. “Sulfur abundant S/FeS<sub>2</sub> for efficient removal of mercury from coal-fired power plants.” *Fuel* **232**:476-484; <https://doi.org/10.1016/j.fuel.2018.06.002>.

Li N, H Wei, Y Duan, H Tang, S Zhao, P Hu, S Ren. 2018. “Experimental study on mercury adsorption and adsorbent regeneration of sulfur-loaded activated carbon.” *Energy Fuels* **32**(10):11023-11029; <https://doi.org/10.1021/acs.energyfuels.8b02527>.

Liao Y, J Weber, BM Mills, Z Ren, CFJ Faul. 2016. “Highly efficient and reversible iodine capture in hexaphenylbenzene-based conjugated microporous polymers.” *Macromolecules* **49**(17):6322-33; <https://doi.org/10.1021/acs.macromol.6b00901>.

Liu D, C Li, J Wu, Y Liu. 2020. “Novel carbon-based sorbents for elemental mercury removal from gas streams: A review.” *Chemical Engineering Journal* **391**:123514; <https://doi.org/10.1016/j.cej.2019.123514>.



- Liu W, H Xu, Y Liao, Z Quan, S Li, S Zhao, Z Qu, N Yan. 2019. "Recyclable CuS sorbent with large mercury adsorption capacity in the presence of SO<sub>2</sub> from non-ferrous metal smelting flue gas." *Fuel* **235**:847-854; <https://doi.org/10.1016/j.fuel.2018.08.062>.
- Luo G, H Yao, M Xu, X Cui, W Chen, R Gupta, Z Xu. 2010. "Carbon nanotube-silver composite for mercury capture and analysis." *Energy & Fuels* **24**(1):419-426; <https://doi.org/10.1021/ef900777v>.
- Ma Y, T Xu, X Zhang, J Wang, H Xu, W Huang, H Zhang. 2022. "Excellent adsorption performance and capacity of modified layered ITQ-2 zeolites for elemental mercury removal and recycling from flue gas." *Journal of Hazardous Materials* **423**:127118; <https://doi.org/10.1016/j.jhazmat.2021.127118>.
- Ma Y, T Xu, X Zhang, Z Fei, H Zhang, H Xu, Y Ma. 2021. "Manganese bridge of mercury and oxygen for elemental mercury capture from industrial flue gas in layered Mn/MCM-22 zeolite." *Fuel* **283**:118973; <https://doi.org/10.1016/j.fuel.2020.118973>.
- Maeck WJ, DT Pence. 1970. "Application of metal zeolites to radioiodine air cleaning problems." *Proceedings of the 11<sup>th</sup> Air Cleaning Conference*, CONF-700816, pp607-620, Idaho Nuclear Corporation, Idaho Falls, Idaho.
- Matlack KS and IL Pegg. 2003. *Destruction of Alcohols in DM1200 Melter System During LAW and HLW Vitrification*. VSL-03L4850-1, Rev. 0; 24590-101-TSA-W000-0009-149-00001, Rev. 00A. Vitreous State Laboratory, The Catholic University of America, Washington, District of Columbia.
- Matlack KS, H Abramowitz, and IL Pegg. 2019. *Summary Report: Iodine Speciation Effects in LAW Feeds*. VSL-19S4740-1, Rev. 0, Vitreous State Laboratory, The Catholic University of America, Washington, District of Columbia.
- Matlack KS, H Abramowitz, IS Muller, I Joseph, IL Pegg. 2020. *Final Report: Iodine Speciation Effects in LAW Feeds*. VSL-20R4740-1, Rev. A, Vitreous State Laboratory, The Catholic University of America, Washington, District of Columbia.
- Matlack KS, W Gong, T Bardakci, N D'Angelo, M Brandys, W Kot, IL Pegg. 2005. *Regulatory Off-gas Emissions Testing on the DM1200 Melter System Using HLW and LAW Simulants*. VSL-05R5830-1, Rev. 0; 24590-101-TSA-W000-0009-166-00001, Rev. 00B. Vitreous State Laboratory, The Catholic University of America, Washington, District of Columbia.
- Matyáš J, GE Fryxell, BJ Busche, K Wallace, LS Fifield. 2011. "Functionalized silica aerogels: advanced materials to capture and immobilize radioactive iodine." In *Proceedings of Ceram. Eng. Sci.: Ceram. Mater. Energy Appl.* eds. H-T Lin, et al., vol. **32**, pp. 23-33, Wiley-The American Ceramic Society.
- Matyáš J, N Canfield, S Sulaiman, M Zumhoff. 2016. "Silica-based waste form for immobilization of iodine from reprocessing plant off-gas streams." *Journal of Nuclear Materials* **476**:255-261; <https://doi.org/10.1016/j.jnucmat.2016.04.047>.
- Matyáš J; ES Ilton, L Kovařík. 2018. "Silver-functionalized silica aerogel, Towards an understanding of aging on iodine sorption performance." *RSC Advances* **8**(56):31843–31852; <https://doi.org/10.1039/C8RA05137B>.
- Oh Y, CD Morris, and MG Kanatzidis. 2012. "Polysulfide chalcogels with ion-exchange properties and highly efficient mercury vapor sorption." *Journal of the American Chemical Society* **134**(35): 14604-14608; <https://doi.org/10.1021/ja3061535>.

Oh Y, S Bag, CD Malliakas, and MG Kanatzidis. 2011. “Selective surfaces: high-surface-area zinc tin sulfide chalcogels.” *Chemistry of Materials* **23**(9): 2447-2456; <https://doi.org/10.1021/cm2003462>.

Otani Y, H Emi, C Kanaoka, I Uchijima, H Nishino. 1988. “Removal of mercury vapor from air with sulfur-impregnated adsorbents.” *Environmental Science & Technology* **22**(6):708-711; <https://doi.org/10.1021/es00171a015>.

Pence DT, FA Duce, WJ Maeck. 1972. “Developments in the removal of airborne iodine species with metal-substituted zeolites.” *Proceedings of the 12<sup>th</sup> AEC Air Cleaning Conference*, CONF-720823, pp417-433, MW First (ed.); Division of Occupational Safety, Division of Waste Management and Transportation, U.S. Atomic Energy Commission, Oak Ridge National Laboratory.

Poulston S, EJ Granite, HW Pennline, CR Myers, DP Stanko, H Hamilton, L Rowsell, AWJ Smith, T Ilkenhans, W Chu. 2007. “Metal sorbents for high temperature mercury capture from fuel gas.” *Fuel* **86**(14):2201-2203; <https://doi.org/10.1016/j.fuel.2007.05.015>.

Prindville KA. 2016. *Inventory Data Package for the Integrated Disposal Facility Performance Assessment*. RPP-ENV-58562, Rev. 3. Washington River Protection Solutions, LLC. Richland, Washington.

Qi H, W Xu, J Wang, L Tong, and T Zhu. 2015. “Hg<sup>0</sup> removal from flue gas over different zeolites modified by FeCl<sub>3</sub>.” *Journal of Environmental Sciences* **28**:110-117; <https://doi.org/10.1016/j.jes.2014.05.050>.

Qian X, B Wang, Z-Q Zhu, H-X Sun, F Ren, P Mu, C Ma, W-D Liang, A Li. 2017. “Novel N-rich porous organic polymers with extremely high uptake for capture and reversible storage of volatile iodine.” *Journal of Hazardous Materials* **338**:224-32; <https://doi.org/10.1016/j.jhazmat.2017.05.041>.

Rashid K, KSK Reddy, A Al Shoaibi, A Srinivasakannan. 2013. “Sulfur-impregnated porous carbon for removal of mercuric chloride: optimization using RSM.” *Clean Technologies and Environmental Policy* **15**(6):1041-1048; <https://doi.org/10.1007/s10098-012-0564-4>.

Reddy, KSK, A Al Shoaibi, C Srinivasakannan. 2014. “Elemental mercury adsorption on sulfur-impregnated porous carbon – A review.” *Environmental Technology* **35**(1):18-26; <https://doi.org/10.1080/21622515.2013.804589>.

Reiser JT, AR Lawter, NA Avalos, J Bonnett, BJ Riley, S Chong, N Canfield, SA Saslow, A Bourchy, and M Asmussen. 2022. “Review and experimental comparison of the durability of iodine waste forms in semi-dynamic leach testing.” *Chemical Engineering Journal Advances* **11**:100300; <https://doi.org/10.1016/j.cej.2022.100300>.

Rickettson H. 2011. *Engineering Specification for Activated Carbon Bed Absorbers*. 24590-WTP-3PS-MWK0-T0001, Rev. 5. (Bechtel National, Inc.) River Protection Project Waste Treatment Plant, Richland, Washington.

Riley BJ, DA Pierce, J Chun, J Matyáš, WC Lepry, T Garn, J Law, MG Kanatzidis. 2014. “Polyacrylonitrile-chalcogel hybrid sorbents for radioiodine capture.” *Environmental Science & Technology* **48**(10):5832-5839; <https://doi.org/10.1021/es405807w>.

Riley BJ, DA Pierce, WC Lepry, JO Kroll, J Chun, KS Subrahmanyam, MG Kanatzidis, FK Alblouwy, A Bulbule, EM Sabolsky. 2015. “Consolidation of tin sulfide chalcogels and xerogels with and without adsorbed iodine.” *Industrial & Engineering Chemistry Research* **54**(45):11259-11267; <https://doi.org/10.1021/acs.iecr.5b02697>.

Riley BJ, J Chun, JV Ryan, J Matyáš, XS Li, DW Matson, SK Sundaram, DM Strachan, JD Vienna. 2011. “Chalcogen-based aerogels as a multifunctional platform for remediation of radioactive iodine.” *RSC Advances* **1**:1704-715; <https://doi.org/10.1039/C1RA00351H>.

Riley BJ, J Chun, W Um, WC Lepry, J Matyas, MJ Olszta, X Li, K Polychronopoulou, MG Kanatzidis. 2013. “Chalcogen-based aerogels as sorbents for radionuclide remediation.” *Environmental Science & Technology* **47**(13):7540-7547; <https://doi.org/10.1021/es400595z>.

Riley BJ, JO Kroll, JA Peterson, J Matyáš, MJ Olszta, X Li, JD Vienna. 2017. “Silver-loaded aluminosilicate aerogels as iodine sorbents.” *ACS Applied Materials & Interfaces* **9**(38):32907-32919; <https://doi.org/10.1021/acsami.7b10290>.

Riley BJ, S Chong, CL Beck. 2021. “Iodine vapor reactions with pure metal wires at temperatures of 100-139 °C in air.” *Industrial & Engineering Chemistry Research* **60**(47):17162-73; <https://doi.org/10.1021/acs.iecr.1c03902>.

Riley BJ, S Chong, J Marcial, N Lahiri, MK Bera, S Lee, T Wu, K Kruska, J Matyáš. 2022. “Silver-loaded xerogel nanostructures for iodine capture: A comparison of thiolated versus unthiolated sorbents.” *ACS Applied Nano Materials* **5**(7):9478-9494; <https://doi.org/10.1021/acsanm.2c01741>.

Riley BJ, S Chong, MJ Olszta, JA Peterson. 2020. “Evaluation of getter metals in Na-Al-Si-O aerogels and xerogels for the capture of iodine gas.” *ACS Applied Materials & Interfaces* **12**(17):19682-19692; <https://doi.org/10.1021/acsami.0c03155>.

Riley BJ, S Chong. 2020. “Environmental remediation with functional xerogels and xerogels,” *Global Challenges* **2020**(4):2000013; <https://doi.org/10.1002/gch2.202000013>.

Rungnim C, V Promarak, S Hannongbua, N Kungwan, S Namuangruk. 2016. “Complete reaction mechanisms of mercury oxidation on halogenated activated carbon.” *Journal of Hazardous Materials* **310**:253-260; <https://doi.org/10.1016/j.jhazmat.2016.02.033>.

Sava DF, KW Chapman, MA Rodriguez, JA Greathouse, PS Crozier, H Zhao, PJ Chupas, TM Nenoff. 2013. “Competitive I<sub>2</sub> sorption by Cu-BTC from humid gas streams.” *Chemistry of Materials* **25**:2591-2596; <https://doi.org/10.1021/cm401762g>.

Sava DF, MA Rodriguez, KW Chapman, PJ Chupasa, JA Greathouse, PS Crozier, TM Nenoff. 2011. “Capture of volatile iodine, a gaseous fission product, by zeolitic imidazolate framework-8.” *Journal of the American Chemical Society* **133**:12398-12401; <https://doi.org/10.1021/ja204757x>.

Stiver B. 2018. *Specification Change Notice: Appendix B, C and M – LAW and HLW Buyer Third Party Testing*. 24590-WTP-3PN-MWK0-00013, Rev. 0. (Bechtel National, Inc.) River Protection Project Waste Treatment Plant, Richland, Washington.

Stiver B. 2019. *Engineering Study for Determining Path Forward on LAW Iodine Decontamination Factor and Removal Efficiencies for use in the Radioactive Air Permit and Performance Assessment Permit*. 24590-WTP-ES-PE-19-001, Rev. 0. (Bechtel National, Inc.) River Protection Project Waste Treatment Plant, Richland, Washington.

Strachan D, J Chun, CH Henager Jr., J Matyas, BJ Riley, JV Ryan, PK Thallapally. 2010. *Summary Report for the Development of Materials for Volatile Radionuclides*. PNNL-20007, Pacific Northwest National Laboratory, Richland, Washington; <https://doi.org/10.2172/1015528>.

Subrahmanyam KS, D Sarma, CD Malliakas, K Polychronopoulou, BJ Riley, DA Pierce, J Chun, MG Kanatzidis. 2015. “Chalcogenide aerogels as sorbents for radioactive iodine.” *Chemistry of Materials* **27**(7):2619-2626; <https://doi.org/10.1021/acs.chemmater.5b00413>.

Sun H, S Zhao, Y Ma, J Wu, P Liang, D Yang, H Zhang. 2018. “Effective and regenerable Ag/4A zeolite nanocomposite for Hg<sup>0</sup> removal from natural gas.” *Journal of Alloys and Compounds*. **762**:520-527; <https://doi.org/10.1016/j.jallcom.2018.05.222>.

Sweeney S. 2020. *Mechanical Data Sheet – Activated Carbon Adsorber*. 24590-LAW-MVD-LVP-00003, Rev. 7. (Bechtel National, Inc.) River Protection Project Waste Treatment Plant, Richland, Washington.

Tardiff BM, VC Nguyen, MS Fountain, CL Bottenus, ME Stone, AM Howe. 2022. *DFLAW Flowsheet Impacts from Recycling the Caustic Scrubber Effluent to the EMF Evaporator*. RPP-RPT-63579, Rev. 0, Washington River Protection Solutions Inc., Richland, Washington.

Tardiff BM. 2022. *Maximum Allowable I-129 Concentration for Effluent Treatment Facility Based on Hanford Waste Treatment and Immobilization Plant Effluent Waste Profile*. RPP-RPT-63887, Rev. 0, Washington River Protection Solutions Inc., Richland, Washington.

Thomas TR, BA Staples, LP Murphy, JT Nichols. 1977. *Airborne Elemental Iodine Loading Capacities of Metal Exchanged Zeolites and a Method for Recycling Silver Zeolite*, ICP-1119, Allied Chemical Corporation, Idaho Falls, Idaho.

Tian Y, G Zhu. 2020. “Porous Aromatic Frameworks (PAFs).” *Chemical Reviews* **120**(16):8934-86; <https://doi.org/10.1021/acs.chemrev.9b00687>.

Tian Z, T-S Chee, L Zhu, T Duan, X Zhang, L Lei, C. Xiao. 2021. “Comprehensive comparison of bismuth and silver functionalized nickel foam composites in capturing radioactive gaseous iodine.” *Journal of Hazardous Materials* **417**:125978; <https://doi.org/10.1016/j.jhazmat.2021.125978>.

Tuck J. 2016. *Drawing – LAW Carbon Bed LVP-ADBR-00001A&B General Arrangement*. 24590-QL-POA-MWK0-00001-05-00197, Bechtel River Protection Project Waste Treatment Plant, Richland, Washington.

Valizadeh B, TN Nguyen, B Smit, KC Stylianou. 2018. “Porous metal-organic framework@polymer beads for iodine capture and recovery using a gas-sparged column,” *Advanced Functional Materials* **28**(30):1801596; <https://doi.org/10.1002/adfm.201801596>.

Vidic RD, DP Siler. 2001. “Vapor-phase elemental mercury adsorption by activated carbon impregnated with chloride and chelating agents.” *Carbon* **39**:3-14; [https://doi.org/10.1016/S0008-6223\(00\)00081-6](https://doi.org/10.1016/S0008-6223(00)00081-6).

WA7890008967. 2019. *Hanford Facility Resource Conservation and Recovery Act Permit, Dangerous Waste Portion, Revision 8, for the Treatment, Storage, and Disposal of Dangerous Waste*. U.S. Department of Energy Hanford Facility, Richland, Washington.

Wajima T, K Sugawara. 2011. “Adsorption behaviors of mercury from aqueous solution using sulfur-impregnated adsorbent developed from coal.” *Fuel Processing Technology* **92**(7):1322-1327; <https://doi.org/10.1016/j.fuproc.2011.02.008>.

Wang J, C Wang, H Wang, B Jin, P Zhang, L Li, S Miao. 2021. "Synthesis of N-containing porous aromatic frameworks via Scholl reaction for reversible iodine capture." *Microporous and Mesoporous Materials* **310**:110596; <https://doi.org/10.1016/j.micromeso.2020.110596>.

Wang L, K Zhang, J Li, X Shen, N Yan, HZ Zhao, Z Qu. 2022. "Engineering of defect-rich Cu<sub>2</sub>WS<sub>4</sub> nano-homojunctions anchored on covalent organic frameworks for enhanced gaseous elemental mercury removal." *Environmental Science & Technology* **56**:16240-16248; <https://doi.org/10.1021/acs.est.2c04799>.

Wang P, Q Xu, Z Li, W Jiang, Q Jiang, D Jiang. 2018. "Exceptional iodine capture in 2D covalent organic frameworks." *Advanced Materials* **30**(29):1801991; <https://doi.org/10.1002/adma.201801991>.

Wang S, Y Liu, Y Ye, X Meng, J Du, X Song, Z Liang. 2019. "Ultrahigh volatile iodine capture by conjugated microporous polymer based on N,N,N',N'-tetraphenyl-1,4-phenylenediamine." *Polymer Chemistry* **10**(20):2608-15; <https://doi.org/10.1039/C9PY00288J>.

WERF MACT Study Team. 1998. *WERF MACT Feasibility Study Report*. INEEL/EXT-98-01166, Idaho National Engineering and Environmental Laboratory, Idaho Falls, Idaho.

Wong A. 2017. *Calculation Cover Sheet – LAW Activated Carbon Bed Operating Conditions and Process Design Requirements*. 24590-LAW-MKC-LVP-00005, Rev. 4, (Bechtel National, Inc.) River Protection Project Waste Treatment Plant, Richland, Washington.

Wren JC, W Long, CJ Moore, KR Weaver. 1999. "Modeling the removal and retention of radioiodine by TEDA-impregnated charcoal under reactor accident conditions." *Nuclear Technology* **125**(1):13-27; <https://doi.org/10.13182/NT99-A2929>.

Wu L, JA Sawada, DB Kuznicki, T Kuznicki, and SM Kuznicki. 2014. "Iodine adsorption on silver-exchanged titania-derived adsorbents." *Journal of Radioanalytical Nuclear Chemistry* **302**(1):527-532; <https://doi.org/10.1007/s10967-014-3252-5>.

Wu X, Y Duan, J Meng, X Geng, A Shen, and J Hu. 2021. "Experimental Study on the Mercury Removal of a H<sub>2</sub>S-Modified Fe<sub>2</sub>O<sub>3</sub> Adsorbent." *Industrial & Engineering Chemistry Research* **60**(48):17429-17438; <https://doi.org/10.1021/acs.iecr.1c01998>.

Xie W, D Cui, S-R Zhang, Y-H Xu, D-L Jiang. 2019. "Iodine capture in porous organic polymers and metal-organic frameworks materials." *Materials Horizons* **6**(8):1571-95; <https://doi.org/10.1039/C8MH01656A>.

Xie Y, T Pan, Q Lei, C Chen, X Dong, Y Yuan, WA Maksoud, L Zhao, L Cavallo, I Pinnau, Y Han. 2022. "Efficient and simultaneous capture of iodine and methyl iodide achieved by a covalent organic framework." *Nature Communications* **13**(1):2878; <https://doi.org/10.1038/s41467-022-30663-3>.

Yadav A, S Chong, BJ Riley, JS McCloy, A Goel. 2022. "Iodine capture by Ag-loaded solid sorbents followed by Ag recycling and iodine immobilization: An end-to-end process." under review at *Industrial & Engineering Chemistry Research*.

Yan Z, Y Yuan, Y Tian, D Zhang, G Zhu. 2015. "Highly efficient enrichment of volatile iodine by charged porous aromatic frameworks with three sorption sites." *Angewandte Chemie International Edition* **54**(43):12733-37; <https://doi.org/10.1002/anie.201503362>.



Yang X, D Xie, W Wang, S Li, Z Tang, S Dai. 2023. "An activated carbon from walnut shell for dynamic capture of high concentration gaseous iodine." *Chemical Engineering Journal* **454**(4):140365; <https://doi.org/10.1016/j.cej.2022.140365>.

Yu Q, X Jiang, M Duan. 2021. "Nano-flower-shaped SnS<sub>2</sub> doped polyacrylonitrile hybrid beads for effective capture of radioactive gaseous iodine." *Social Science Research Network* <http://dx.doi.org/10.2139/ssrn.3978461>.

Yu Q, X Jiang, Z Cheng, Y Liao, Q Pu, M Duan. 2020. "Millimeter-sized Bi<sub>2</sub>S<sub>3</sub>@polyacrylonitrile hybrid beads for highly efficient iodine capture." *New Journal of Chemistry* **44**:16759; <https://doi.org/10.1039/D0NJ03229H>.

Zhang L, J Li, H Zhang, Y Liu, Y Cui, F Jin, K Wang, G Liu, Y Zhao, Y Zeng. 2021. "High iodine uptake in two-dimensional covalent organic frameworks." *Chemical Communications* **57**(45):5558-61; <http://dx.doi.org/10.1039/D1CC00737H>.

Zhang X, B Shen, S Zhu, H Xu, L Tian. 2016. "UiO-66 and its Br-modified derivatives for elemental mercury removal." *Journal of Hazardous Materials* **320**:556-563; <https://doi.org/10.1016/j.jhazmat.2016.08.039>.

Zhao S, H Xu, Z Qu, P Liu, Y Cui, N Yan. 2018b. "Combined effects of Ag and UiO-66 for removal of elemental mercury from flue gas." *Chemosphere* **197**:65-72; <https://doi.org/10.1016/j.chemosphere.2018.01.025>.

Zhao S, J Mei, H Xu, W Liu, Z Qu, Y Cui, N Yan. 2018a. "Research of mercury removal from sintering flue gas of iron and steel by the open metal site of Mil-101 (Cr)." *Journal of Hazardous Materials* **351**:301-307; <https://doi.org/10.1016/j.jhazmat.2017.12.016>.

Zhao S, W Huang, J Xie, Z Qu, N Yan. 2021. "Mercury removal from flue gas using UiO-66-type metal-organic frameworks grafted with organic functionalities." *Fuel* **289**:119807; <https://doi.org/10.1016/j.fuel.2020.119807>.

Zhou J, S Hao, L Gao, Y Zhang. 2014. "Study on adsorption performance of coal based activated carbon to radioactive iodine and stable iodine." *Annals of Nuclear Energy* **72** (2014): 237-241; <https://doi.org/10.1016/j.anucene.2014.05.028>.

Appendix A – Detailed Material Screening, Evaluation, and Ranking Tables

Material Type	Representative Material	Reference	Candidacy	Bulk Material/ Fabrication Cost	Safety Risks (toxic/dust/ flammable)	Hg Vapor Testing	Hg Test Conditions/ Capacity	I Vapor Testing	I Test Conditions/ Capacity	WTP Relevant Test Conditions	Physical Form	Waste Form Demonstrated	Most Significant Gap/Question	Significant Challenge	Other Gaps/Questions	Thermal and Chemical Stability in Service				
				Green - Low Yellow - Medium Red - High	Green - None Yellow - Some Red - Significant	(Y/NA)	Green - Dynamic Yellow - Partial Orange - Static Red - No data	(Y/Other/NA)	Green - Dynamic Yellow - Partial Orange - Static Red - No data	Green - High Yellow - Moderate Orange - Partial Red - Low	Green - Ready Yellow - Alter Red - Raw	Green - Full-scale Yellow - Bench Red - None	Performance under WTP conditions	Stability in humid conditions	Long-term service performance vs. BAT 37 (original)	Thermal Loss of Structure (Fines)	NOx/ Oxidizing	Water	Temp. Capacity Loss (80°C)	Organics
COMMERCIAL GROUP																				
Baseline	BAT-37 II (Assumed similar to BAT-37)	Abramowitz H, KS Matlack, M Brandys, IL Pegg, GA Diener. 2019a. Final Report: Activated Carbon Media Small-Scale Testing. VSL-19R4530-1, Rev. 0; 24590-CM-HC4-MWK0-00002-02-00001, Rev. 00B. Vitreous State Laboratory, The Catholic University of America, Washington, District of Columbia.	Planned replacement of BAT-37 that is sulfur and KI impregnated	L	Flammable	Y	Assume same as BAT-37 DF = 21	Y	DF = 167	BAT-37 Data	Ready	Full	Performance under WTP conditions	Stability in humid conditions	Long-term service performance vs. BAT 37 (original)					
Carbon Based: S-Impregnated AC	Desorex (K43J/HGD)	Donau Carbon Spec Sheet	Commercially available activated carbon designed for Hg capture	L	Flammable	Y	100-1000 mg/g	Y	N/A (950 mg/g capacity)	Dynamic test conditions - up to 70C	Ready	Full	Combined deployment with other activated carbons	N/A	Testing in WTP conditions			150 C		
Carbon Based: TEDA-Impregnated AC	Chemsorb 701G	Abramowitz H, KS Matlack, M Brandys, IL Pegg, GA Diener. 2019. Final Report: Activated Carbon Media Small-Scale Testing. VSL-19R4530-1, Rev. 0; 24590-CM-HC4-MWK0-00002-02-00001, Rev. 00B. Vitreous State Laboratory, The Catholic University of America, Washington, District of Columbia.	Commercially available activated carbon developed for I capture and demonstrated Hg capture	L	Flammable	Y	DF = 497	Y	DF = 438	Dynamic conditions, 70C, simplified off-gas	Ready	Full	Combined deployment with other activated carbons	N/A	Testing in WTP conditions			150 C		
Carbon Based: KI-Impregnated AC	Oxorbion K 40J	Donau Carbon Spec Sheet	Commercially available activated carbon capable of I capture	L	Flammable	N	No Data	Y	No Data	Dynamic test conditions -	Ready	Full	Combined deployment with other activated carbons	N/A	Hg/I testing in WTP condition			150 C		
Carbon Based: Ag-Impregnated AC	AGC-50 CS-Si	Resin Tech Spec Sheet	Commercially available activated carbon capable of I capture	H - Ag	Toxic (Ag)	N	No Data	Y	No Data (maybe liquid)	Physically stable up to 100C in dynamic conditions	Ready	Full	Can it be a dual capture material? (Hg)	Cost	Combination with other activated carbons, Testing in WTP conditions, service lifetime vs cost, is regeneration of sorbent possible					
Porous Inorganic Crystalline Matrices (Faujasite)	Ionex 400	Riley BJ, S Chong, J Marcial, N Lahiri, MK Bera, S Lee, T Wu, K Kruska, J Matyáš. 2022. "Silver-loaded xerogel nanostructures for iodine capture: A comparison of thiolated versus unthiolated sorbents," ACS Applied Nano Materials 5(7):9478-9494; https://doi.org/10.1021/acsanm.2c01741.	Commercially available material developed for I capture	H - Ag	Toxic (Ag)	Y	370 mg/g (&)	Y	330 mg/g	Hg testing in dynamic conditions at 30 C without humidity. Iodine data in static conditions at 150 C.	Ready	Bench	Can it be a dual capture in WTP conditions?	Stability in NOx and cost	Is regeneration of sorbent possible					

				Bulk Material/ Fabrication Cost	Safety Risks (toxic/dust/ flammable)	Hg Vapor Testing	Hg Test Conditions/ Capacity	I Vapor Testing	I Test Conditions/ Capacity	WTP Relevant Test Conditions	Physical Form	Waste Form Demonstrated	Most Significant Gap/Question	Significant Challenge	Other Gaps/Questions	Thermal and Chemical Stability in Service				
Material Type	Representative Material	Reference	Candidacy	Green - Low Yellow - Medium Red - High	Green - None Yellow - Some Red - Significant	(Y/NA)	Green - Dynamic Yellow - Partial Orange - Static Red - No data	(Y/Other/NA)	Green - Dynamic Yellow - Partial Orange - Static Red - No data	Green - High Yellow - Moderate Orange - Partial Red - Low	Green - Ready Yellow - Alter Red - Raw	Green - Full-scale Yellow - Bench Red - None				Thermal Loss of Structure (Fines)	NOx/ Oxidizing	Water	Temp. Capacity Loss (80°C)	Organics
Porous Inorganic Crystalline Matrices (Mordenite)	Ionex 900	Abramowitz H, KS Matlack, M Brandys, IL Pegg, GA Diener. 2019. Final Report: Activated Carbon Media Small-Scale Testing. VSL-19R4530-1, Rev. 0; 24590-CM-HC4-MWK0-00002-02-00001, Rev. 00B. Vitreous State Laboratory, The Catholic University of America, Washington, District of Columbia.	Commercially available material developed for I capture and demonstrated Hg removal	H - Ag	Toxic (Ag)	Y	DF = 203 (with I)	Y	DF = 45 (with Hg)	Testing in dynamic conditions, 70 C, Simplified off-gas	Ready	Bench	Can it be a dual capture in WTP conditions?	Stability in NOx and cost	Is regeneration of sorbent possible, waste form demonstration					
Inorganic Sulfide Sorbents	CuS	Liu W, H Xu, Y Liao, Z Quan, S Li, S Zhao, Z Qu, N Yan. 2019. “Recyclable CuS sorbent with large mercury adsorption capacity in the presence of SO2 from non-ferrous metal smelting flue gas.” Fuel 235:847-854; https://doi.org/10.1016/j.fuel.2018.08.062.	Simple powder product likely capable of both Hg and I capture	L - dependent on metal	H2S Vapor generation	Y	17 mg/g	Y	Other material -	Dynamic conditions, 70 C	raw	None	Can it be a dual capture material?	N/A	WTP conditions, engineered scaffold, does it capture both at same reported capacity, waste form, large scale synthesis/product ion route		SO2			
Metal Substrates and Other Sorbents (Non-metal)	Unstabilized Amorphous nano-Se	Johnson NC, S Manchester, L Sarin, Y Gao, I Kulaots, RH. Hurt. 2008. “Mercury vapor release from broken compact fluorescent lamps and in situ capture by new nanomaterial sorbents.” Environ. Sci. Technol. 42(15):5772-5778; https://doi.org/10.1002/adma.201700665.	Raw material with capacity for Hg	M - dependent on metal	Toxic (Se)	Y	188 mg/g	N	No Data	Partial conditions, 20 C, no competition	raw	none	Can it be a dual capture material?	Stabilization of fine nanopowders	WTP conditions, Need engineered form, does it capture both at same reported capacity, waste form, large scale synthesis/product ion route					
Metal Substrates and Other Sorbents (Metal)	Pure metal wires	Riley BJ, S Chong, CL Beck. 2021. “Iodine vapor reactions with pure metal wires at temperatures of 100-139 °C in air,” Industrial & Engineering Chemistry Research 60(47):17162-73; https://doi.org/10.1021/acs.iecr.1c03902.	Very high iodine loadings for some metals (e.g. Ag, Cu,Sn)	M - dependent on metal	Dependent on metal, maybe toxic	N	No Data	Y	4368 mg/g (Sn 100 C)	Static -up to 139°C, no competition	Alter	Bench	Can they capture Hg?	N/A	Service lifetime, dynamic testing, metal-type for cost, pressure drop, possible volume expansion in capture, flowability into unit, combining different metals					
Metal Substrates and Other Sorbents (Nano-metals)	Nano-Ag	Johnson NC, S Manchester, L Sarin, Y Gao, I Kulaots, RH. Hurt. 2008. “Mercury vapor release from broken compact fluorescent lamps and in situ capture by new nanomaterial sorbents.” Environ. Sci. Technol. 42(15):5772-5778; https://doi.org/10.1002/adma.201700665.	High capacity, could get Hg and I	H	Dust, Toxic (Ag)	Y	0.008 mg/g	N	No Data	Partial conditions, 20 C, no competition	raw	None	Can it be a dual capture material?	N/A	WTP conditions, Need engineered form, possible volume expansion, does it capture both at same reported capacity, waste form, large scale synthesis/product ion route					



Material Type	Representative Material	Reference	Candidacy	Bulk Material/ Fabrication Cost	Safety Risks (toxic/dust/ flammable)	Hg Vapor Testing	Hg Test Conditions/ Capacity	I Vapor Testing	I Test Conditions/ Capacity	WTP Relevant Test Conditions	Physical Form	Waste Form Demonstrated	Most Significant Gap/Question	Significant Challenge	Other Gaps/Questions	Thermal and Chemical Stability in Service				
				Green - Low Yellow - Medium Red - High	Green - None Yellow - Some Red - Significant	(Y/NA)	Green - Dynamic Yellow - Partial Orange - Static Red - No data	(Y/Other/NA)	Green - Dynamic Yellow - Partial Orange - Static Red - No data	Green - High Yellow - Moderate Orange - Partial Red - Low	Green - Ready Yellow - Alter Red - Raw	Green - Full-scale Yellow - Bench Red - None				Thermal Loss of Structure (Fines)	NOx/ Oxidizing	Water	Temp. Capacity Loss (80°C)	Organics
				DEVELOPMENTAL GROUP																
Inorganic Aerogels (Aerogel)	Ag <sup>0</sup> - functionalized silica aerogel	Matyáš J, GE Fryxell, BJ Busche, K Wallace, LS Fifield. 2011. Functionalized silica aerogels: advanced materials to capture and immobilize radioactive iodine. In Proceedings of Ceram. Eng. Sci.: Ceram. Mater. Energy Appl. eds. H-T Lin, et al., vol. 32, pp. 23-33, Wiley-The American Ceramic Society.	High iodine capacity even in in oxidizing conditions and humid air; contains S grout that could capture Hg	H - Ag	Toxic (Ag) but less flammable than carbon, some dust generation	N	No Data	Y	480 mg/g	Testing in dynamic conditions up to 150°C in prototypic off-gas conditions	Alter	Bench	Can it be a dual capture material? (Hg)	N/A	WTP conditions, stability in bed at large scale (may need scaffold), testing for dust generation, large scale synthesis/product ion route					
Inorganic Xerogels	Thiolated AgAlSiO <sub>4</sub> xerogel	Riley BJ, S Chong, J Marcial, N Lahiri, MK Bera, S Lee, T Wu, K Kruska, J Matyáš. 2022. “Silver-loaded xerogel nanostructures for iodine capture: A comparison of thiolated versus unthiolated sorbents,” ACS Applied Nano Materials 5(7):9478-9494; https://doi.org/10.1021/acsanm.2c01741.	High iodine loading in saturated conditions, mechanically robust sorbent	H - Ag	Toxic (Ag) but less flammable than carbon	N	No Data	Y	522 mg/g	Static - up to 150 C, no competitors	Alter	Bench	Can it be a dual capture material? (Hg)	N/A	dynamic condition testing, WTP conditions, stability in bed at large scale (may need scaffold), large scale synthesis/product ion route					
Engineered Membranes	Bi-loaded Carbon Foam	Baskaran K, M Ali, BJ Riley, I Zharov, K Carlson. 2022. “Evaluating the physisorption and chemisorption of iodine on bismuth-functionalized carbon foams.” ACS Materials Letters 4(9):1780-1786; https://doi.org/10.1021/acsmaterialslett.2c00466.	Demonstrated for I, could get Hg	M	No Data	N	No Data	Y	700 mg/g	Static - up to 150 C, no competitors	Alter	None	Can it be a dual capture material? (Hg) FY23 UNR scope	N/A	dynamic condition testing, WTP conditions, deployable form/stability in bed at large scale (may need scaffold)?, large scale synthesis/product ion route					
Inorganic Aerogels (Chalcogel)	Chalcogel (Mo-S)	Subrahmanyam KS, D Sarma, CD Malliakas, K Polychronopoulou, BJ Riley, DA Pierce, J Chun, MG Kanatzidis. 2015. “Chalcogenide aerogels as sorbents for radioactive iodine,” Chemistry of Materials 27(7):2619-2626; https://doi.org/10.1021/acs.chemmater.5b00413.	Tested both I and Hg. The high surface area, polarizability, visible-light response, and rich S–S network render the MoSx chalcogel suitable for catalytic and environmental remediation applications	M (since the ingredients are moderate and require synthesis)	No Data	Y	6 g/g	Y (Separate)	6 g/g (&)	Up to 140 C in static nitrogen	raw	None	Can this be a simultaneous dual capture material for Hg and I or other chalcogels?	Challenging synthesis likely not practical and updated information on other materials may supersede	Can it be a dual capture material simultaneously?, testing in WTP Conditions, Need engineered form, does it capture both at same reported capacity, waste form, large scale synthesis/product ion route					
Improving Existing Materials through Functionalization	Various	N/A	Take existing substrates, similar to above lines, and functionalize for WTP conditions	N/A	N/A	N/A	N/A	N/A	N/A	N/A	N/A	N/A	What other available substrates that are stable in WTP conditions can be altered to meet needs?	N/A	N/A					
Porous Organic Sorbents	Nitrogen Rich Organic Framework	He L, L Chen, X Dong, S Zhang, M Zhang, X Dai, X Liu, P Lin, K Li, C Chen, T Pan, F Ma, J Chen, M Yuan, Y Zhang, L Chen, R Zhou, Y Han, Z Chai, S Wang. 2021. "A nitrogen-rich covalent organic framework for simultaneous dynamic capture of iodine and methyl iodide." Journal of Chem 7(3):699-714	High surface area and has shown capture of iodine and methyl iodide.	M	No Data	Y	DF =5 (&)	Y	6 g/g for iodine and 1.45 g/g for CH3I	Dynamic at 25°C - 150°C (some materials up to 240 C) and with competitors	raw	None	Can a MOF-type be a dual capture material simultaneously?	Cost of MOF at large scale application	WTP conditions, Need engineered form, does it capture both at same reported capacity, waste form, large scale synthesis/product ion route					

Material Type	Representative Material	Reference	Candidacy	Bulk Material/ Fabrication Cost	Safety Risks (toxic/dust/ flammable)	Hg Vapor Testing	Hg Test Conditions/ Capacity	I Vapor Testing	I Test Conditions/ Capacity	WTP Relevant Test Conditions	Physical Form	Waste Form Demonstrated	Most Significant Gap/Question	Significant Challenge	Other Gaps/Questions	Thermal and Chemical Stability in Service							
				Green - Low Yellow - Medium Red - High	Green - None Yellow - Some Red - Significant	(Y/NA)	Green - Dynamic Yellow - Partial Orange - Static Red - No data	(Y/Other/NA)	Green - Dynamic Yellow - Partial Orange - Static Red - No data	Green - High Yellow - Moderate Orange - Partial Red - Low	Green - Ready Yellow - Alter Red - Raw	Green - Full-scale Yellow - Bench Red - None							Thermal Loss of Structure (Fines)	NOx/ Oxidizing	Water	Temp. Capacity Loss (80°C)	Organics
TiO2 Support	15% Ag-TiO2	Khunphonoi R, P Khamdahsag, S Chiarakorn, N Grisdanurak, A Paerungruang, S Predapitakkun. 2015. “Enhancement of elemental mercury adsorption by silver supported material.” Journal of Environmental Sciences 32:207-216; <a href="https://doi.org/10.1016/j.jes.2015.01.008">https://doi.org/10.1016/j.jes.2015.01.008</a> .	Utilizes an alternate substrate that has high stability. Shown to capture Hg and with the Ag component could capture I.	H - Ag	Toxic (Ag) but less flammable than carbon	Y	0.1 mg/g	N	No Data	Static, 60 C, no competitors	raw	None	Can it be a dual capture material?	N/A	dynamic condition testing, WTP conditions, deployable form/stability in bed at large scale (may need scaffold)?, large scale synthesis/product ion route								
Inorganic Sulfide Sorbents (Includes CuS, oS ZnS, H2SFe2O3)	Nanotubes/micr	Johnson NC, S Manchester, L Sarin, Y Gao, I Kulaots, RH. Hurt. 2008. “Mercury vapor release from broken compact fluorescent lamps and in situ capture by new nanomaterial sorbents.” Environ. Sci. Technol. 42(15):5772-5778; <a href="https://doi.org/10.1002/adma.201700665">https://doi.org/10.1002/adma.201700665</a> .	Sulfur used as impregnation element for Hg capture.	M	No Data	Y	2.6x10 <sup>-5</sup> mg/g	N	No Data	Static, 140 C, no competitors	raw	None	Can it be a dual capture material?	N/A	dynamic condition testing, WTP conditions, Need engineered form, does it capture both at same reported capacity, waste form, large scale synthesis/product ion route								

## Distribution List

All distribution of the current report will be made electronically.

DOE EM-3.2 Office of Technology Development

Gerdes, K  
Machara, N

DOE Office of River Protection

Kruger, AA  
Porcaro, EN

Washington River Protection Solution

Skeen, RS  
Swanberg, DJ  
Wagnon, TJ

University of Nevada, Reno

Carlson, K

Pacific Northwest National Laboratory

Arm, ST  
Brouns, TM  
Peeler, DK  
Project File  
Information Release  
Project File  
Information Release

# **Pacific Northwest National Laboratory**

902 Battelle Boulevard  
P.O. Box 999  
Richland, WA 99354  
1-888-375-PNNL (7665)

***[www.pnnl.gov](http://www.pnnl.gov)***